UNIVERSITY OF TURIN

DOCTORAL SCHOOL IN LIFE AND HEALTH SCIENCES

PhD Programme in Complex Systems for Life Sciences

Cycle XXXI

PHARMACOKINETICS AND PHARMACOGENETICS OF DEFERASIROX FOR IRON OVERLOAD TREATMENT IN BETA-THALASSAEMIA PATIENTS

Tutor: ***Student:***

Prof. Antonio D'Avolio ***Dr. Sarah Allegra***

2015-2018

PUBLICATIONS ARISING FROM THIS THESIS

Published Journals Paper

1. **Allegra S**, Cusato J, De Francia S, Longo F, Pirro E, Massano D, Piga A and D'Avolio A. **Effect of pharmacogenetic markers of vitamin D pathway on deferasirox pharmacokinetics in children.**
   Pharmacogenetics and Genomics vol. 28, p. 17-22, doi: 10.1097/FPC.0000000000000315

Submitted Journals Papers

1. **Allegra S**, Cusato J, De Francia S, Longo F, Pirro E, Massano D, Piga A and D'Avolio A. **Role of *CYP1A1*, *ABCG2*, *CYP24A1* and *VDR* gene polymorphisms on the evaluation of cardiac iron overload in thalassaemia patients.**
   Pharmacogenetics and Genomics
2. **Allegra S**, Cusato J, De Francia S, Longo F, Pirro E, Massano D, Piga A and D'Avolio A. **The effect of vitamin D pathway genes and deferasirox pharmacogenetics on liver iron in thalassaemia major patients.**
   Pharmacogenomics Journal

Oral Presentations

1. **Sarah Allegra**, Jessica Cusato, Silvia De Francia, Arianna Arduino, Filomena Longo, Davide Massano, Antonio Piga and Antonio D'Avolio. **Impact of pharmacogenetic markers of vitamin D pathway on deferasirox pharmacokinetics in children.**
   SIF, Rimini 20-22/09/2016
2. **Sarah Allegra**, Silvia De Francia, Jessica Cusato, Arianna Arduino, Elisa Pirro, Davide Massano, Filomena Longo, Antonio Piga and Antonio D'Avolio. **Role of *CYP24A1*, *VDR* and *GC* gene polymorphisms on deferasirox pharmacokinetics and clinical outcomes.**
   Monotematico SIF "Il ruolo della Farmacologia Clinica in Italia: prospettive future nell'ambito del SSN", Napoli 15-16/12/2016

Poster Presentations

1. **Sarah Allegra**, Jessica Cusato, Silvia De Francia, Arianna Arduino, Filomena Longo, Davide Massano, Elisa Pirro, Antonio Piga, Antonio D'Avolio. **Impact of pharmacogenetic markers of vitamin d pathway on liver stiffness in β-thalassemia major patients.**
   SIGU, Torino 23-26/11/2016

TABLE OF CONTENTS

LIST OF ABBREVIATION

ABC: ATP-binding cassette;

ADME: absorption, distribution, metabolism, and excretion;

AUC: area under the curve;

BCRP: breast cancer resistance protein;

Cl: clearance;

Cmax: maximum concentration;

Cmin: minimum concentration;

Ctrough: concentration at the end of dosing interval

CYP: cytochrome P450;

DFX: deferasirox;

EMA: European Medicines Agency;

FDA: Food and Drug Administration;

GC: gc-globulin (group-specific component);

HPLC: high performance liquid chromatography;

HW: Hardy-Weinberg equilibrium;

IQR: interquartile range;

IS: internal standard;

IV: intervening sequence;

LD: linkage disequilibrium;

LOD: limit of detection;

LOQ: limit of quantification;

LPI: labile plasma iron;

MAF: minimum allele frequency;

MEC: minimum effective concentration;

MRI: magnetic resonance imaging;

MRP: multidrug resistance-associated protein;

MTC: maximum tolerated concentration;

NBF: nucleotide ATP binding folds;

NTBI: non-transferrin bound iron;

ObsHET: observed heterozygous;

PCR: polymerase chain reaction;

PredHET: predicted heterozygous;

PTH: parathyroid hormone;

QC: quality control;

RXR: retinoid X receptor;

SNP: single nucleotide polymorphisms;

SQUID: superconducting quantum interference device;

STD: calibration standard

$t_{1/2}$: half-life;

TDM: therapeutic drug monitoring;

Tm: melting temperature;

UGT: UDP-glucuronosyltransferase;

UPLC: ultra performance liquid chromatography;

UV: ultraviolet;

Vd: volume of distribution;

VDBP: vitamin D binding protein;

VDIR: vitamin D receptor -interacting repressor;

VDR: vitamin D receptor;

VDRE: vitamin D response element.

ABSTRACT

Cardiac and hepatic iron burden is one of the leading cause of morbidity and mortality in β-thalassaemia major patients, thus monitoring and treating this ion overload is crucial in transfusion-dependent thalassaemia patients. The oral agent deferasirox (DFX) showed an important variability in drug pharmacokinetics. Based on Chirnomas *et al.* (2009) responders/non responders definitions, we introduced an efficacy DFX Ctrough cut-off (20 µg/mL), negatively predicted by *CYP1A1* -27+606 and *CYP1A2* 1548 polymorphisms. Moreover, we proposed efficacy (360 µg/mL/h) and non-response (250 µg/mL/h) AUC thresholds. *UGT1A3* -66 and *ABCG2* 1194+928 variants resulted efficacy predictors.

Different studies on β-thalassaemia major showed extremely low vitamin D levels in these patients. We here reported the influence of *CYP24A1* (encoding the hydroxylase metabolizing the vitamin) 22776, 3999 and 8620 variants on DFX pharmacokinetics. Furthermore, *VDR* (vitamin D receptor) Cdx2 and *GC* (encoding the vitamin D binding protein) 1296 variants were retained in regression analysis as AUC efficacy cut-off negative predictors.

Eventually, we investigated if polymorphisms within *VDR*, *CYP24A1*, *CYP27B1*, *GC* and DFX metabolism and transport related genes could influence cardiac and hepatic T2* values and liver stiffness.

Considering liver parameters, *UGT1A1* -364 and *CYP27B1* (encoding the hydroxylase activating the vitamin) -1260 showed a predictive role on T2* and stiffness cut-offs, respectively. In addition *UGT1A1* -364 and *VDR* TaqI and BsmI, *GC* 1269 and *CYP27B1* -1260 polymorphisms influenced liver stiffness values.
Evaluating cardiac iron accumulation, the influence of *CYP1A1* +1189, *ABCG2* 421, *UGT1A1* -364, *UGT1A3* -751, *CYP24A1* 8620 and *VDR* TaqI variants has been observed.

This work has been performed in the Laboratory of Clinical Pharmacology and Pharmacogenetics (Department of Medical Sciences) in collaboration with Centre for Microcitemie (S. Luigi Gonzaga Hospital) and Clinical Pharmacology Service "Franco Ghezzo" (Department of Biological and Clinical Sciences).

To our knowledge, this is the first study aimed at evaluating the role of DFX and vitamin D pharmacogenetics on cardiac and hepatic T2* magnetic resonance and on liver stiffness. However, we have not compared the achieved results to that obtained with liver biopsy and our analyses lack of the evaluation of vitamin D serum levels quantification.

This research discoveries may be useful for personalizing medicine and the proposed method could be applied in patients with hereditary hemochromatosis and myelodysplastic syndromes.

INTRODUCTION

1. Beta-thalassaemia

Beta-thalassaemia results from a deficient or absent synthesis of beta-globin chains (Figure 1), leading to reduced haemoglobin, decreased red blood cells production and anaemia. It is caused by mutations in *beta-globin* gene (chromosome 11) able to affect the gene expression by a variety of mechanisms [1-3]. Roughly 200 different gene mutations, and related disorders, have been described. Nevertheless the most *beta-globin* gene mutations are substitutions, deletions or insertions involving a single or few nucleotides; large deletions of the entire or multiple genes have been reported [1].

Beta-thalassaemias are a group of disorders inherited in an autosomal recessive manner. The disease is usually suspected in children, younger than two years of age, with severe microcytic anaemia, mild jaundice and hepatosplenomegaly [2].

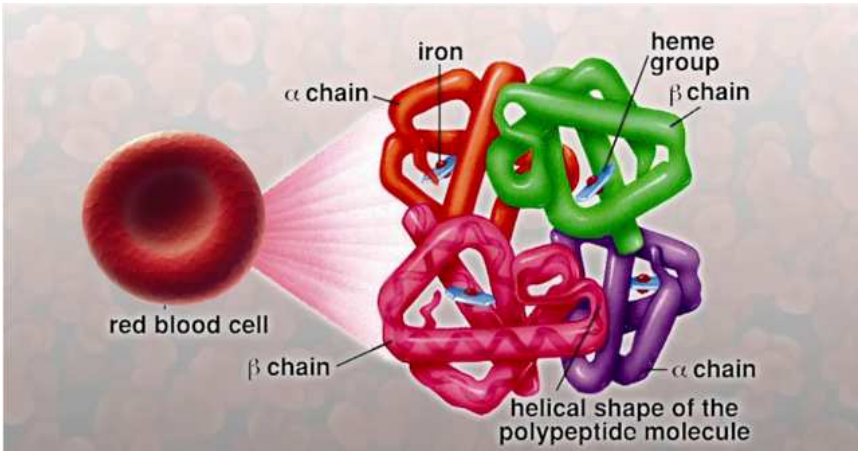

Figure 1 Haemoglobin Structure 1997 [3].

1.1 Classification of beta-thalassaemia

Beta-thalassaemia includes three main forms (Table 1):

- Thalassaemia Major;
- Thalassaemia Intermedia;
- Thalassaemia Minor.

Cause	Clinical nomenclature	Genotype	Disease
Severe gene mutations	***Major***	β°/β°	Severe: red blood cells transfusions
		β°/β+	
		β+/β+	
Two mutations	***Intermedia***	β°/β	Severe
		β+/β+	
Minor point mutation	***Minor***	β/β°	Asymptomatic
		β/β+	

Table 1 The classification of beta-thalassaemia.

1.1.1 *Beta-Thalassaemia Major*

Variably referred to as "Cooley's Anaemia" and "Mediterranean Anaemia", is the most severe form of beta-thalassaemia because both mutations of both *beta-globin* alleles result in severely impaired chain production. Three allele combinations are responsible for this phenotype: β°/β°, β°/β+ and β+/β+ (Table 1) [4]. In these patients, the excess unpaired alpha-globin chains aggregate and form inclusion bodies, which damage red blood cells membranes, leading to intravascular hemolysis. Moreover, damaged red blood cells and the destruction of premature erythrocytes precursors are the cause of an ineffective erythropoies [5]. For these reasons, a regular transfusion program, to maintain a minimum haemoglobin concentration of 9.5 to 10.5 g/dL is needed for patients' survival.

1.1.2 *Beta-Thalassaemia Intermedia*

It comprehends a clinically and genetically heterogeneous group of disorders, which clinical severity varies widely between patients and over time [6]. It presents later in life and can be

characterized by poor growth and bone abnormalities. Two allele combinations are responsible for this phenotype: β°/β and β+/β+ (Table 1) [7].

1.1.3 Beta-Thalassaemia Minor

It is also called "beta-thalassaemia carrier", "beta-thalassaemia trait" or "heterozygous beta-thalassaemia". This is the most common form of beta-thalassaemia and the affected individuals are asymptomatic [8]. Two allele combinations are responsible for this phenotype: β/β° and β/β+ (Table 1) [9].

1.2 Geographic distribution of beta-globin gene mutation

The mutation of the intervening sequences (IVs) and three exons of *beta-globin* gene differ in frequency geographically. Globally, the region IVs-I is the most susceptible to mutations followed by exon 1 and exon 2, IVs-II is less frequent and exon 3 is the least common [10]. Table 2 sums up the common beta-thalassaemia mutations in the world [11].

Regions	Types	Mutation	Remarks
Southeast Asia	ß0	CD41/42–TTCT	Chinese, SE Asians
		CD17, A→T	Chinese, SE Asians
		CD43, G →T	Chinese, Thai
		IVS2–654, C→T	Chinese, SE Asians
		CD71/72, +A	Chinese, Thai
		CD27/28, +C	Chinese, Thai
		CD14/15, +G	Chinese
		IVS1-5, G→C	SE Asians
	ß+	–28, A→G	Chinese, SE Asians
		CAP +40 to +43	Chinese
		–29, A→G	Chinese
		IVS1-I, G→T	SE Asian, Chinese
		–32, C→A	Taiwanese
		–30, T→C	Chinese
Indian subcontinent	ß0	IVS1-5, G→C	India, Pakistan, Bangladesh, Sri Lanka, Mauritius
		IVS1-I, G→A	Sri Lanka
		IVS1-I, G→T	India

		CD47/48, +ATCT	India
		619 bp deletion	India, Pakistan
		Codon 41/42, –TCCT	India
	ß+	Codon 8/9, +G	India, Bangladesh
		Codon 15, G→A	India
		Codon 8/9, +G	India, Pakistan
		–88, C→T	India
Middle East	ß0	Codon 36/37 –T	Iran
		IVS1-I	Iran, Iraq, Kurd, Syria
		IVS1-5	Iraq, Iran
		IVS2-I	Iran, Arab, Syria
		CD5, –CT	Syria
	ß+	IVS2-745	Iran
		IVS1-6	Syria, Iraq, Kurd, Arab
		IVS1-110	Syria, Iraq, Kurd, Arab
		Codon 8/9, +G	Iraq, Iran, Arab
African origin	ß0	CD39, C→T	Tusnia, Algeria, Morocco
		IVS1-I	Tusnia, Algeria, Morocco
		Codon 8, -AA	Morocco
	ß+	IVS1-6	Tusnia, Algeria, Morocco
		–29, A→G	Algeria, Morocco
Mediterranean	ß0	Codon 39	Mediterranean
		IVS1-I	Mediterranean
		–IVS-2-1	Mediterranean
	ß+	IVS-1-110	Mediterranean
		IVS-2-745	Mediterranean
		IVS-1-6	Mediterranean
		IVS-1-5	Mediterranean
		IVS-2-745	Mediterranean

Table 2 Geographical distribution of common beta-thalassaemia mutations [11].

2. Iron Overload

Thalassaemia major patients, as a consequence of repeated long-life red blood cells transfusions essential for survival, accumulate over time iron in the body. The iron burden in children occurs with growth retardation and lack or alteration of sexual development; in adult patients, it can lead to complications affecting heart (dilatation of the myocardium and arrhythmias), liver (fibrosis and cirrhosis) and/or endocrine glands (diabetes mellitus, hypogonadism and insufficiency of the parathyroid, thyroid, pituitary gland and, less commonly, of the adrenal glands). Furthermore, this condition may increase the risk of hypersplenism, chronic hepatitis (resulting from HBV and HCV infections), HIV infection, venous thrombosis and osteoporosis [2].

Iron is a transition metal with many functions in human body, including a role in oxygen transport and erythropoiesis. We take iron through food, partially excreted through the processes of dermal and gastrointestinal regeneration and, for women, through menstruation. Metal absorption disturbances or severe blood loss can cause iron deficiency, compromising important processes, such as erythropoiesis. However, if an excess of iron circulates, this accumulates in soft tissues such as liver, heart and other organs: this is the so-called "iron overload" [12].

It is called "primary iron overload" the spontaneous mutation of genes encoding proteins involved in iron homeostasis [13].

In thalassaemia patients, a so-called "secondary iron overload", can be observed as a consequence of the repeated transfusions. When additional iron is added to the body, there is an increase in the production of ferritin, a molecule found in liver, spleen, bone marrow and, in small quantities, in blood (serum ferritin); its goal is to deposit the iron excess in these tissues [13-15]. Moreover, iron is stored in hepatocytes and absorbed by the duodenal enterocytes (Table 3) [16].

To minimize the iron entry into cells, the body attempts to reduce the production of transferrin (the main protein transporting iron in blood (Table 3)) and its receptors [17]. However, when the iron increase, the system is overwhelmed: ferritin no longer store the ion, and saturated transferrin is no

longer able to bind it. As a consequence it settles in different organs, with toxic effects [18] (Figure 2).

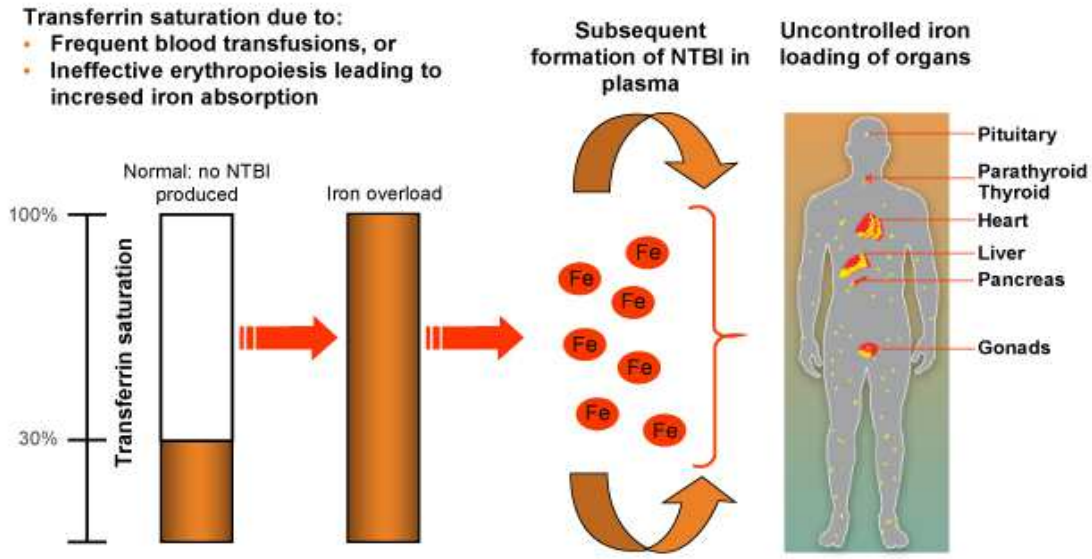

Figure 2 Consequences of transferrin saturation. NTBI: non-transferrin bound iron.

When an iron burden occurs, its physiological carrier is also saturated and a portion of free iron is formed, not bound to transferrin (NTBI: non-tranferrin-bound plasma iron) and into cell (LPI: labile plasma iron) (Table 3); NTBI and LPI are involved in redox reactions with the formation of highly reactive free radicals, responsible for cell and tissue damage, compromising different organs functionality and with negative impact on patient's survival. Since most of the iron excess accumulates in liver, the most common techniques measure the hepatic iron levels (LICs, liver iron concentrations). However, LIC correlation with the amount of cardiac hemosiderosis is poor (Table 4) [19-22].

Molecules	Amount	Properties
Transferrin	Trace amount	Transport of ferric iron If transferrin saturation > 45%, non–transferrin-bound iron forms If transferrin saturation > 75%, non–transferrin-bound iron/labile plasma iron forms, creating reactive radicals responsible for tissue damage
Ferritin	1–2 g in healthy subjects	Iron reservoir 4500 atoms Water soluble
Hemosiderin	0–1 g in healthy subjects	Similar to iron core of ferritin Results from ferritin degradation Not water soluble Forms clusters

Table 3 Molecule for transport or storage of iron.

2.1 Monitoring of serum ferritin

Serum ferritin should reflect the organic iron deposit levels. It is measured by a blood collection and it allows frequent monitoring. However, the results can be influenced by several factors, including infections and inflammations [23]. Table 4 shows the threshold values of the main parameters used for martial overload evaluation.

Parameter	**Normal Range**	**Iron Overload State**		
		Mild	**Moderate**	**Severe**
LIC (mg Fe/g dw)	<1.2	3-7	>7	>15
Serum Ferritin (ng/mL)	<300 (male) <200 (female)	>1000 to <2500		>2500

Table 4 Thresholds for the main parameters used to evaluate iron overload.

2.2 Liver biopsy

Biopsy is the most precise direct method for the assessment of hepatic hemosiderosis. It allows to evaluate:

- the quantitative determination of siderosis;
- the pattern of metal accumulation in hepatocytes and Kupffer cells;
- the evaluation of inflammation, fibrosis and any cirrhosis.

Hepatic siderosis is measured by cytochemical staining for iron (Perls method), according to the Scheuer gradation (grades I-IV). The pattern of martial overload at the level of hepatocytes, Kupffer cells (Figure 3), sinusoids and the main structures of portal spaces can also be evaluated [24].

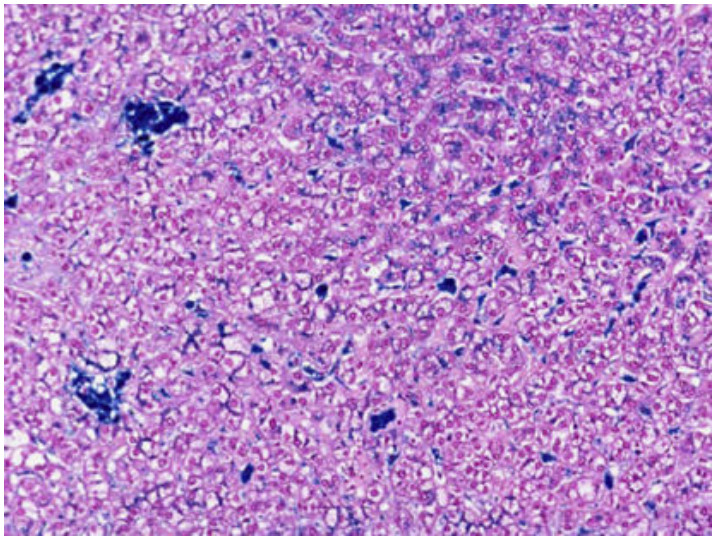

Figure 3 Macrophage (Kupffer cell) hemosiderosis secondary to transfusions [25].

2.3 Transient elastography

Many ultrasound elastographic approaches have been developed [26]. Transient elastography, performed using a FibroScan device (Figure 4), uses a low-frequency pulsed excitation able to generate shear waves in liver tissue. The shear waves velocity has been related to the tissue stiffness [27]. The comparison between the METAVIR classification (from F0, healthy liver state, to F4, the most severe stage of fibrosis [28]) and stiffness values, reported by the Fibroscan system, shows an excellent correlation [29]. The rate of successful measurements was calculated as the ratio between the number of those validated and total measurements [27]. The results were expressed as a median value of the total measurements in kPa. Values < 7.0 kPa are indicative for not significant fibrosis [30].

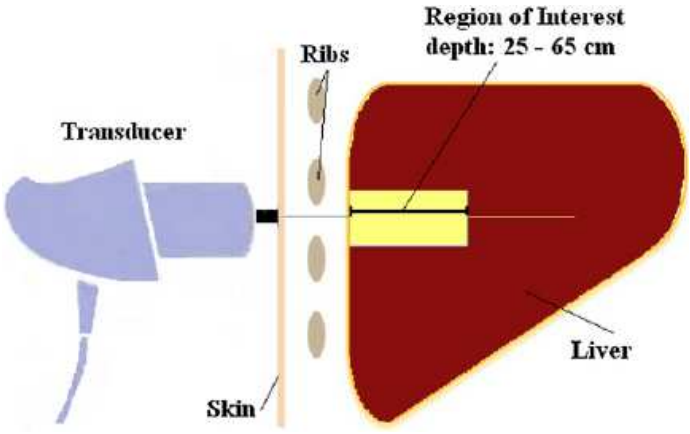

Figure 4 Schematic of a transient elastography system used for measuring liver stiffness [26].

2.4 Hepatic biomagnetic susceptibility by means of SQUID

The Superconducting Quantum Interference Device (SQUID, Figure 5) is based on the physical properties of ferritin and hemosiderin (pigment containing iron, consisting of ferritin molecules and other structural elements aggregates, which is found in liver, spleen and bone marrow) (Table 3). This non-invasive method provides a LIC value that can be completely overlapped with that obtained with liver biopsy, but does not allow the assessment of inflammation and fibrosis. SQUID determines iron concentration in liver and spleen [31].

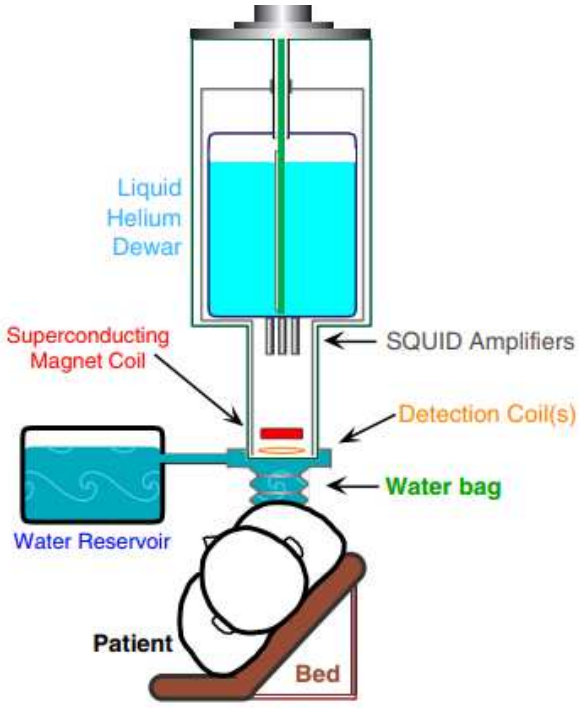

Figure 5 Schematic SQUID system

2.5 Magnetic Resonance Imaging

Magnetic Resonance Imaging (MRI) is a non-invasive technique based on nuclear magnetic resonance; to date, quantification of iron with MRI is considered the standard of care in diagnosis and monitoring of iron overload diseases [32]. It is extremely sensitive in assessing iron concentration and distribution throughout the body, therefore not only in liver, but also in other organs, including heart. Currently there are several MRI methods available [33].

T2* MRI imaging is accomplished using a breath-hold multiple echo gradient echo pulse sequence to acquire a series of images with increasing echo times. This sequences can be used in liver and heart. The value of T2* =20 ms corresponds to the lower limit of normality; lower is the T2* value and higher can be the risk for serious, and sometimes fatal, cardiac event in a short time [22, 34]. Considering liver, MRI T2* normal values are $\geq$ 6.3 ms [19].

3. Chelation therapy

In absence of physiological mechanisms to excrete exceeding iron, the administration of an iron-chelation therapy is necessary and this results in a negative net iron balance [35-37].

3.1 Goals of therapy

Chelation is a chemical reaction in which a metallic atom, acting as Lewis acid, is bound by a chelating reagent, through more than one coordinating bond. The structure of the resulting compound constitutes a very stable complex which sees the central atom surrounded by the chelator. The chelator is often a polydentate binder (specifically, bidentate, tridentate, etc.). Once chelated, the metal loses its characteristics and then it can be eliminated linked to the chelator (Figure 6).

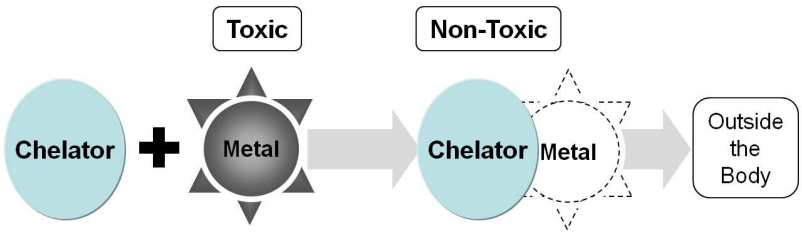

Figure 6 Metallic ion chelation sequence.

The goal of chelation therapy in beta-thalassaemia patients is to bind and remove iron from the body; it must also try to satisfy other important needs [38]:

- the elimination rate must be equal to or greater than iron input rate with the transfusion, so it is important that the therapy allows a flexible dosage;

- it must provide 24-hours chelation coverage, to avoid the iron accumulation and thus to prevent the adverse effects of its overload; this translates into the need of a molecule with a long half-life;

- the route and timing of administration (treatment regimen) must guarantee the maximum adherence to therapy;

- the number of days in which patients receive the chelation therapy is more important than the total dose taken during treatment; thus the exposure length of chelation therapy is crucial;

- the treatment-related adverse effects must be minimal.

3.2 Available drugs

The main drugs currently used in iron chelation therapy are deferoxamine, deferiprone and deferasirox (DFX).

Deferoxamine (Desferal®) (Figure 7) was the first commercial iron chelator, approved in 1970. It is a large hexadentated molecule with a short half-life (20-30 minutes), which binds iron with high affinity; Fe-deferoxamine complex is eliminated in urine and feces [39]. Deferoxamine intake requires a slow parenteral infusion of 8-12 hours, 5 to 7 times a week. This therapy regimen has a significant impact on adherence and a large number of patients do not get the full benefits from therapy and die early. Moreover, a 24-hours chelation coverage is not possible with the use of deferoxamine due to its short half-life [38]. The deferoxamine-iron chelate is charged and does not readily enter and leave cells. Eventually, this drug leads to many side effects, such as local reaction at the site of infusion, hypoacusia, ocular toxicity, retarded growth and skeletal changes [2, 40].

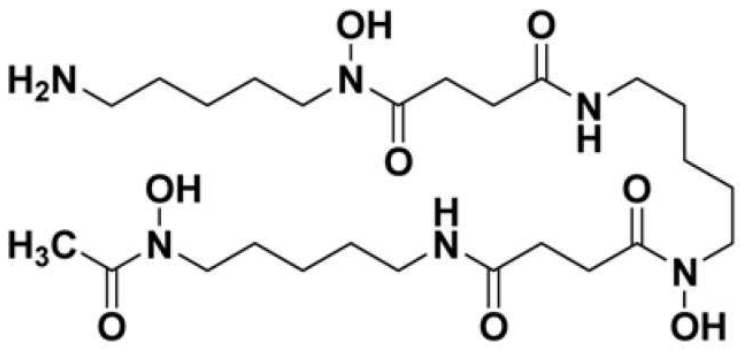

Figure 7 The chemical structure of deferoxamine.

The first oral chelator, deferiprone (Ferriprox®) (Figure 8) is a bidentate chelator (3 molecules bond an iron ion), approved in 1987; the Fe-deferiprone complex is not loaded and therefore can easily cross the membranes, allowing a rapid removal of the iron accumulation from cells [39]. It is taken orally 3 times a day and has a half-life of 3-4 hours; thus, as deferoxamine, it is not able to guarantee a 24-hours chelation coverage. Furthermore, treatment with deferiprone has been correlated with rare, but severe, agranulocytosis, mild neutropenia, abdominal discomfort and erosive arthritis [2, 41, 42].

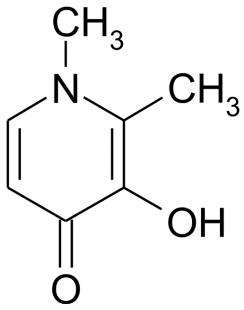

Figure 8 The chemical structure of deferiprone.

Combination therapy with deferiprone and deferoxamine has been investigated for the removal of cardiac iron and the normalization of its body stores [43].

The urgent need for an effective and safe once-daily orally administered iron chelator leads to the expedited approval of DFX [44, 45].

4. Deferasirox

For its clinical and pharmacokinetics properties, DFX was considered the most suitable to be an "ideal chelator" (Table 5) [39].

	"Ideal chelator"	Deferoxamine	Deferiprone	Deferasirox
Route of administration	Oral	Parenteral, usually subcutaneous or intravenous	Oral	Oral
Plasma half-life	Long enough to give constant protection from labile plasma iron	Short (minutes); requires constant delivery	Moderate (< 2 hours). Requires at least 3-times-per-day dosing	Long, 8-16 hours; remains in plasma at 24 h
Therapeutic index	High	High at moderate doses in iron-overloaded subjects	Idiosyncratic side effects are most important	Probably high in ironoverloaded subjects*
Molar iron chelating efficiency; charge of iron (III) complex	High, uncharged	High (hexadentate); charged	Low (bidentate); uncharged	Moderate (tridentate); uncharged
Important side effects	None or only in iron-depleted subjects	Auditory and retinal toxicity; effects on bones and growth; potential lung toxicity, all at high doses; local skin reactions at infusion sites	Rare but severe agranulocytosis; mild neutropenia; common abdominal discomfort; erosive arthritis	Abdominal discomfort; rash or mild diarrhea upon initiation of therapy; mild increased creatinine level
Ability to chelate intracellular cardiac and other tissue iron in humans	High	Probably lower than deferiprone and deferasirox	High in clinical and in vitro studies	Insufficient clinical data available; promising in laboratory studies

*Nephrotoxicity observed in non—iron-loaded animals has been minimal in iron-overloaded humans, but effectiveness is demonstrated only at higher end of tested doses, as discussed in Cappellini et al.[1]

Table 5 Comparison of available iron chelators to an ideal chelation drug [39].

4.1 Chemical structure

DFX (4- [3,5-bis (2-hydroxyphenyl) -1,2,4-triazol-1-yl] benzoic acid, 373 g / mol) is a tridentate iron chelator (Figure 9).

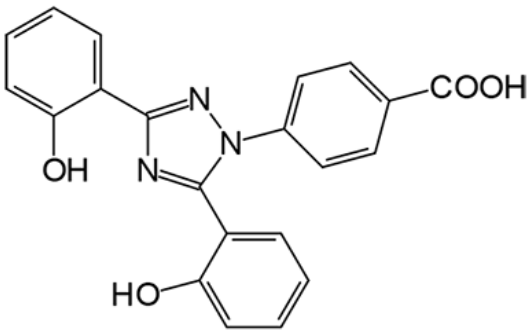

Figure 9 The chemical structure of DFX.

4.2 Mechanism of action and pharmacodynamics

DFX is composed of two molecules forming a stable complex with an iron ferric atom (Fe3+) (Figure 10). The lipophilic active molecule (ICL670) is highly bound to protein, above all albumin. It induces a mean net iron excretion per day of 0.119 mg Fe/Kg body (10 mg/Kg/day DFX dose), 0.329 mg Fe/Kg body (20 mg/Kg/day DFX dose) and 0.445 mg Fe/Kg body (40 mg/Kg/day DFX dose) mg Fe/Kg body, classified under the clinical relevant range (0.1-0.5 mg/Kg/day) [46].

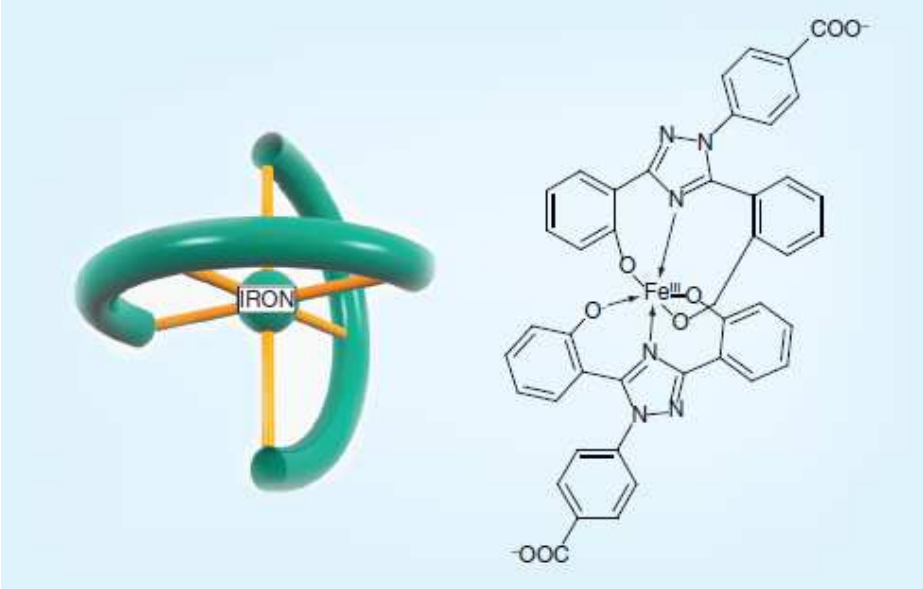

Figure 10 Two molecules of DFX (one depicted in black and the other in blue) form a soluble complex with one iron (Fe3+) ion (red) [47].

DFX chelating properties are:

- high and specific affinity for Fe3+;

- oral bioavailability, facilitating use in paediatric patients;

- high efficiency and effectiveness;

- long half-life (8-16 hours), which determines a chelating coverage of 24 hours, allowing a once-daily dosage;

- flexible therapeutic regimen;

- generally well tolerated.

DFX was approved as a first-line therapy for blood-transfusion-related iron overload by the Food and Drug Administration (FDA) in 2005 and the European Medicines Agency (EMA) in 2006. It is indicated in patients aged ≥ 2 years and with chronic iron overload due to transfusion-dependent or nontransfusion-dependent thalassaemia or anaemia. The EMA guidelines states that DFX treatment should only be initiated after the transfusion of ≥ 100 mL/kg of red blood cells (e.g. ≥20 units for an individual weighing 40 kg) or when serum ferritin levels are > 1000 µg/L [48].

The recommended initial daily dose is 20 mg/Kg, except for those with a higher iron burden (30/mg/Kg), taken on an empty stomach at least 30 minutes before food. To achieve therapeutic goals, dose adjustments in steps of 5-10 mg/Kg/day, up to 40 mg/Kg/day, can be made [47]. The tablet can be dissolved in water, orange juice or apple juice and any residue can be resuspended in a smaller volume of drink. DFX should be taken on an empty stomach, no less than 30 minutes before taking food [39].

4.2 Metabolism

DFX is mainly metabolized in liver (glucuronidation) and eliminated through hepatobiliary excretion in faeces [45, 49-52]. UDP-glucuronyltransferase 1A1 (UGT1A1) is the main UGT isoform responsible for DFX glucuronidation [44, 53-56]; *in vitro* studies showed the role of cytochrome-P450 (CYP) 1A1, 1A2 and to a lesser extent 2D6 enzymes (Figure 11) [49].

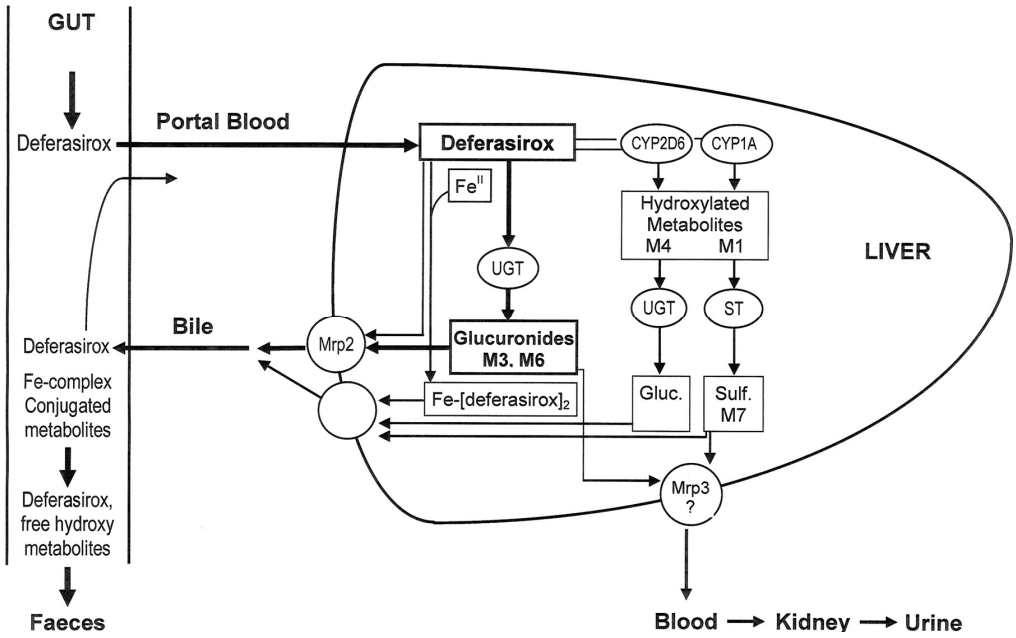

Figure 11 Proposed scheme DFX disposition in humans after oral administration [52]. ST, sulfotransferase; Gluc., glucuronic acid conjugate; Sulf., sulfate conjugate.

Particularly, UGT transforms DFX in M3 (acyl glucoronide) and M6 (2-O-glucoronide) metabolites; the 6% of the pro-drug is metabolized by CYPs to M1 (5-hydroxy DFX) and M4 (5'-hydroxy DFX), respectively (Figure 12) [52].

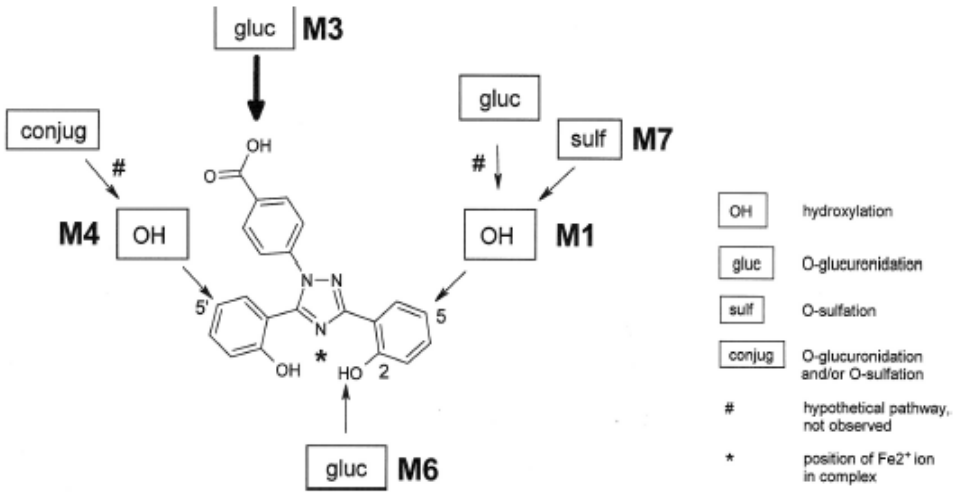

Figure 12 DFX metabolites [52].

DFX and metabolites are mostly excreted in bile through multidrug resistance protein 2 (MRP2, also known as ABCC2) [49]; breast cancer resistance protein (BCRP1, also known as ABCG2) may influence drug toxicity [53].

4.3 Efficacy

Chirnomas *et al*. defined as inadequate responders patients with a rising ferritin trend over 3 consecutive months, at least one higher than 1500 ng/mL, or a rising LIC, documented by biopsy or non invasively and on a dose of more than 30 mg/Kg per day of DFX; instead, adequate responders have a ferritin trend below 1000 ng/mL (evaluating the interval between the LIC at the beginning and at the end of the study) documented declining liver iron burden by MRI or biopsy and a dfx administration of 30 mg/Kg per day or less (Figure 13) [57].

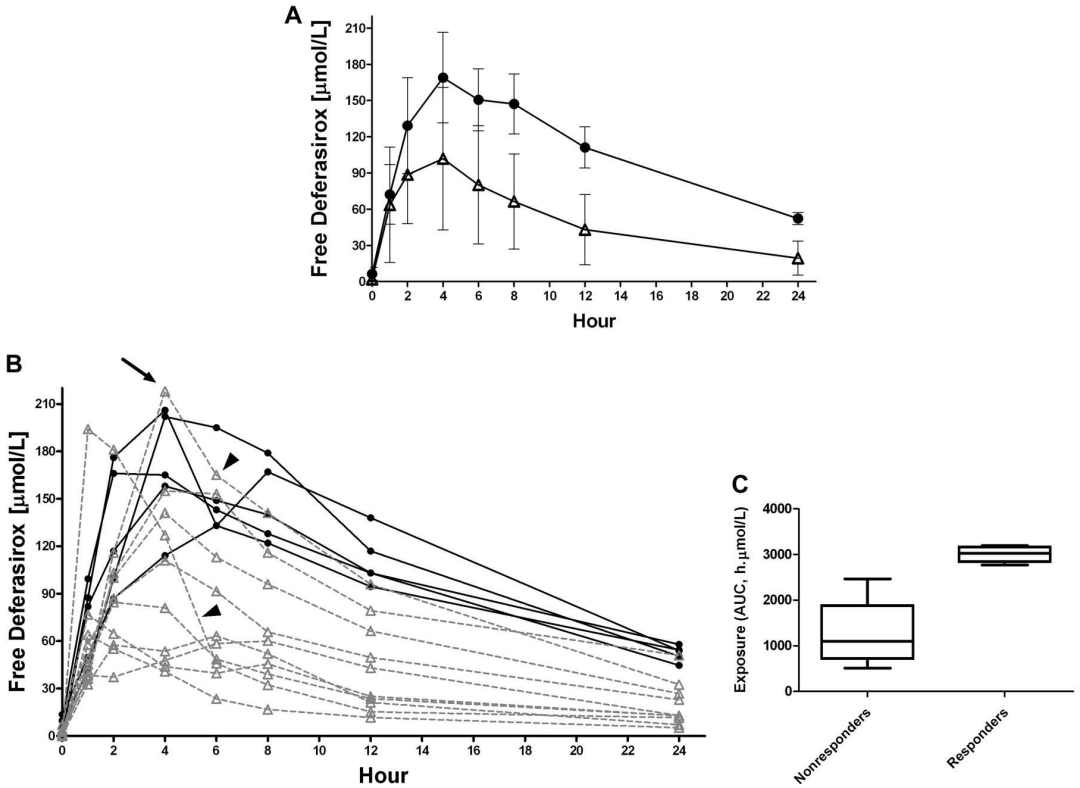

Figure 13 Pharmacokinetic assessments A. Mean DFX AUC 24hours. Error bars represent standard error. (Adequate responders [●]; inadequate responders [▵].)
B. AUC of free DFX. The actual average dose per kilogram was 34.7 plus or minus 1.12 mg (SD). (Adequate responders [●]; inadequate responders [▵]).
C. Box and whisker plots of DFX AUC in responders versus inadequate responders ($p < 0.001$). Box represents median interquartile range and whiskers are minimum to maximum range. Generated with the Mann-Whitney test [57].

Based on Chirnomas efficacy definition, we determined an efficacy DFX concentration at the end of dosing interval (Ctrough) threshold of 20,000 ng/mL and an area under the curve (AUC) concentrations efficacy (360 μg/mL/h) and non-response (250 μg/mL/h) cut-offs [58, 59].

4.4 Side effects

DFX is well tolerated by adults and children with different chronic anaemias. Phase II and III studies described and defined the clinical safety profile of DFX in patients of all ages, including patients younger than 2 years [60]. The most common adverse effects are gastro-intestinal disorders (diarrhoea, abdominal pain, nausea and vomiting) and rash (mild, moderate or severe). In one third of patients treated a non-progressive increase in serum creatinine values, proportional to the chelating dose, was observed, which resolves spontaneously and decreases with the reduction of drug dose. Recent studies also report cases of:

- cytopenia (agranulocytosis, neutropenia and thrombocytopenia);
- acute renal injury (also in paediatric patients);
- hepatic toxicity;
- adverse effects involving hearing and sight.

The length of treatment period does not seem to correlate with the increase in adverse effects [38].

5. Pharmacogenetics and pharmacokinetics

The use of several drugs has some limitations: among these, the most important is the choice of the optimal dose to obtain the best result with fewer side effects.

To solve these and many other respects, over the years the following scientific disciplines emerged: pharmacodynamics, pharmacokinetics and pharmacogenetics.

5. 1 Pharmacokinetics and pharmacodynamics

Pharmacokinetic is the study of absorption, distribution, metabolism and excretion (ADME system) of a drug. These parameters will influence drug concentrations in different compartments of the body. The pharmacodynamics is the study of biochemical and physiological drugs effects, as well as their mechanism of action. The kinetic and dynamic aspects are closely related to each other, since the proportion of the effect depends on drug concentration in the specific site of action (dose-effect relation).

The main pharmacokinetic parameters are reported below (Figure 14):

- **AUC** (Area Under the Curve): it is represented by the area under the plasma concentration curve over the time between one dose and the next one; it describes drug exposure.
- **Cmax** (Maximum Concentration): it is the highest concentration reached by the AUC, often used as a drug toxicity marker; its value has to be within the therapeutic range. The **Tmax** (Time to reach the maximum serum concentration) is the time at which Cmax is attained.
- **Cmin** (Minimum Concentration): it is minimum concentration reached by AUC; once reached steady-state (Figure 15), the state of equilibrium in which the amount of eliminated drug corresponds to the one introduced for each administration. It is important that Cmin value doesn't fall below the value of the minimum effective concentration (MEC).

- **Ctrough** (Trough Concentration): it is the plasma concentration of the drug immediately before the next dose. The values of Cmin and Ctrough may not be equal, but they are generally very close.
- **Vd** (Volume of distribution): it indicates the ability of diffusion and penetration of the drug in various organs and tissues.
- **MTC** (Maximum Tolerated Concentration): it is the maximum plasma concentration of the drug beyond which toxic side effects and/or non-tolerable toxicity occur.
- **MEC** (Minimum Effective Concentration): it indicates the plasma drug level below which therapeutic effects will not occur.
- $\mathbf{T_{1/2}}$ (half-life): it represents the time required to reduce plasma drug concentration by 50%.
- **Cl** (Clearance): it indicates the rate of drug elimination divided by its plasma concentration.

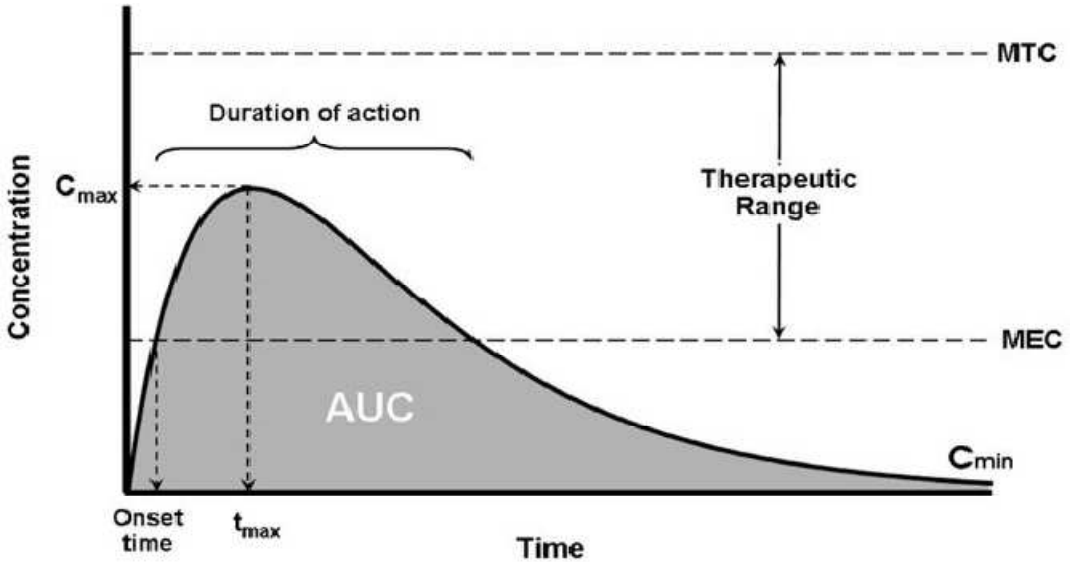

Figure 14: Area under the curve and pharmacokinetics parameters [61].

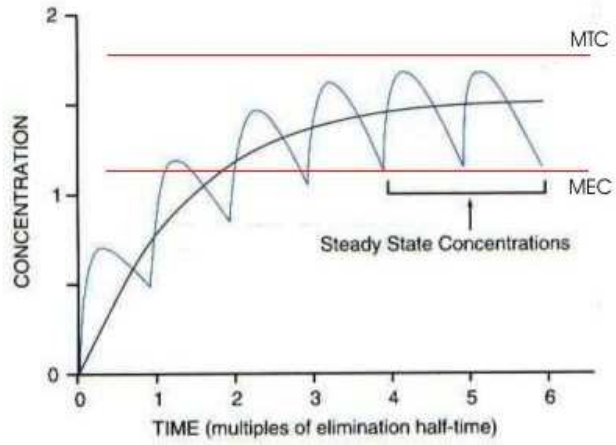

Figure 15 Schematic diagram of attaining steady state [62].

5.1.1 *Deferasirox pharmacokinetics*

DFX is rapidly adsorbed and distributed throughout the body with a Vd of 14.37±2.69 L in adults; the Tmax is 1-4 hours post-dose; Cmax and AUC linearly increase with dose after single administration and under steady-state condition (Figure 16) [47].

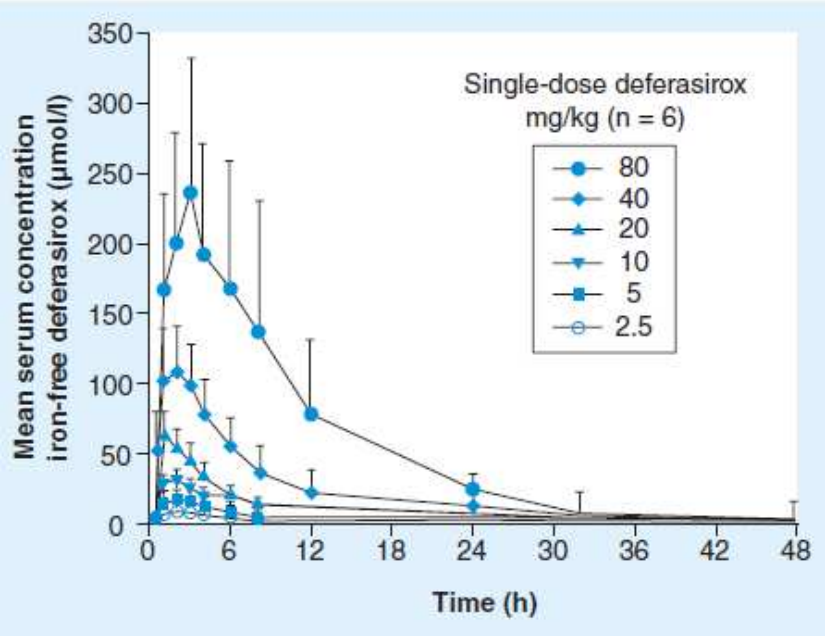

Figure 16 Mean plasma concentrations of DFX are proportional to dose [47, 63].

Mean plasma DFX Ctrough is about 25% of peak levels [64]. Its long $t_{1/2}$, 11-19 hours, leads to once daily oral regimen [65].

5. 2 *Pharmacogenetics*

The inter-individual variability in treatment response has always been one of the most relevant challenge in clinical practice. In some patients, with the same therapeutic strategy and compliance, can be observed reduced or even absent therapeutic effects, adverse reactions or adverse events.

In the past this inter-individual variability was mainly attributed to the influence of non-genetic factors: compliance, age, sex, nutritional status, renal and hepatic function, life habits, with particular reference to diet, alcohol and smoking abuse and other drugs concomitant use.

Now is well known that hereditary factors, in addition to those mentioned above, play a very important role in the individual response to drugs. Studies on monozygotic and dizygotic twins suggested that genetic factors are involved in determining pharmacokinetic variability [66, 67].

The pharmacogenetic studies the variability in drugs response on a hereditary basis. This approach is based on the identification of single nucleotide polymorphisms (SNPs) in genes involved ADME and transport of drugs, as well as on molecular targets of drugs themselves.

5.2.1 *Deferasirox pharmacogenetics*

- UDP-glucuronosyltransferase 1A

The *UGT1A* gene cluster encodes the set of enzymes, which are important components of the glucuronidation pathway, necessary for the conversion of lipophilic to water soluble molecules for excretion; UGT1A gene products contribute to the regulation of bilirubin clearance/ excretion [68].

Chirnomas *et al*. performed a pharmacogenetic study on fifteen patients (adults and paediatrics) who had transfusional iron overload and on DFX for at least 6 months at some point in their chelation history. They analyzed selected *UGT1A1* and *UGT1A3* gene polymorphisms, without finding statistically significant correlations between pharmacokinetics and pharmacogenetics [57].

In 2013, Lee *et al*., in paediatric patients (mean age 9 years), showed a correlation between the *UGT1A1**6 and the increase in creatinine, in those with a body weight lower than 40 kg [56].

In an our study on adult beta-thalassaemic patients, *UGT1A3* -66 GG genotype showed a significant correlation with higher AUC concentrations, Cmax, Tmax and lower Vd compared to AA/AG group; moreover carriers of G allele had higher values of $t_{1/2}$. CT and TT patients of *UGT1A3* -751 showed lower drug AUC concentrations, $t_{1/2}$, Cmax and higher Tmax and Vd than CC ones [59, 69]. *UGT1A3* -66 A>G, in linkage disequilibrium (LD) with -751 T>C, is the mayor determinant of *UGT1A3* haplotypes that impact the expression of the gene and the pharmacokinetics/ pharmacodynamics of atorvastatin [70, 71]. Study on anti-HIV drugs ritonavir and atazanavir showed hyperbilirubinemia associated with -66 GG genotype [72]. This is in line with higher DFX AUC concentrations showed in GG patients in our population; we supposed a reduced *UGT* expression, thus glucuronidation activity and excretion, for GG genotype. Moreover, it is confirmed by the reduced Vd. Considering treatment response, *UGT1A3* -66 GG genotype remained in the multivariate analysis as a response predictor considering AUC cut-offs, confirming the involvement of this SNP in the prediction of DFX therapy outcome [59, 69]. Evaluating -751 variant, T allele carriers showed lower DFX AUC concentrations and higher Vd, thus enhanced via UGT elimination. Related to *UGT1A1* -364 C>T (*UGT1A1*28*), CC genotype was associated with lower $t_{1/2}$ [59, 69]. This SNP is located in the promoter region of the gene, 310 bp away from the $(TA)_n$ repeat. It was shown that this variant results in a reduction in enzyme activity of up to 70% [73-75]. Moreover, it has been related to serum bilirubin in adults in many populations [76-78]. Bilirubin comparison showed minor alleles of the $(TA)_n$ repeat; -364 and 5226 SNPs were associated with higher bilirubin levels [79]. Zhou *et al*. proposed the protective effect of this polymorphism, attributed to its strong LD with $(TA)_n$ repeat [79]. Moreover, we observed a relationship of -364 variant and DFX plasma Ctrough: CC and CT genotypes showed lower concentration than TT one [80].

Moreover, we performed a study on paediatric beta-thalassaemia major patients, and we observed reduced ferritin and gamma glutamyl transferase levels in -66 GG and -751 CC carriers, respectively [81].

- Cytochrome P450 enzyme

The oxidative metabolism of many drugs is mediated by CYP enzymes family, composed of numerous isoforms involved in phase I metabolism. Each isoform is characterized by a different specificity. In humans, 57 CYPs were identified, which can be subdivided into 18 families and 42 sub-families, based on the identity percentage of amino acid sequences. Polymorphisms of genes encoding for CYP, can lead to altered enzymes activity: slow metabolizer (xenobiotic accumulation) or rapid metabolizer (rapid drug elimination) [82].

Bruin and colleagues reported the involvement of CYP1A1, CYP1A2 and CYP2D6 enzymes in DFX metabolism [49].

In an our study, patients with *CYP1A2* -9-154 AA genotype had lower DFX Ctrough compared to AC and CC ones [59]. Evaluating the effect of pharmacogenetic on DFX toxic effect in children, we found AA carrier association with higher creatinine levels, compared to AC/CC; conversely, AA patients showed lower LIC value. In regression model, CC genotype resulted as ferritin negative predictor factor and AC/CC group as LIC positive one [81]. *CYP1A2* -9-154 A>C polymorphism is located in the intron 1 of *CYP1A2* gene [83, 84] and it is related with reduced enzyme activity [85, 86]. Several papers reported the influence of this SNP on response and side effects of antipsychotic drugs use: the A allele leading to lower plasma drug concentration and higher risk for nonresponse; the C allele presence causes an increase of plasma exposure and risk for adverse effects [87-91]. Another *CYP1A2* variant selected by our group is the exonic 1548 C>T: it determines a synonymous substitution affecting mRNA stability [92]. In a population of beta-thalassaemic patients treted with DFX, CC and CT genotypes have been related to higher drug Ctrough compared to TT one [58].

The intron located *CYP1A1 C>A* -27+606 C>A polymorphism determines enhanced gene expression in presence of specific substrates (C allele) or in their absence (A allele) [93, 94]. This suggested a gain of function in AA carriers, confirmed in an our previous study: CC and CA genotypes had higher DFX Ctrough, compared to AA [58]. Evaluating paediatrics, we observed this SNP influence on Ctrough and $t_{1/2}$; in addition, CA/AA genotype group resulted as predictive factor of LIC [81]. Another variant located in intronic region of *CYP1A1* gene is the +1189 T>C, in which the C allele has been related to an increased enzyme activity [95-97]. In children we observe TC/CC influence on Tmax and on creatinine levels [81].

Eventually, both genotypes *CYP1A1* -27+606 AA and *CYP1A2* 1548 TT resulted able to predict drug concentrations below 20 µg/mL, the efficacy cut-off [58].

CYP2D6 1457 C>G gene polymorphism is considered a susceptibility factor to various diseases, including cancers, Parkinson's disease, Systemic Lupus erythematosus, nephropathy and ankylosing spondylitis [98]. *In vitro* studies showed that CYP2D6 is involved in DFX metabolism, but only to a lesser extent [49]. Interesting, we found a negative effect of CG/GG group on Cmax increase in paediatrics, probably due to an increased activity in mutant allele carrier [81].

- ATP-binding cassette

It is the largest family of transmembrane proteins that bind ATP and use the energy obtained to modulate the transport of various molecules in all cell membranes, characterized by ATP binding domains, known as "NBF folds" (Nucleotide ATP Binding folds). These pumps are primarily unidirectional. In eukaryotes, the majority of ABC proteins transport compounds from the cytoplasm to the extracellular side or in specific compartments (endoplasmic reticulum, mitochondria, peroxisomes) and work as transporters or "half transporters" forming homodimers or heterodimers. These genes are widely dispersed in the genome and are highly conserved between species. The human genome carries 49 ABC genes, arranged in seven subfamilies, designated A to G [99].

MRP2 (ABCC2) 1249 G>A nonsynonimous variant was associated with A allele minor enzyme function, resulting in reduced transport [100, 101]. We previously reported lower DFX Ctrough in GG genotype carrier in comparison with GA [58]. Also in paediatrics we observed a reduced DFX exposure (AUC) and larger Vd value in GG compared to GA [81]. Lee *et al*. reported hepatotoxicity elevation in association with *MRP2* haplotype [56].

The BCRP1 (ABCG2) transporter is expressed in gastrointestinal tract and liver and it is involved in absorption, distribution and excretion of a wide variety of drugs. Germ line polymorphisms in its gene have been described as affecting expression, cellular localization and substrate recognition of the encoded protein; more than 24 variations have been reported [102]. The missense SNP 421 G>A has been associated with different drugs pharmacokinetic [103-108]. In paediatrics treated with DFX, this SNP was retained in multivariate linear regression analysis as predictor factor of higher Tmax [81]. *BCRP1* 1194+928 T>C SNP is localized in chromosome 4; *C* allele has been associated with enhanced molecular response in chronic myelogenous leukemia patients, treated with imatinib; moreover, it may positively affect response [109, 110]. In adults we found a positive prediction of DFX therapy efficacy AUC cut-off value for CC genotype [59, 69]. Moreover, in paediatrics we observed borderline association with higher Vd and CC genotype [81].

5.3 Therapeutic Drug Monitoring

Up to now, the most frequently used approach to analyse the toxic effects or the inefficacy of pharmacological treatments was the change of treatment suspension, the change of treatment or the "*ad juvantibus*" change in drug dosage. Recently, the better knowledge of the pharmacokinetics/pharmacodynamics and pharmacogenetics properties of drugs allowed the use of this information in order to guide the dose adjustment during therapy.

In fact, since the concentration of the drug is rarely measurable in its site of activity, the Therapeutic Drug Monitoring (TDM) in plasma (or sometimes in blood) plays a crucial role. It is based on the determination of drug concentration in patients undergoing therapy, in order to monitor factors difficult to control, such as the "compliance" and/or drug-drug interaction. It is moreover useful for particular conditions such as pregnancy.

Although TDM is mainly performed on plasma samples, it can be carry out with different techniques, among which chromatography is considered the gold-standard. These technologies include liquid (such as High/Ultra Performance Liquid Chromatography, HPLC/UPLC) and gas chromatography using different detectors: ultraviolet (UV), potodiode array, fluorescence and mass spectrometers (standard, tandem quadrupole detector or time-offly).

TDM, together with pharmacogenetic testing, can be a powerful tool for treatment personalization and management. However, in order to correctly use TDM, several conditions are needed:

- Deep knowledge of pharmacokinetic properties, such as the dose-proportionality of drug concentrations, the drug $t_{1/2}$ and the Tmax;
- Deep knowledge of the pharmacodynamics properties, such as MEC and MTC, thus the therapeutic range;
- Adequate technology to support the quantitative determination of drugs concentrations in the biological matrix;
- Fully validated robust bioanalytical methods to quantify drugs.

5.3.1 *Deferasirox therapeutic drug monitoring*

It has been reported that some patients, particularly those with heavily iron loaded, do not achieve adequate chelation and a negative iron balance, even when receiving DFX doses exceeding 30 mg/kg/day (poor responders). Others may experience DFX related adverse events at the dose required to maintain the iron burden balance (intolerant patients). If adverse events are managed by decreasing the DFX dose or interrupting treatment, these patients will not be able to achieve adequate iron chelation and maintain a negative iron balance during their regular blood transfusions [57]. Therefore the inter-individual variability of drug exposure, investigated by TDM, can lead to potential inadequate chelation treatment or to a toxicity increase [55, 80], particularly considering plasma Ctrough [55, 58, 59, 69, 81, 111-115]. In addition, an inverse correlation between preadministration LPI and DFX Ctrough has been shown, sustaining the hypothesis that DFX concentrations could be related to treatment response [116].

5.4 Deferasirox plasma quantification

In recent years, numerous papers reported the use of high throughput bioanalytical procedures for the quantification of iron chelating drugs [49, 52, 57, 63, 117-120]. Some of them reporting the use of HPLC-UV methods [49, 57, 63, 117, 119], based on the methodology developed by Rouan *et al.* [120]. Moreover, also chromatographic methods based on mass spectrometry detection have been developed to quantify DFX [117, 118].

5.4.1 *High performance liquid chromatography system*

HPLC is an analytical chemistry technique used to separate different compounds in a mixture, identifying and quantifying each of them. It relies on pumps to erogate a precise pressurized liquid solvent flow containing the sample mixture, through a column filled with a solid matrix, functionalized with different chemical sorbents. Each component in the sample interacts slightly differently with the sorbent, causing different retention for each different compound and leading to the separation of the components as they flow out the column. During the run, the mobile phase can

always be identical or can change over time, subjecting the molecules to a gradient of solvents: when the mobile phase affinity to the stationary phase overcomes the molecules one, the molecule detaches from the matrix and elutes.

The use of autosamplers allowed to apply such techniques for the analysis of large batchs of samples, containing the analytical variability and making possible the use of calibration curves, running simultaneously with the samples.

HPLC system consists of a pumping unit, an autosampler, a column heater and a detector (Figure 17). The pumping unit delivers mobile phases flow with a limit pressure of 5800 – 7000 psi (400 – 500 bar).

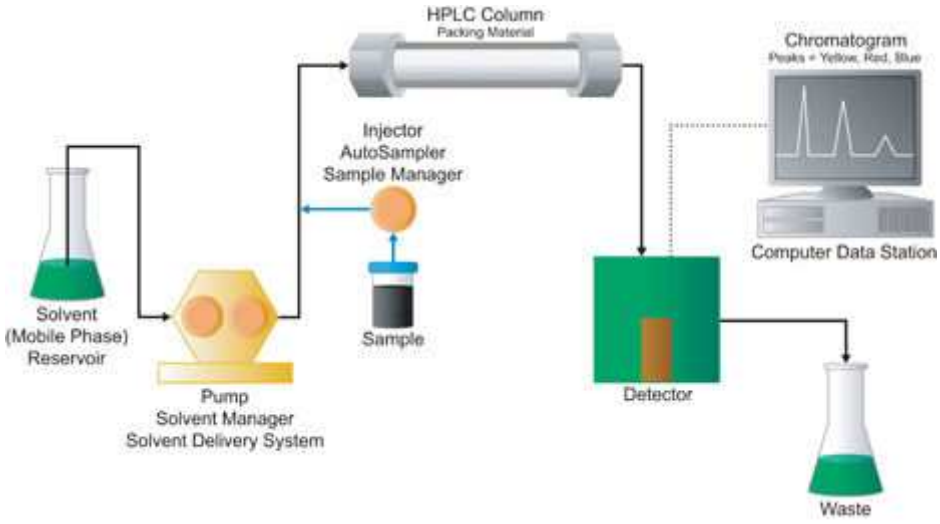

Figure 17 Schematic Diagram of HPLC system

5.4.2 High performance liquid chromatography system columns

The HPLC is based on the use of stationary phases consisting of particles with diameter of 3 to 5 μm: separation of the sample components requires a bonded phase that provides both retention and selectivity. Many bonded phases are available for HPLC separations; each column chemistry provides a different combination of hydrophobicity, silanol activity, hydrolytic stability and chemical interaction with analytes (Figure 18).

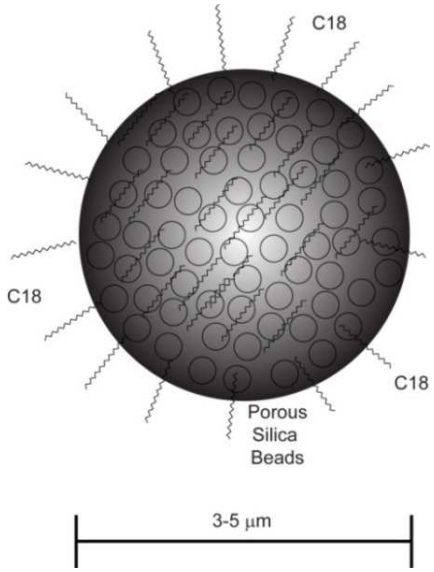

Figure 18 an example of C18 silica beads.

5.4.3 Sample preparation

Since most samples encountered in a laboratory are not in a form to be directly analysed by the chromatographic instrument, some preparations are required. The sample preparation could be as simple as "dilute and shoot" or as complex as multistage sample handling. Sample matrices can be broadly classified as organic, biological or inorganic, and may be further subdivided into solids, semi-solids, liquids, and gases. For liquids and suspensions, the main preparation techniques include: protein precipitation, solid phase extraction, liquid-liquid extraction, dilution, evaporation,

distillation, microdialysis, lyophilization, filtration, centrifugation, sedimentation, solid phase microextraction and stir bar sorbent extraction.

5.4.4 *Ultraviolet Detector*

A chromatographic detector has to be capable of establishing both the identity and concentration of eluting components in the mobile phase stream. A broad range of detectors is available to meet different sample requirements. The standard UV detector for HPLC measures the absorbance of monochromatic light of fixed wavelength in the UV or visible wavelength range (typically between 190 nm [UV] and 400 nm [blue light]) against a reference beam and relates the magnitude of the absorbance to the concentration of analyte in the eluent passing through a flow cell contained within the instrument. Molecules suitable for UV detection typically contain unsaturated bonds, aromatic groups, or functional groups containing heteroatoms, which contain nonbonding orbitals into which electrons are promoted to absorb the incident energy. These nonbonding orbitals contain a wide distribution of vibrational and rotational energy levels that lead to a distribution of absorbance energies and therefore spectra with broad, rather than sharp features.

6. VITAMIN D

Different studies on beta-thalassaemia major showed extremely low vitamin D levels in these patients [121-124]; the deficiency could be due to reduced intestinal absorption, subicteric tint and/or iron induced higher pigmentation, which interfere with vitamin skin synthesis, and to liver impairment and siderosis, leading to limited hepatic hydroxylation [121]. Napoli *et al.* suggested a possible role of iron burden in inducing vitamin D deficiency, suggested by a negative correlation between 25(OH)D3 and ferritin levels, higher in beta-thalassaemia subjects[123]. Considering cardiac function, has been demonstrated that R2* (R2* = 1000/T2*) and left ventricular fraction were associated with vitamin D deficiency. In addition, low vitamin levels has been linked to reduced heart function, myocytes weakness, glucose insensitivity and cardiac failure [125].

Vitamin D belongs to a hydrophobic secosteroids group, fundamental for one of the well known functions in different ions adsorption such as calcium, iron, magnesium, phosphate and zinc [126, 127]. As well as this function, vitamin D results to have many other roles [128, 129]:

- skeletal calcium balance by promoting calcium absorption and bone resorption by modulating osteoclasts activity;
- involvement in cell proliferation and differentiation both in adults and fetal stage;
- regulation of the immune response.

In liver, vitamin D is hydroxylated at C-25 by CYP2R1, CYP2D11 and CYP2D25, with the formation of 25-hydroxyvitamin D3 (25(OH)D3, calcitriol) [130]. 25(OH)D3 is transported by the vitamin D binding protein (VDBP, encoded by *GC* gene) to kidney, where magalin, a member of the low-density lipoprotein receptor superfamily, allows the endocytic internalization of the vitamin [131]. In the proximal renal tubule, calcitriol is hydroxylated in C-1 of the A ring, resulting in the hormonally active form of vitamin D, 1,25-dihydroxyvitamin D3 (1,25(OH)2D3)[130]. The CYP27B1, which metabolizes 25(OH)D3 to 1,25(OH)2D3, is expressed predominantly in kidney, but also in placenta, monocytes and macrophages [130, 132-135]. The CYP24A1 is the

multicatalytic CYP responsible for the catabolism of vitamin D via the C23- and C24-oxidation pathways. The metabolic degradation of vitamin D, catalyzed by CYP24A1, involves sequential oxidations of the C20-C26 side chain, leading to the formation of excretory products [136]. The enzyme is expressed in many, but not all, target cells containing the vitamin D receptor (VDR), including kidney, bone and intestine, and it is strongly inducible by VDR agonists in such tissues [137, 138]. The VDR, a trans-acting transcriptional regulatory factor, binds active form of vitamin D and it modulates many immune, endocrinal and neural activities [139-142]. VDR exerts its classical genomic action through the formation of a heterodimer with the retinoid-X receptor (RXR). This complex interacts with vitamin D response elements (VDREs) on gene promoter region and enhances genes transcription; microarray analyses with different human cells reveal that more than 100 genes have VDREs in their promoter regions (Figure 19) [143-145].

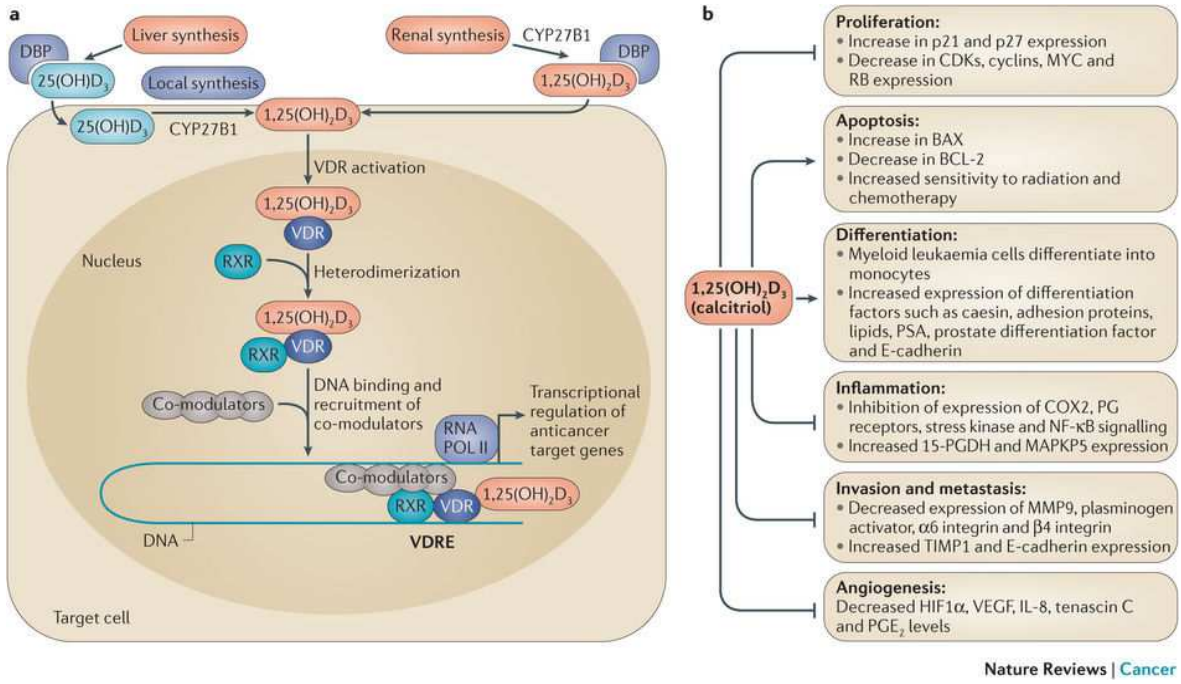

Figure 19 Genomic mechanism of calcitriol action through the VDR [146].

Whereas, if VDR-RXR complex binds the VDR-interacting repressor (VDIR), *CYP27B1* and *PTH* (parathyroid hormone) genes transcription is repressed [147]. VDR is also located in caveolae-enriched plasma membranes, where it binds vitamin D and exerts a rapid, non genomic thus

transcription independent, response through second messengers production; this results in the activation of many physiological pathways (Figure 20) [148-150].

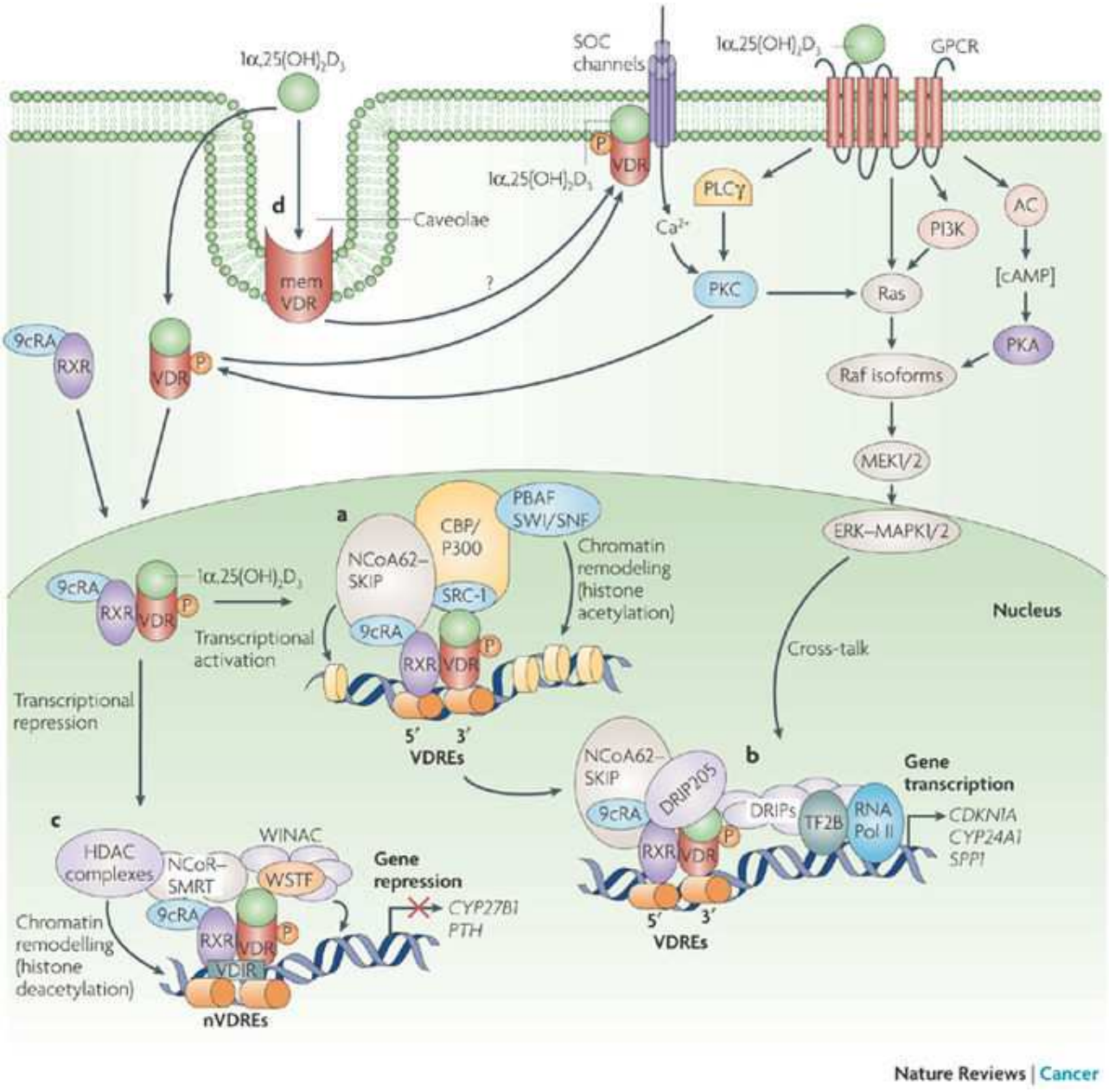

Figure 20 Non-genomic, rapid actions of 1α,25(OH)2D3, involving cytosolic VDR and membrane VDR (memVDR), also found in caveolae [151].

GOALS OF THE STUDY

As previously mentioned, DFX is the first once-daily oral chelator for iron overload treatment in beta-thalassaemia major. However, a high inter-individual variability in DFX exposure may occur, leading to inadequate chelation treatment or to toxicity increase.

Since it has been demonstrated the correlation between iron burden and vitamin D deficiency [121-124] and among DFX pharmacokinetics and treatment outcome and pharmacogenetics [55, 58, 59, 69, 81, 112-115, 152, 153], our goal was to retrospectively evaluate the role of SNPs in genes encoding for proteins involved in DFX metabolism (*UGT1A1*, *UGT1A3*, *CYP1A1*, *CYP1A2*, *CYP2D6*, *MRP2*, *BCRP* genes) and transport and in vitamin D pathway (*CYP24A1*, *CYP27B1*, *GC* and *VDR* genes) on DFX treatment personalization.

Overall, in this work three main points were analyzed:

1. Role of deferasrirox and vitamin D pharmacogenetics on drug pharmacokinetics and clinical outcomes [152];
2. Role of deferasrirox and vitamin D pharmacogenetics on the evaluation of cardiac iron overload;
3. Role of deferasrirox and vitamin D pharmacogenetics on liver iron accumulation.

MATERIALS AND METHODS

1. Patients and inclusion criteria

We carried out a monocentric study in patients with beta-thalassaemia major, treated at the Haemoglobinopathies Centre of San Luigi University Gonzaga Hospital in Orbassano (Turin, Italy) between September 2011 and December 2015.

Inclusion criteria were:

- beta-thalassaemia with transfusional iron overload;
- at least 18 years of age;
- DFX treatment for at least 6 months;
- self-reported adherence of 90%;
- no concomitant administration of drugs with known interactions;
- no co-morbidities;
- no vitamin D consumption;
- no renal dysfunction.

Study protocol ("Studio dei determinanti farmacogenetici nella farmacocinetica e nella risposta clinica del deferasirox", registration number 79/2012) was approved by the local Ethics Committee. A written informed consent for the study was obtained from each subject. The study was performed in accordance with the Helsinki Declaration of 1975.

Data available for all the enrolled patients were:

-sex;
- age;
- weight;
- height;
- ethnicity;
- ferritin serum levels;
- DFX dose;
- cardiac T2* value;
- hepatic T2* value;
- liver stiffness value.

2. Clinical End-point

Based on Chirnomas *et al.* adequate/inadequate responders definitions [57], we proposed an efficacy DFX Ctrough cutoff (20 µg/mL) [58]. Moreover, we defined efficacy (360 µg/mL/h) and non-response (250 µg/mL/h) AUC cutoffs [59, 69].

3. Pharmacokinetic analysis

Pharmacokinetic analysis was performed in the Laboratory of Clinical Pharmacology Service "Franco Ghezzo" (Department of Biological and Clinical Sciences, University of Turin).

3.1 Chemicals, reagents and plasma

Acetonitrile HPLC grade, methanol HPLC grade and triethylamine were purchased from VWR International (Milan, Italy). HPLC grade water was produced with Milli DI system coupled with a Synergy 185 system by Millipore (Milan, Italy). DFX and imatinib, used as Internal Standard (IS), were kindly provided by Novartis Pharma AG (Basel, Switzerland). Blank plasma from healthy donors was kindly supplied by the Blood Bank of San Luigi Hospital (Orbassano, Italy). All powders were stored at -20°C in the dark, to prevent any possible degradation.

3.2 Biological samples and timing of collection

Plasma DFX concentrations were determined from samples obtained before (Ctrough) and after 2, 4, 6 and 24 hours drug administration. The AUC over 24 hours values were defined using the mixed log-linear rule (Kinetica software, Waltham, Massachusetts, USA).

Each blood sample (in lithium-heparin tube, 5 mL) was centrifuged at 50 rounds/sec (Hz) for 10 minutes at 4°C within 30 minutes and plasma was stored at -20°C before the experiments.

3.3 Stock solutions, calibration standards and quality controls

Stock solution of DFX was prepared by dissolving an accurately weighed amount of drug in ethanol to obtain a final concentration of 1 mg/mL, then stored at −20 °C till analysis. IS stock solution was

prepared by dissolving an accurately weighed amount of drug in methanol to obtain a final concentration of 1 mg/mL, then stored at −20 °C till analysis, stable up to 3 months [24]. The highest calibration standard (STD10: 40 µg/mL) and 3 quality controls (QCs), QChigh (20 µg/ml), QCmedium (5 µg/mL) and QClow (0.3125 µg/mL) were prepared adding a determined volume of stock solution to blank plasma. Others STDs were prepared by serial dilution from STD10 to the lowest calibration standard (STD1: 0.078125 µg/mL) with blank plasma, to obtain 10 different spiked concentrations. A blank sample plus IS (STD0) was also included. Calibration range, from STD10 to STD1, and QCs concentrations are listed in Table 6 [55].

Concentrations (µg/ml)												
STD_1	**STD_2**	**STD_3**	**STD_4**	**STD_5**	**STD_6**	**STD_7**	**STD_8**	**STD_9**	**STD_{10}**	**QC_l**	**QC_m**	**QC_h**
0.078125	0.15625	0.3125	0.625	1.25	2.5	5	10	20	40	0.3125	5	20

Table 6 Calibrations standards from STD1 to STD10 and quality controls (low, medium, high) concentrations [55].

3.4 Sample preparation

The extraction procedure was based on protein precipitation (Figure 21): 100 µL of IS working solution, made at the final concentration of 100 µg/mL in methanol and used immediately, was added to 500 µL of plasma sample. Then 750 µL of protein precipitation solution (methanol:acetonitrile 50:50, v/v) was added to each sample. After brief mixing (30 s), samples were centrifuged at 12,000 rpm for 15 min and 800 µL of the obtained supernatant were transferred to vials, for injection in column (20 µL). All procedures (stock solutions, STDs and QCs preparation and extraction steps) were carried out at room temperature.

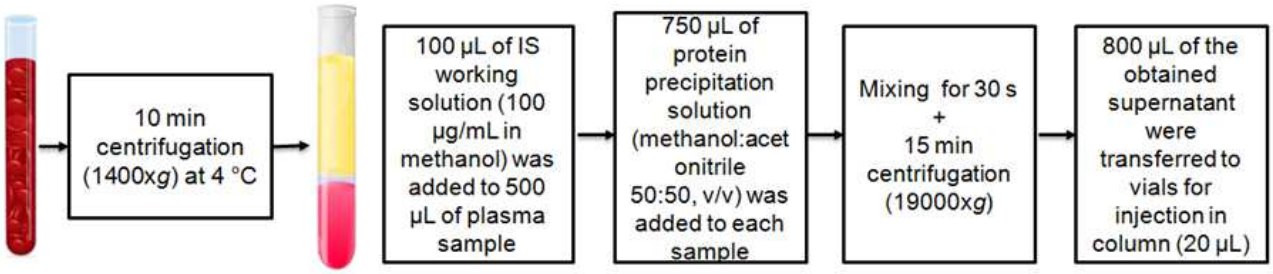

Figure 21 Protein precipitation workflow.

3.5 Chromatographic system and conditions

The described method has been validated following FDA procedures [55]. HPLC was performed with a VWR Hitachi system (LaChrom Elite) equipped with autosampler, spectrophotometer, and heated column compartment (Figure 22).

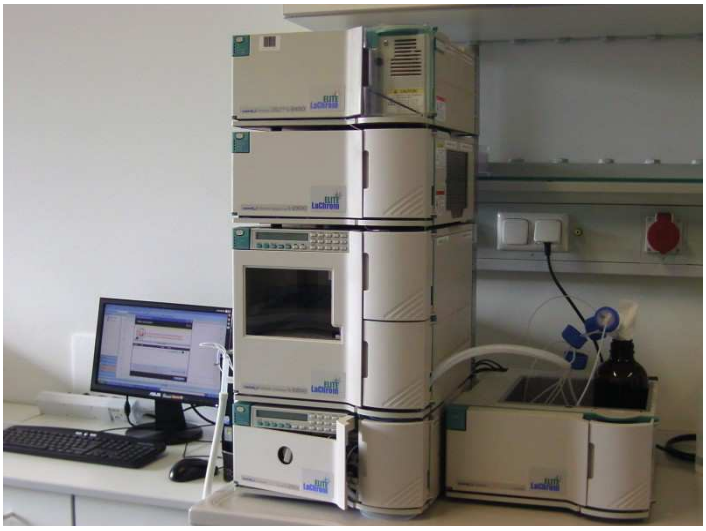

Figure 22 VWR Hitachi system (LaChrom Elite).

Separation was achieved with GraceSmart© RP18 column, 5 µ, 250 mm × 4.6 mm (Grace, Milan, Italy), preceded by a Security Guard Cartridge C18 4 mm × 3 mm (Phenomenex, Milan, Italy). Mobile phase consisted of:

- 40% solvent A (water (72.5%) methanol (25%) and triethylamine (2.5%), adjusted for pH 9.3 byorthophosphoric acid);
- 20% methanol;
- 40% acetonitrile.

Analysis was carried out at the constant flow rate of 1 mL/min at 25 °C in isocratic condition. The eluate was monitored at 295 nm. Total runtime was 8 min.

Parameters for method validation:

- Linearity: calibration curves were linear over the concentrations range selected for validation, with a mean regression coefficient (r2) of 0.99;
- Variability and accuracy: all observed data had a relative standard deviation (RSD) below 15% (Table 6);
- Recovery, limit of detection (LOD) and limit of quantification (LOQ): final extraction recovery value for DFX was obtained as mean from 9 ratios (Table 6). The LOD was defined as 0.078125 g/mL, while LOQ was set at calibration stanard 2 (0.15625 g/mL). Accuracy for LOQ was 11.55%, intra and inter day variability was 3.98 and 19.85% (Table 7);
- Selectivity and stability: no signal increase due to endogenous plasma substances was observed at the retention time of DFX and IS. Analyses of freeze and thaw, short-term and long-term stability were all within 15% of nominal concentration;
- Carry-over: no signal increase due to carry over of substances was observed at the retention time of DFX and IS.

QC_{low} 0.3125 μg/ml				QC_{medium} 5 μg/ml				QC_{high} 20 μg/ml			
Accuracy (%)	Variability (RSD%)[a]		Recovery (%)	Accuracy (%)	Variability (RSD%)		Recovery (%)	Accuracy (%)	Variability (RSD%)		Recovery (%)
	Intra-day	Inter-day			Intra-day	Inter-day			Intra-day	Inter-day	
5.77	7.77	12.42	87.12	2.29	2.95	3.75	90.31	5.55	3.96	6.23	97.56

[a] Relative standard deviation.

Table 7 Validation data [55].

4. Pharmacogenetic Analysis

This work was performed in the Laboratory of Clinical Pharmacology and Pharmacogenetics (Department of Medical Sciences, University of Turin).

4.1 Chemicals and reagents

QIAamp DNA minikit was purchased from Qiagen (Valencia, CA) for DNA extraction. TaqMan assay was used to allelic discrimination and all "Master Mix" and primers-probes were purchased from Applied Biosystems (Foster City, CA). Ultrapure water was produced by Milli-Di coupled to Synergy 185, Millipore (Milan, Italy).

4.2 Biological samples and timing of collection

Venous blood aliquots were obtained from patients who gave written informed consent according to standards of the local ethic committees and arrived in the laboratory in 3-7 mL tubes containing EDTA. Then, each sample was inactivate at 58 °C for 35 minutes and stored inside cryovials at -80 °C for pharmacogenetics analysis.

4.3 Analysed single nucleotide polymorphisms

Basing on results obtained from previously described studies focused on transporters, receptors and enzymes involved in the ADME and/or clinical effects of DFX-treated patients and vitamin D, the choice of which genetic polymorphisms to analyze are resumed in Table 8:

Gene	SNP name	rs	Alleles	Position
UGT1A1	*UGT1A1 -364*	rs887829	C>T	234668570
UGT1A3	*UGT1A1 -66*	rs3806596	A>G	234302446
UGT1A3	*UGT1A3 -751*	rs1983023	C>T	234301761
CYP1A1	*CYP1A1 -27+606*	rs2606345	C>A	75017176
CYP1A1	*CYP1A1*1189*	rs4646903	T>C	75011641
CYP1A2	*CYP1A2 -9-154*	rs762551	A>C	75041917
CYP1A2	*CYP1A2 1548*	rs2470890	C>T	75047426
CYP2D6	*CYP2D6 1457*	rs1135840	C>G	42522613
ABCC2	*ABCC2 1249*	rs2273697	G>A	101563815
ABCG2	*ABCG2 421*	rs2231142	G>A	89052323
ABCG2	*ABCG2 1194+928*	rs13120400	T>C	89033527
CYP27B1	*CYP27B1 2838*	rs4646536	C>T	58157988
CYP27B1	*CYP27B1 -1260*	rs10877012	G>T	58162085
CYP24A1	*CYP24A1 8620*	rs2585428	A>G	52786897
CYP24A1	*CYP24A122776*	rs927650	C>T	52772741
CYP24A1	*CYP24A1 3999*	rs2248359	T>C	52791518
VDR	ApaI	rs7975232	C>A	48238837
VDR	TaqI	rs731236	T>C	48238757
VDR	FokI	rs10735810	T>C	46559162
VDR	BsmI	rs1544410	G>A	48239835
VDR	Cdx2	rs11568820	A>G	48302545
GC	*GC 1296*	rs7041	T>G	71752617

Table 8 Analyzed SNPs characteristics: gene, variant name (SNP name), rs number, alleles and position.

4.4 DNA extraction

The "QIAamp DNA minikit" (Qiagen, Valencia, CA) was used for genomic DNA extraction, including mini-columns to purify a sufficient amount of DNA from 200 µL of treated patients blood.

Extraction protocol is reported as follow (Figure 23):

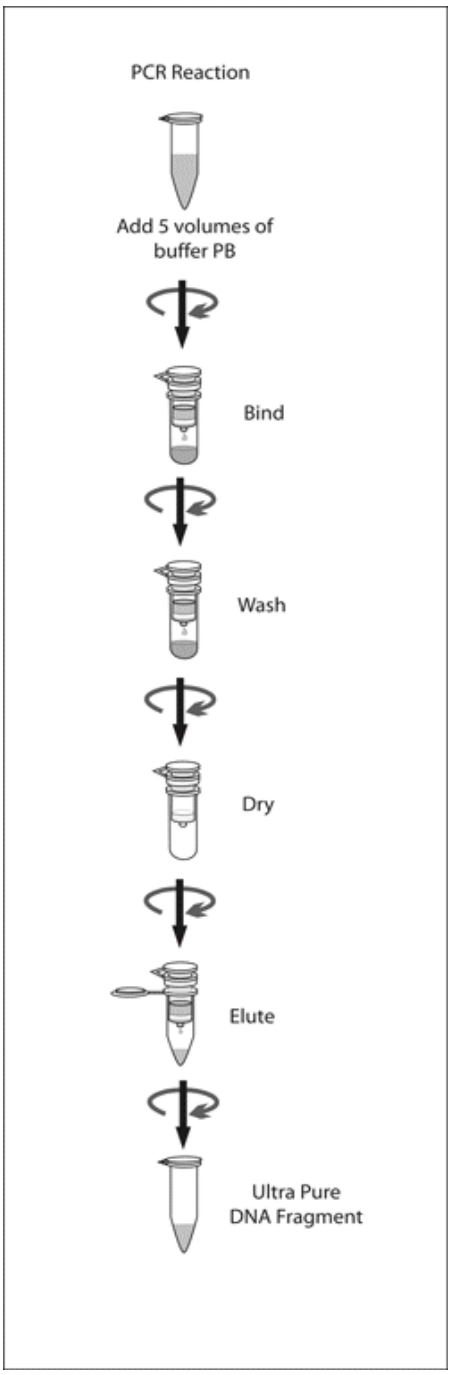

Figure 23 DNA extraction workflow.

1) For each sample, firstly 20 µL of Proteinase K was spiked in 1,5 mL PFTE tubes, subsequently 200 µL of blood sample and 200 µL of Lysis Buffer were introduced. Afterwards, these samples have been vortexed for 10 seconds, leaved at 56 °C for 10 minutes to activate proteinase K and then centrifuged for 1 minute at 6080Xg.

2) For each PFTE tube 200 µL of Ethanol 99% were added in order to crio-preserve samples for long-term and being ensure that every trace of the virus was eliminated. Thus, samples were vortexed for 10 seconds and centrifuged for 1 minute at 6080Xg.

3) Each sample was transferred in the appropriate column and centrifugated (1 minute at 6080Xg). In this way, DNA binds beads present in the silical filter and the waste was eliminated. The column was recovered, then underwent two washing steps, which the first one is followed by centrifugation (1 minute at 6080Xg).

4) Afterwards, a centrifuge step (3 minutes at 18630Xg) eliminated all scrap residues. Finally, each column was transferred in the appropriate 1.5 mL PFTE tubes and underwent elution step with Elution Buffer. It was necessary waiting for 1 minute, leaving the PFTE tubes in vertical position at room temperature and then make a final centrifuge step (1 minute at 6080Xg). Thus, it was possible trough away the column and preserving each PFTE tube at -80 °C.

4.5 Allelic discrimination

Allelic discrimination consists in determining the two possible variants on a DNA sequence by "5 nuclease fluorogenic assay". In detail, this technique exploits the 5' to 3' esonuclease activity of Taq polymerase: when the enzyme meets an oligonucleotide perfectly matched with the DNA sequence, this one is used by Taq polymerase as plate for continuing elongation during the reaction.

In this way, it is possible to investigate SNPs. As well as a valid flexibility and efficiency, it is realizable to genotype a wide amount of samples simultaneously by a single PCR (Polymerase Chain Reaction) race, without using other additional techniques. TaqMan® Allelic Discrimination was adopted to analyze samples. The process is based on a Real Time PCR (RT-PCR), namely an amplification and an evaluation of DNA samples in real time, following each amplification step phase to phase.

The real-time PCR needs three important elements:

1. primer "sense" or 5';
2. primer "anti-sense" or 3';
3. "probe".

The latter is an oligonucleotide formed of two parts linked to opposite extremities:

- "Quencer" (TAMRA fluorochrome), which is a particular fluorescence silencer. In a deeper analysis, the silencing occurs through energy transfer between both fluorochromes, but only when these ones are near.
- "Reporter" (FAM or VIC fluorochrome), which is the real responsible of fluorescence signal.

The presence of this probe allows to make both a quantitative analysis, because of emission signal is proportional to how much DNA derives from each sample, and a qualitative analysis evaluating the energy emission of one of two allelic-specific probes linking different kind of fluorochromes (FAM or VIC fluorochrome). During the extension, esonuclease activity of Taq polymerase occurs only when there is a perfect match with the template, improving the analysis specificity: thus

whether Taq polymerase moves away the probe matched with the "wild-type" SNP will be possible to observe a type of signal (i.e. FAM); conversely if the probe links the "mutant variant", the other fluorochrome (i.e. VIC) will release and be detectable from the instrument. For these reasons, real-time PCR appears as a simple and rapid approach to genotype a great amount of samples for different SNPs (Figure 24).

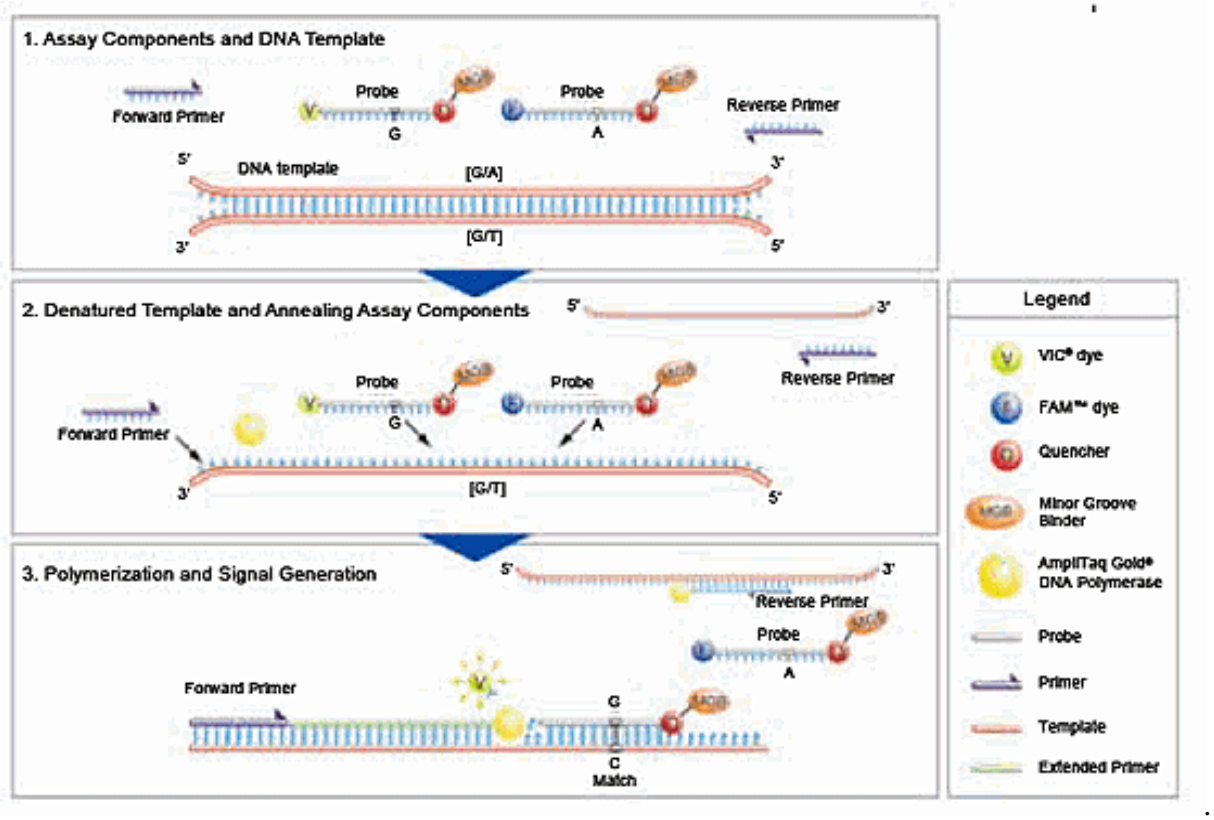

Figure 24 Real-time PCR (RT-PCR) schematic overview.

There are some requirements that should be always respected in a real-time PCR:

- *Lower Melting Temperature of probes (T_m)* compared to T_m of DNA (at least 5 °C) in order to avoid cross-reactions and allowing a specific linkage to the sequence during the synthesis of complementary strand;
- *Length of probes*, the amount of nucleotides have to be at least 20 nucleotides, but no many more avoiding unspecific binding. Therefore, the percentage of GC should be around 50%;
- *Extension phase must occur at temperature under 72 °C*, usually used in PCR, in order to maintain the probes on the complementary sequence during this step;

- *High $MgCl_2$ concentration*, for the same reason of the previous point;
- Accurate probe design, avoiding either unspecific or absent reactions;
- The fluorometer is located inside the instrument and reveals the emission signals at a wave length included between 500 and 600 nm ($500 < \lambda < 600$). Subsequently, a software coupled with the instrument elaborates data and develops a clusterization of fluorescent signals in groups corresponding to different genotypes.

5. Evaluation of cardiac and hepatic stiffness.

5.1 T2 cardiac magnetic resonance imaging*

Iron loading and cardiac function was assessed using T2* cardiac magnetic resonance [28]. The evaluation of the cardiac iron concentration was monitored in the period between two consecutive determinations (about one year). Patients were scanned with a 1.5T scanner (Sonata, Siemens Medical Solutions, Erlangen, Germany) using previously reported techniques [154]. In brief, cardiovascular magnetic resonance was performed using a cardiac gated, single breath-hold, 8-echo sequence (2.6 – 16.7 ms, increasing in 2.02 ms increments) of a single mid-ventricular short axis slice. Long axis cines and a contiguous stack of short axis cines were also acquired to assess left ventricular dimensions and function using standard techniques [155]. Data analysis was performed using CMRtools and its plug-in ThalassemiaTools (Cardiovascular Imaging Solutions, London UK) for T2* (a large region of the interventricular septum excluding regions in proximity to the coronary veins), as well as left ventricular ejection fraction using semi-automated planimetry of endocardial borders [155]. Cardiac T2* values > 20 ms were considered normal [22].

5.2 T2 hepatic magnetic resonance imaging*

MRI T2* liver examinations were performed using the Philips Achieva 1.5 Tesla MR systems (Philips Healthcare, the Netherland). The procedure was performed according to previous report [156]. A single breath-hold, 20 echo sequence (1.07–0.21ms) of a transaxial slice of the liver was acquired. Data analysis was performed using CMRtools and its plug-in ThalassemiaTools (Cardiovascular Imaging Solutions, London UK) for the liver T2*, evaluating a large region of interest excluding vascular structures. Normal values were ≥ 6.3 ms. The evaluation of the liver iron concentration was monitored by T2* magnetic resonance imaging, in the period between two consecutive drug concentration determinations (about one year).

5.3 Transient elastography

Transient elastography was performed using the FibroScan device (Echosens, Paris, France). All participants were studied by using the M probe (3.5 MHz frequency, 7-mm external transducer, depth of assessment 35-65 mm) of the Fibroscan device after fasting for at least 6 hours. Measurements were performed following the examination procedure described elsewhere [27]. The rate of successful measurements was calculated as the ratio between the number of those validated and total measurements. The results were expressed as a median value of the total measurements in kPa. Only the examinations with at least 10 validated measurements, a success rate of at least 60%, and an interquartile range (IQR) of the median stiffness value lower than 30% were considered reliable. Patients with ascites were excluded from the study. A cut-off value < 7.0 kilopascal (kPa) was considered indicative for not significant fibrosis [30]. The transient elastography has been evaluated in the period between two consecutive drug concentration determinations (about one year).

6. Statistical Analysis

To carry out the descriptive analysis, continuous and non normal variables were summarized as median and the IQR (quartile 1; quartile 3), to evaluate the statistical dispersion of the data; categorical variables were represented as frequency and percentage. All the variables were tested for normality with the Shapiro-Wilk test. The correspondence of each parameter was evaluated with a normal or non-normal distribution, through the Kolmogorov-Smirnov test.

All the SNPs were tested for HW equilibrium by the $\chi 2$ test with the OEGE software (Online Encyclopedia for Genetic Epidemiology studies[157]), to determine the observed genotype frequencies: $\chi 2$ indicates the difference among expected and observed values for genotype counts and a $\chi 2 < 3.84$ was considered in HW equilibrium.

Linkage disequilibrium (LD) was evaluated with Haploview 4.2 software (Cambrige, Massachusetts, USA). We measured LD among a pair of SNPs by the statistic D': |D'| of 1 indicates complete LD and 0 corresponds to no LD.

Kruskal-Wallis and Mann-Whitney tests have been used to evaluate the influence of SNPs on pharmacokinetic parameters, considering the level of statistical significance (*p value*<0.05).

Any predictive power of the considered variables (genetic factors, age, ethnicity, body mass index, gender, DFX Ctrough, DFX dose and serum ferritin) was finally evaluated through univariate and multivariate linear (for pharmacokinetic parameters) and logistic (considering efficacy, T2* and liver stiffness cut-offs) regression analyses. Factors (β, β coefficient for linear model; Exp(B), exponentiation of the B coefficient for logistic model; IC, interval of confidence at 95% for the parameter B, for linear model, or Exp(B) for logistic model) with a *p value* < 0.2 in univariate analysis were included in the multivariate analysis (*p value* < 0.05). Suggested genetic polymorphism associations by the univariate analysis were corrected by the Bonferroni method (*q value* = 0.2/number of evaluated SNPs). All the tests were performed with IBM SPSS Statistics 22.0 for Windows (Chicago, Illinois, USA).

RESULTS

1. Role of deferasirox and vitamin D pharmacogenetics on drug pharmacokinetics and clinical outcomes [152]

1.1. Study population

Ninety-nine patients, treated with DFX, were enrolled. Data required to calculate AUC parameters were available only for 58 subjects. Their demographical, clinical and pharmacokinetic characteristics were resumed in Table 9.

Variable	All patients (N=99)	AUC patients (N=58)
Gender		
Male, n (%)	53 (53.5)	34 (58.6)
Female, n (%)	46 (46.5)	24 (41.4)
Age (years)		
Median (IQR)	34 (18-53)	34 (18-53)
Body mass index (BMI) Kg/m^2		
Median (IQR)	22 (15-32)	21.95 (15-32)
Ethnicity		
Caucasian, n (%)	93 (93.9)	55 (94.8)
Other, n (%)	6 (6.1)	3 (5.2)
Serum ferritin ng/mL		
Median (IQR)	1139 (49.50-8470.50)	1132.07 (63-6737.50)
Efficacy		
Responders, n (%)	27 (27.3)	16 (27.6)
Non responders, n (%)	72 (72.7)	42 (72.4)
DFX AUC < 250 µg/mL/h		
n (%)		26 (44.8)
DFX AUC > 360 µg/mL/h		
n (%)		22 837.9)
DFX dose mg/day/Kg		
Median (IQR)	29 (13.61-40)	28 (17-40)
DFX Ctrough µg/mL		
Median (IQR)	10.36 (0-85.95)	4.98 (0-85.95)
DFX AUC µg/mL/h		
Median (IQR)		267.14 (63.76-965.54)
DFX Vd mL		
Median (IQR)		920.38 (208.73-16608.77)
DFX $t_{1/2}$ hours		
Median (IQR)		7.51 (22.51)
DFX Cmax µg/mL		
Median (IQR)		22.51 (6.90-72.90)
DFX Tmax hours		
Median (IQR)		4 (2-6)

Table 9 Demographic, clinical and pharmacokinetic characteristics of all the enrolled patients (N=99) and of AUC patients subgroup (N=58).

1.2 Hardy-Weinberg and Linkage Disequilibrium analyses

All the SNPs were in HW equilibrium (Table 10).

	ALL PATIENTS (N=99)				AUC PATIENTS (N=58)			
SNP name	**ObsHET**	**PredHET**	**HW *p value***	**MAF**	**ObsHET**	**PredHET**	**HW *p value***	**MAF**
CYP27B1 +2838	0.323	0.397	0.1038	0.273	0.345	0.348	1	0.224
CYP27B1 -1260	0.333	0.382	0.2846	0.258	0.362	0.357	1	0.233
CYP24A1 +8620	0.545	0.494	0.4309	0.444	0.500	0.496	1	0.457
CYP24A1 +22776	0.495	0.500	1	0.490	0.431	0.499	0.4015	0.474
CYP24A1 +3999	0.424	0.478	0.3406	0.394	0.431	0.475	0.6182	0.388
ApaI	0.455	0.497	0.4871	0.460	0.466	0.499	0.7564	0.474
TaqI	0.444	0.485	0.4947	0.414	0.466	0.467	1	0.371
FokI	0.354	0.418	0.1769	0.298	0.379	0.400	0.8835	0.276
BsmI	0.434	0.490	0.3280	0.429	0.466	0.482	0.9537	0.405
Cdx2	0.343	0.422	0.0960	0.303	0.259	0.357	0.0771	0.233
GC +1296	0.434	0.466	0.6130	0.369	0.362	0.467	0.135	0.371

Table 10 Analyzed SNPs characteristics: variant name (SNP name), observed heterozygous (ObsHET), predicted heterozygous (predHET), HW equilibrium $\chi 2$ (HW *p value*) and minimum allele frequency (MAF), considering all our cohort (N=99) and AUC patients subgroup (N=58).

LD analysis was shown in Figure 25. The extent of LD decreases in proportion to the number of generations since the LD-generating event; an alternative explanation is that the recombination rates in the studied regions might be markedly less than the genome-wide average [158].

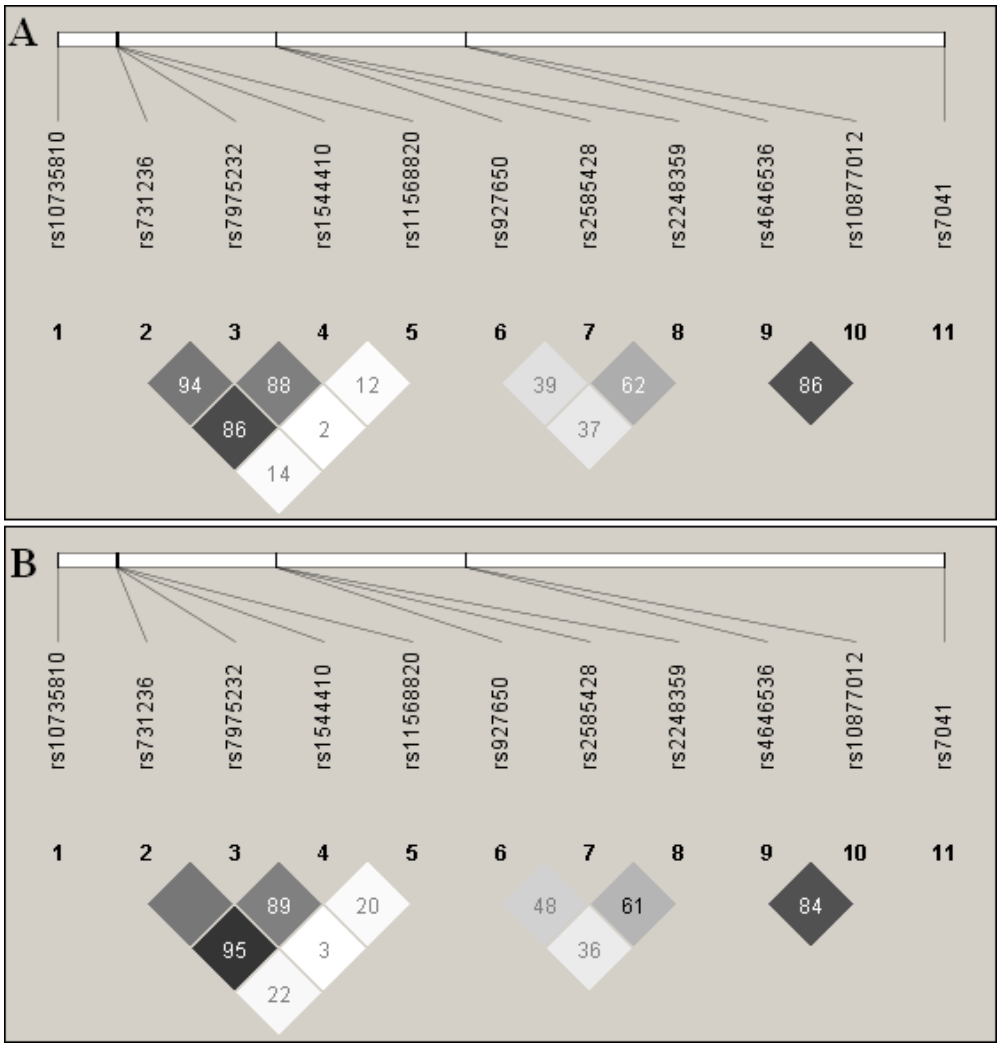

Figure 25 The panel shows pairwise LD of the studied population among the studied SNPs. Each value in the box represents r2. Dark grey, regions with high r2 values; light grey, regions with low r2 values. Intensity of shading indicates the degree of confidence in the r2 value and numbers in blocks denote r2 values. Dark filled squares indicate a r2 value of 1 with LOD (logarithm of odds) < 2.0. r2 was calculated as follows: r2 = r scales D by the standard deviation of the allele frequencies at two loci, where statistic D is the range of values regardless of the frequencies of the SNPs compared. LOD was defined as log10(L1/L0), where L1 = likelihood of the data under LD, and L0 = likelihood of the data under LD. The physical position of each SNP is showed in the top diagram.
A. Pairwise LD considering all the 99 patients.
B. Pairwise LD considering AUC subgroup (58 patients).

1.3 Effect of VDR, CYP24A1, CYP27B1 and GC SNPs on DFX Ctrough

CYP24A1 8620 GG and 3999 CC SNPs significantly influenced Ctrough (p= 0.047 and p= 0.010, respectively; Figure 23). Evaluating 8620 A>G variant, median concentrations was 12.350 µg/mL (IQR 0-85.95 µg/mL) for AA/AG (N=71) group and 3.797 µg/mL (IQR 0-84.23 µg/mL) for GG (N=28) (Figure 23A); considering 3999 T>C SNP, median value was 14.050 µg/mL (IQR 0-85.95 µg/mL) in *TT/TC* (N=60) and 3.556 µg/mL (IQR 0-84.23 µg/mL) in CC (N=39) (Figure 23B).

Only sex had a significant *p value* in linear regression model (*p*= 0.030; β= -0.218; IC95% [-14.682; -0.771]) (data not shown).

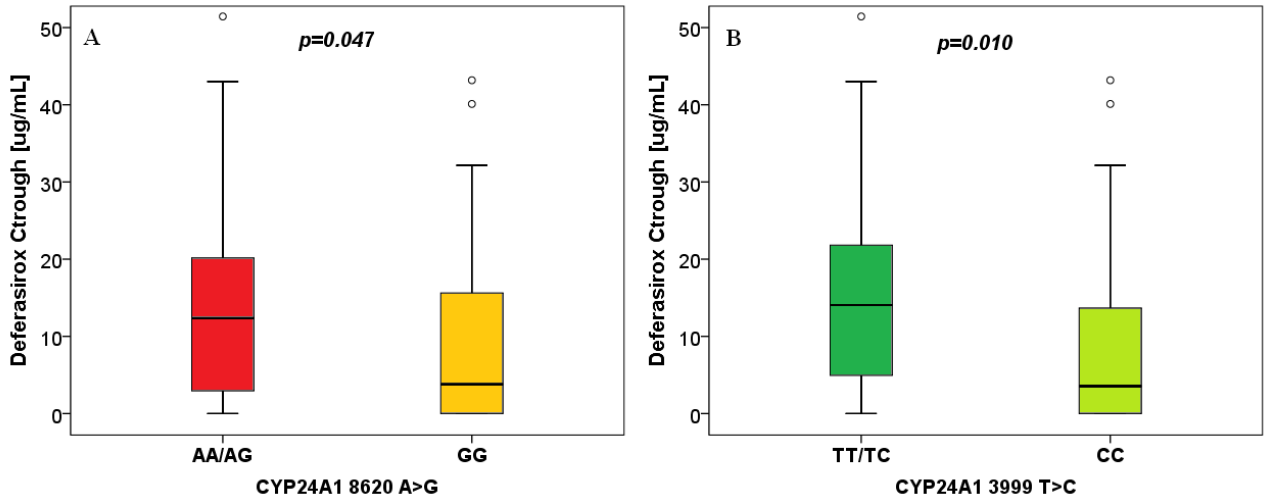

Figure 26 Box plot of *CYP24A1* 8620 A>G and 3999 T>C SNPs influence on DFX Ctrough (µg/mL); boxes and black lines in boxes represent respectively interquartile ranges (IQR) and median values; open dots and stars represent outlier values. Median values (horizontal line), IQR (bars), patient values (black square), highest and lowest value (whiskers) and *p* value are shown.
A. *CYP24A1* 8620 AA/AG (N=71; median Ctrough value 12.350 µg/mL; IQR 0-85.95 µg/mL) versus GG (N=28; median Ctrough value 3.797 µg/mL; IQR 0-84.23 µg/mL).
B. *CYP24A1* 3999 TT/TC (N=60; median Ctrough value 14.050 µg/mL; IQR 0-85.95 µg/mL) versus CC (N=39; median Ctrough value 3.556 µg/mL; IQR 0-84.23 µg/mL).

1.4 Effect of VDR, CYP24A1, CYP27B1 and GC SNPs on DFX AUC

AUC resulted significantly influenced by *CYP24A1* 8620 GG genotype (*p*= 0.021; Figure 27): AG/GG (N=41) group had median value of 330.551 µg/mL/h (IQR 76.56-965.54 µg/mL/h) and GG (N=17) one had 183.550 µg/mL/h (IQR 63.76-629.21 µg/mL/h). This variant was also retained in multivariate linear regression analysis (*p*= 0.031; β= -0.283; IC95% [-2879.092; -13.812]; and *q*= 0.031 after Bonferroni correction) (Table 11).

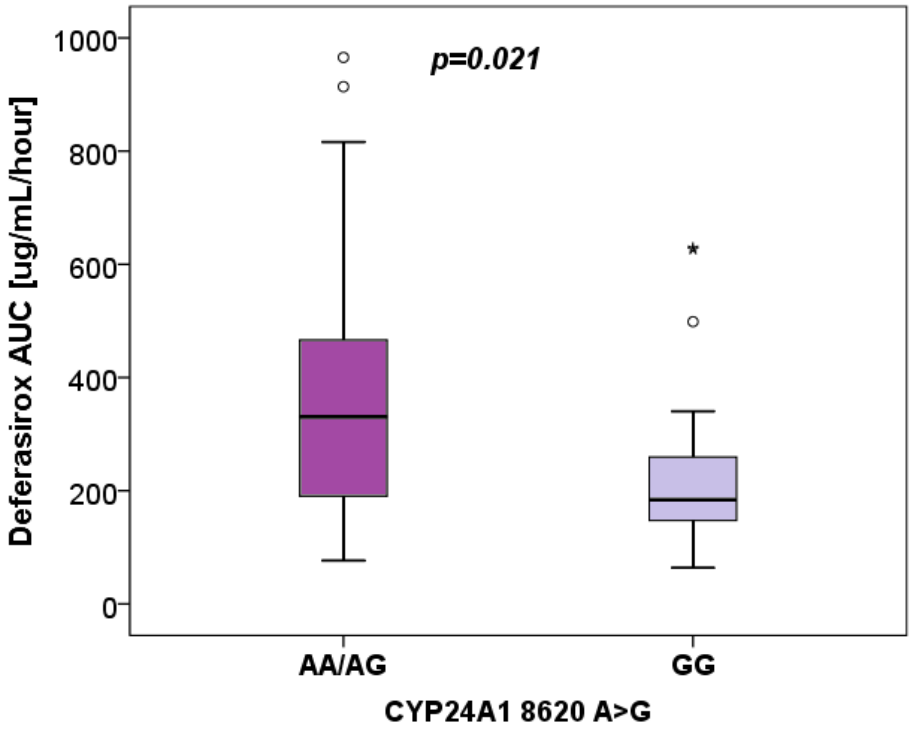

Figure 27 Box plot of *CYP24A1* 8620 A>G SNP influence on DFX AUC (µg/mL/h). *CYP24A1* 8620 AA/AG (N=41; median AUC value 330.551 µg/mL/h; IQR 76.56-965.54 µg/mL/h) versus GG (N=17; median AUC value 183.550 µg/mL/h; IQR 63.76-629.21 µg/mL/h).

		UNIVARIATE	*q*	MULTIVARIATE
FACTOR	***GENOTYPE***	***p*;β (IC95%)**		***p*;β (IC95%)**
Age		0.673; -0.057 (-11.84; 7.70)		
Gender		0.942; 0.010 (-123.16; 132.49)		
BMI		0.580; -0.074 (-26.37; 14.90)		
Ethnicity		0.636; -0.161 (-451.51; 109.62)		
DFX dose (mg/Kg/day)		0.960; 0.007 (-10.11; 10.63)		
CYP27B1 +2838	***CT/TT***	0.510; 0.088 (-189.34; 376.99)	1.403	
	TT	0.912; 0,015 (-115.43; 129.04)	0.967	
CYP27B1 -1260	***GT/TT***	0.690; 0.052 (-97.63; 146.53)	0.759	
	TT	0.510; -0.088 (-376.99; 189.34)	1.603	
CYP24A1 8620	***AG/GG***	0.476; -0.093 (-199.63; 94.352)	1.745	
	GG	**0.031; -0.283 (-279.09; -13.81)**	0.682	**0.031; -0.283 (-279.09; -13.81)**
CYP24A1 22776	***CT/TT***	0.667; -0.058 (-165.15; 106.57)	0.776	
	TT	0.602; 0.068 (-103.40; 176.73)	1.019	
CYP24A1 3999	***TC/CC***	**0.117; -0.208 (-292.62; 33.42)**	1.287	0.243; -0.152 (-255.77; 66.30)
	CC	0.531; -0.082 (-162.16; 84.53)	1.062	
FokI	***TC/CC***	0.326; 0.131 (-112.28; 332.46)	1.793	
	CC	0.987; 0.002 (-120.30; 122.34)	0.987	
Cdx2	***AG/GG***	0.455; -0.097(-277.96; 126.12)	2.002	
	GG	0.517; -0.085 (-172.43; 87.73)	1.137	
ApaI	***CA/AA***	0.644; -0.062 (-180.86; 112.83)	0.995	
	AA	0.514; -0.087 (-173.27; 87.73)	1.256	
TaqI	***TC/CC***	0.657; -0.058 (-152.30; 96.77)	0.803	
	CC	0.655; -0.060 (-223.17; 141.33)	0.848	
BsmI	***GA/AA***	0.654; -0.059 (-153.98; 97.39)	0.899	
	AA	0.575; -0.075 (-212.99; 119.41)	1.054	
GC 1296	***TG/GG***	**0.139; -0.197 (-217.18; 31.06)**	1.019	0.154; -0.184 (-207.33; 33.51)
	GG	0.650; -0.042 (-175.89; 123.02)	0.953	

Table 11 Factors, in univariate and multivariate linear regression analyses, able to predict DFX levels, considering AUC. Significant *q* value (0.2/11) > 0.018.

1.5 Effect of VDR, CYP24A1, CYP27B1 and GC SNPs on DFX $t_{1/2}$

CYP24A1 8620 GG genotype significantly affected $t_{1/2}$ with a *p value* of 0.031 (Figure 28). AA/AG (N=41) genotypes showed median $t_{1/2}$ of 8.411 hours (IQR 1.28-47.99 hours), while GG (N=17) group 6.476 hours (IQR 1.41-10.47 hours). No factors were retained in the final regression model (data not shown).

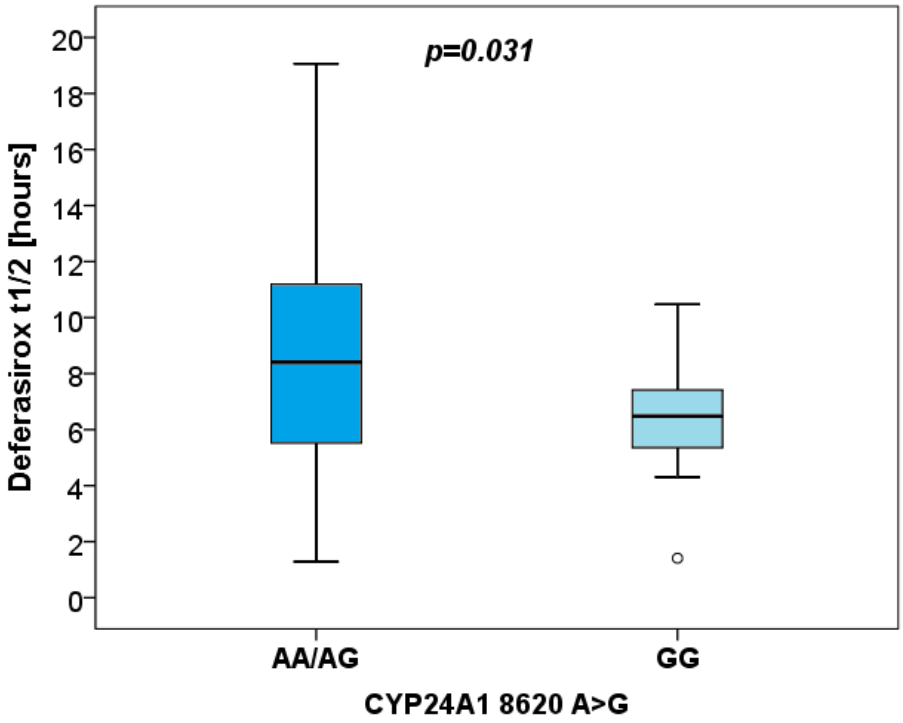

Figure 28 Box plot of *CYP24A1* 8620 A>G SNP influence on DFX $t_{1/2}$ (hours). *CYP24A1 8620* AA/AG (N=41; median 8.411 hours; IQR 1.28-47.99 hours) versus GG (N=17; median 6.476 hours; IQR 1.418-10.47 hours).

1.6 Effect of VDR, CYP24A1, CYP27B1 and GC SNPs on DFX Cmin

CYP24A1 8620 GG, 3999 CC and 22776 TT SNPs were related to Cmin (p= 0.010, p= 0.040 and p= 0.011, respectively; Figure 29). 8620 AA/AG (N=41) genotype showed 12.280 µg/mL (IQR 0-85.95 µg/mL) median Cmin, whereas GG (N=17) had 0 µg/mL (IQR 0-84.23 µg/mL) (Figure 29A); 3999 TT/TC (N=43) group median Cmin was 11.160 µg/mL (IQR 0-85.95 µg/mL) and CC (N=15) one was 0 µg/mL (IQR 0-22.56 µg/mL) (Figure 29B); considering 22776, median Cmin was 14.430 µg/mL (IQR 0-85.95 µg/mL) for CC/CT (N=35) and 1.148 µg/mL (IQR 0-84.23 µg/mL) for TT (N=23) (Figure 29C). In regression analyses only *CYP24A1* 22776 TT resulted statistically significant (p= 0.036; β=-0.271; IC95% [-23.982; -0.808]) (Table 12).

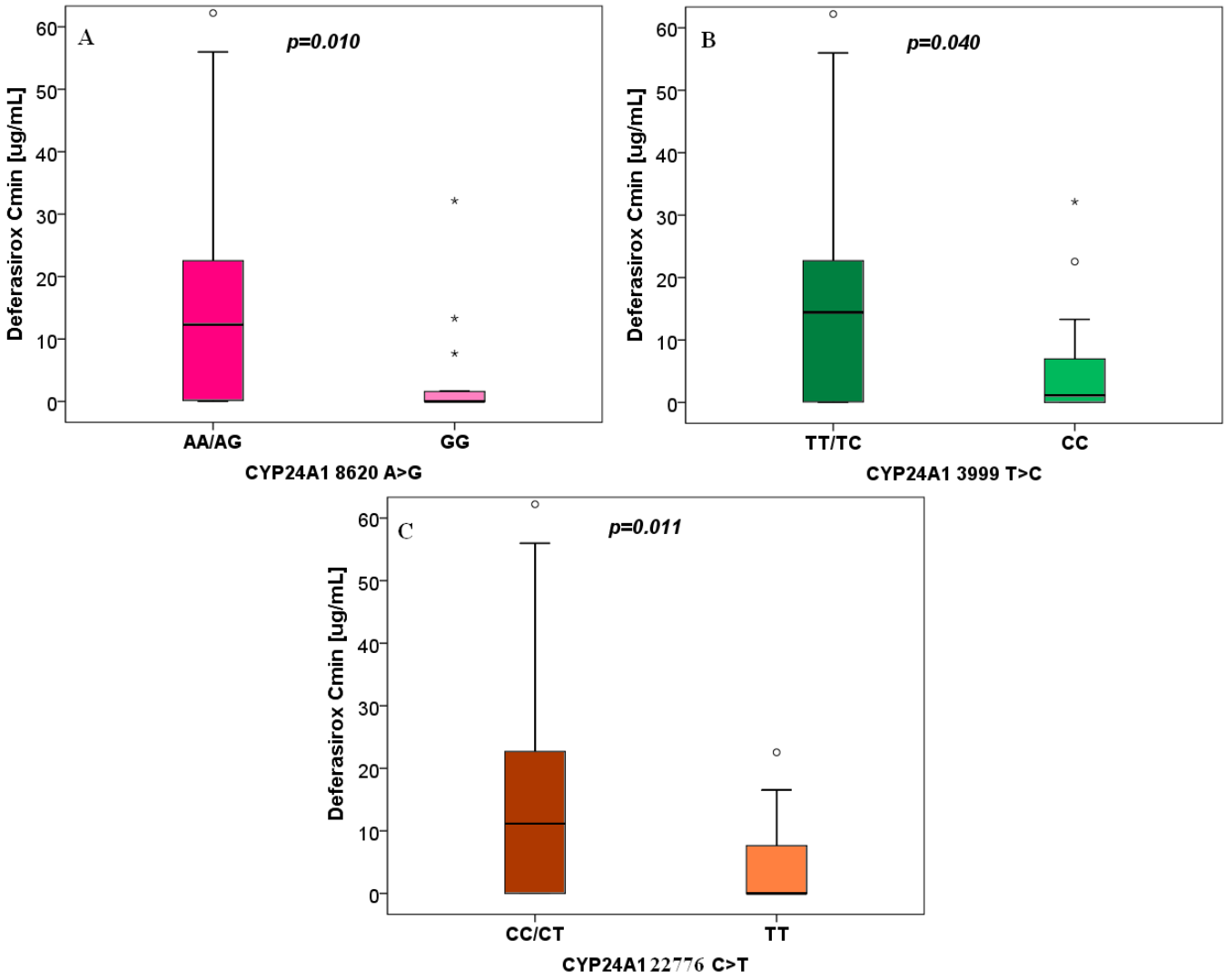

Figure 29 Box plot of *CYP24A1* 8620 A>G, 3999 T>C and 22776 C>T SNPs on DFX Cmin (µg/mL).
***A. CYP24A1* 8620 AA/AG (N=41; median value 12.280 µg/mL; IQR 0-85.95 µg/mL) versus GG (N=17; median value 0 µg/mL; IQR 0-84.23 µg/mL).**
***B. CYP24A1* 3999 TT/TC (N=43; median value 11.160 µg/mL; IQR 0-85.95 µg/mL) versus CC (N=15; median value 0 µg/mL; IQR 0-22.56 µg/mL).**
***C. CYP24A1* 22776 CC/CT (N=35; median value 14.430 µg/mL; IQR 0-85.95 µg/mL) versus TT (N=23; median value 1.148 µg/mL; IQR 0-84.23 µg/mL).**

		UNIVARIATE	*q*	MULTIVARIATE
FACTOR	***GENOTYPE***	***p*;β (IC95%)**		***p*;β (IC95%)**
Age		0.970; 0.005 (-0.82; 0.85)		
Gender		0.220; -0.164 (-17.37; 4.08)		
BMI		**0.102; 0.217 (-0.29; 3.14)**		0.077; 0.228 (-0.17; 3.17)
Ethnicity		0.226; -0.162 (-38.45; 9.27)		
DFX dose (mg/Kg/day)		**0.150; -0.192 (-1.15; 0.23)**		0.251; -0.146 (-1.31; 0.35)
CYP27B1 +2838	***CT/TT***	0.823; -0.030 (-23.87; 21.46)	0.823	
	TT	0.928; -0.012 (-10.974; 10.022)	0.801	
CYP27B1 -1260	***GT/TT***	0.465; 0.098 (-6.84; 14.80)	0.883	
	TT	0.783; 0.036 (-17.87; 23.60)	0.826	
CYP24A1 8620	***AG/GG***	0.533; -0.084 (-17.04; 8.75)	0.844	
	GG	**0.182; -0.178 (-19.39; 3.77)**	0.864	0.519; -0.090 (-16.10; 8.23)
CYP24A1 22776	***CT/TT***	0.416; -0.017 (-15.83; 6.63)	0.988	
	TT	**0.047; -0.262 (-23.77; -0.16)**	0.893	**0.036; -0.271 (-23.98; -0.81)**
CYP24A1 3999	***TC/CC***	0.746; -0.043; -16.13; 11.62)	0.834	
	CC	**0.067; -0.243 (-20.54; 0.70)**	0.636	0.799; -0.043 (-15.41; 11.93)
FokI	***TC/CC***	0.733; 0.045 (-15.51; 21.91)	0.870	
	CC	**0.199; -0.171 (-17.44; 3.71)**	0.756	0.110; 0.203 (-18.20; 1.92)
Cdx2	***AG/GG***	0.913; 0.014 (-15.24; 17.01)	0.826	
	GG	0.657; 0.060 (-8.64; 13.60)	0.892	
ApaI	***CA/AA***	0.535; 0.082 (-8.21; 15.63)	0.921	
	AA	0.441; -0.103 (-16.23; 7.17)	0.931	
TaqI	***TC/CC***	0.722; 0.047 (-8.67; 12.40)	0.914	
	CC	0.587; -0.073 (-19.71; 11.26)	0.858	
BsmI	***GA/AA***	0.862; 0.023 (-9.79; 11.68)	0.818	
	AA	0.332; -0.130 (-20.92; 7.19)	1.051	
GC 1296	***TG/GG***	0.335; -0.127 (-15.33; 5.31)	0.909	
	GG	**0.179; -0.179 (-22.56; 4.32)**	1.134	0.222; -0.159 (-21.29; 5.06)

Table 12 Factors, in univariate and multivariate linear regression analyses, able to predict DFX levels, considering Cmin. Significant $q = 0.018$.

1.7 Effect of VDR, CYP24A1, CYP27B1 and GC SNPs on DFX Cmax

No factors significantly influenced Cmax or were retained in regression analysis (data not shown).

1.8 Effect of VDR, CYP24A1, CYP27B1 and GC SNPs on DFX Tmax

Concerning Tmax no associations were found. Anyway, *CYP12A1* 3999 CC (p= 0.008; β=-0.339; IC95% [-1.607; -0.252]), with DFX dose (mg/Kg/day) (p= 0.013; β=0.315; IC95% [0.02; 0.12]), were retained in the linear regression model (Table 13).

		UNIVARIATE	q	MULTIVARIATE
FACTOR	***GENOTYPE***	***p*;β (IC95%)**		***p*;β (IC95%)**
Age		0.411; -0.110 (-0.08; 0.03)		
Gender		0.225; 0.162 (-0.28;1.16)		
BMI		0.809; -0.032 (-0.13;0.10)		
Ethnicity		0.754; 0.042 (-1.37; 1.88)		
DFX dose (mg/Kg/day)		**0.059; 0.250 (-0.00; 0.11)**		**0.013; 0.315 (0.02; 0.12)**
CYP27B1 +2838	***CT/TT***	**0.153; 0.190 (0.44; 2.75)**	0.153	0.096; 0.205 (-0.23; 2.71)
	TT	0.840; -0.027 (-0.87; 0.71)	0.133	
CYP27B1 -1260	***GT/TT***	0.441; -0.101 (-1.09; 0.48)	0.132	
	TT	**0.153; -0.190 (-2.75; 0.44)**	0.153	
CYP24A1 8620	***AG/GG***	0.609; -0.067 (-1.22; 0.72)	0.131	
	GG	0.212; -0.166 (-1.27; 0.29)	0.127	
CYP24A1 22776	***CT/TT***	0.628; -0.064 (-1.06; 0.642)	0.126	
	TT	**0.160; -0.187 (-1.18; 0.23)**	0.120	0.674; -0.057 (-1.00; 0.65)
CYP24A1 3999	***TC/CC***	0.572; 0.074 (-0.432; 0.774)	0.143	
	CC	**0.037; -0.27 (-1.16; -0.05)**	0.111	**0.008; -0.339 (-1.61; -0.25)**
FokI	***TC/CC***	0.719; 0.047 (-0.64; 0.92)	0.120	
	CC	0.291; 0.141 (-0.33; 1.09)	0.125	
Cdx2	***AG/GG***	0.703; 0.050 (-0.98; 1.44)	0.124	
	GG	0.311; -0.135 (-1.12; 0.36)	0.117	
ApaI	***CA/AA***	0.890; 0.019 (-0.78; 0.90)	0.134	
	AA	0.672; 0.056 (-0.68; 1.05)	0.126	
TaqI	***TC/CC***	0.577; 0.073 (-0.57; 1.02)	0.133	
	CC	0.273; 0.146 (-0.46; 1.60)	0.137	
BsmI	***GA/AA***	0.991; -0.002 (-0.81; 0.80)	0.142	
	AA	0.540; 0.082 (-0.66; 1.24)	0.147	
GC 1296	***TG/GG***	**0.107; -0.214 (-1.28; 0.13)**	0.161	0.515; -0.084 (-0.92; 0.47)
	GG	0.381; -0.115 (-1.44;0.56)	0.127	

Table 13 Factors, in univariate and multivariate linear regression analyses, able to predict DFX levels, considering Tmax. Significant q = 0.018.

1.9 Effect of VDR, CYP24A1, CYP27B1 and GC SNPs on DFX Vd

No factors significantly affected Vd or were retained in the regression analysis.

1.10 Effect of VDR, CYP24A1, CYP27B1 and GC SNPs on DFX concentration outcome cut-offs.

The 20 µg/mL efficacy cut-off was not predicted by any analyzed SNP (data non shown). In logistic regression model, AUC efficacy cut-off (360 µg/mL/h) was predicted by *GC* 1296 TT/TG and Cdx2 AA/AG (*p= 0.010*; β=0.178; IC95% [0.048; 0.663] and *p*= 0.022; β=0.092; IC95% [0.12; 0.707], respectively) (Table 14). Any factor resulted able to predict AUC non-response cut-off (250 µg/mL/h) (data not shown).

		UNIVARIATE	*q*	MULTIVARIATE
FACTOR	***GENOTYPE***	***p; ExpB* (IC95%)**		***p; ExpB* (IC95%)**
Age		0.639; 0.774 (0.27; 2.62)		
Gender		0.623; 0.764 (0.26; 2.36)		
BMI		0.955; 0.969 (0.33; 2.85)		
Ethnicity		0.999; 0 (0-1)		
DFX dose (mg/Kg/day)		0.342; 1.680 (0.58; 4.89)		
CYP27B1 +2838	***CT/TT***	0.816; 0.850 (0.22; 3.35)	0,952	
	TT	0.689; 1.25 (0.42; 3.73)	0,965	
CYP27B1 -1260	***GT/TT***	0.623; 1.310 (0.45; 3.83)	0,935	
	TT	0.745; 0.789 (0.19; 3.29)	0,978	
CYP24A1 8620	***AG/GG***	0.419; 1.571 (0.53; 4.70)	1,100	
	GG	**0.049; 0.248 (0.06; 1.00)**	0,515	0.210; 0.376 (0.08; 1.74)
CYP24A1 22776	***CT/TT***	0.207; 0.481 (0.16; 1.50)	0,725	
	TT	0.871; 0.920 (0.34; 2.51)	0,915	
CYP24A1 3999	***TC/CC***	**0.124; 0.333 (0.08; 1.35)**	0,868	0.061; 0.219 (0.05; 1.07)
	CC	0.205; 1.835 (0.72; 4.70)	1,206	
FokI	***TC/CC***	0.402; 2.625 (0.27; 25.14)	0,861	
	CC	0.858; 1.083 (0.45; 2.60)	0,948	
Cdx2	***AG/GG***	**0.146; 0.265 (0.04; 1.59)**	0,767	**0.022; 0.092 (0.01; 0.71)**
	GG	0.561; 0.722 (0.241; 2.162)	0,982	
ApaI	***CA/AA***	0.535; 0.706 (0.24; 2.12)	1,021	
	AA	0.790; 0.852 (0.26; 2.76)	0,976	
TaqI	***TC/CC***	0.480; 0.711 (0.28; 1.83)	1,008	
	CC	0.423; 0.500 (0.09; 2.73)	0,987	
BsmI	***GA/AA***	0.480; 0.711 (0.28; 1.83)	1,008	
	AA	0.572; 0.954 (0.15; 2.85)	0,924	
GC 1296	***TG/GG***	**0.027; 0.286 (0.09; 0.87)**	0,567	**0.010; 0.178 (0.05; 0.66)**
	GG	0.943; 1.045 (0.36; 3.57)	0,943	

Table 14 Factors, in univariate and multivariate logistic regression analyses, able to predict DFX AUC efficacy cut-off (>360 µg/mL/h). Significant *q* = 0.018.

2. Role of deferasirox and vitamin D pharmacogenetics on the evaluation of cardiac iron overload

2.1 Study population

One-hundred and five patients, treated with DFX, have been enrolled. Their demographical, clinical and pharmacokinetic features were resumed in Table 15.

Variable	N=105
Gender	
Male, n (%)	58 (55.2)
Female, n (%)	47 (44.8)
Age (years)	
Median (IQR)	37.00 (27.50-40.00)
Body mass index (BMI) Kg/m^2	
Median (IQR)	22.00 (19.91-23.76)
Ethnicity	
Caucasian, n (%)	93 (88.6)
Other, n (%)	12 (11.4)
Serum ferritin ng/mL	
Median (IQR)	1167.00 (388.00-2635.00)
Cardiac T2* values (ms mean /year)	
Median (IQR)	39.45 (20.69-46.50)
Cardiac T2* values ≥ 20 ms	
Normal values (≥ 20 ms), n (%)	80 (76.2)
Critical values (< 20 ms), n (%)	25 (23.8)
Hepatic T2* values (ms mean /year)	
Median (IQR)	11.00 (4.00-20.60)
Hepatic T2* values ≥ 6.3 ms	
Normal values (≥ 6.3 ms), n (%)	58 (55.2)
Critical values (< 6.3 ms), n (%)	47 (44.8)
Liver stiffness values (KPa mean /year)	
Median (IQR)	5.50 (4.55-7.75)
Liver stiffness values ≤ 7 KPa	
Normal values (≤ 7 KPa)	75 (71.4)
Non normal values (> 7 KPa)	30 (26.8)
Efficacy	
Responders, n (%)	27 (25.7)
Non responders, n (%)	78 (74.3)
DFX dose mg/Kg/day	
Median (IQR)	29.00 (21.96-30.88)

Table 15 Demographic, clinical and pharmacokinetic characteristics of the enrolled patients.

2.2 Hardy-Weinberg and Linkage Disequilibrium analysis

All the SNPs were in HW equilibrium (Table 16).

LD analysis was shown in Figure 30.

Gene	SNP name	rs	Alleles	Position	ObsHET	PredHET	HW *p value*	MAF
UGT1A1	*UGT1A1* -364	rs887829	C>T	234668570	0.491	0.454	0.5347	0.349
UGT1A3	*UGT1A1* -66	rs3806596	A>G	234302446	0.56	0.498	0.2654	0.47
UGT1A3	*UGT1A3* -751	rs1983023	C>T	234301761	0.543	0.489	0.3417	0.427
CYP1A1	*CYP1A1* -27+606	rs2606345	C>A	75017176	0.509	0.46	0.3665	0.358
CYP1A1	*CYP1A1**1189	rs4646903	T>C	75011641	0.362	0.375	0.8481	0.25
CYP1A2	*CYP1A2* -9-154	rs762551	A>C	75041917	0.336	0.313	0.6622	0.194
CYP1A2	*CYP1A2* 1548	rs2470890	C>T	75047426	0.603	0.488	0.0196	0.422
CYP2D6	*CYP2D6* 1457	rs1135840	C>G	42522613	0.431	0.467	0.5018	0.371
ABCC2	*ABCC2* 1249	rs2273697	G>A	101563815	0.353	0.313	0.2821	0.194
ABCG2	*ABCG2* 421	rs2231142	G>A	89052323	0.155	0.158	1.0	0.086
ABCG2	*ABCG2* 1194+928	rs13120400	T>C	89033527	0.388	0.418	0.5439	0.297
CYP27B1	*CYP27B1* 2838	rs4646536	C>T	58157988	0.293	0.366	0.0563	0.241
CYP27B1	*CYP27B1* -1260	rs10877012	G>T	58162085	0.302	0.353	0.1844	0.228
CYP24A1	*CYP24A1* 8620	rs2585428	A>G	52786897	0.526	0.497	0.6947	0.461
CYP24A1	*CYP24A1*22776	rs927650	C>T	52772741	0.491	0.499	0.9787	0.478
CYP24A1	*CYP24A1* 3999	rs2248359	T>C	52791518	0.448	0.479	0.5906	0.397
VDR	ApaI	rs7975232	C>A	48238837	0.431	0.493	0.2266	0.44
VDR	TaqI	rs731236	T>C	48238757	0.448	0.488	0.4627	0.422
VDR	FokI	rs10735810	T>C	46559162	0.371	0.438	0.1396	0.323
VDR	BsmI	rs1544410	G>A	48239835	0.466	0.496	0.5972	0.457
VDR	Cdx2	rs11568820	A>G	48302545	0.336	0.403	0.11	0.28
GC	*GC* 1296	rs7041	T>G	71752617	0.431	0.467	0.5018	0.371

Table 16 Analyzed SNPs characteristics: gene, variant name (SNP name), rs number, position, alleles, ObsHET, predHET, HW equilibrium $\chi 2$ (HW *p value*) and MAF.

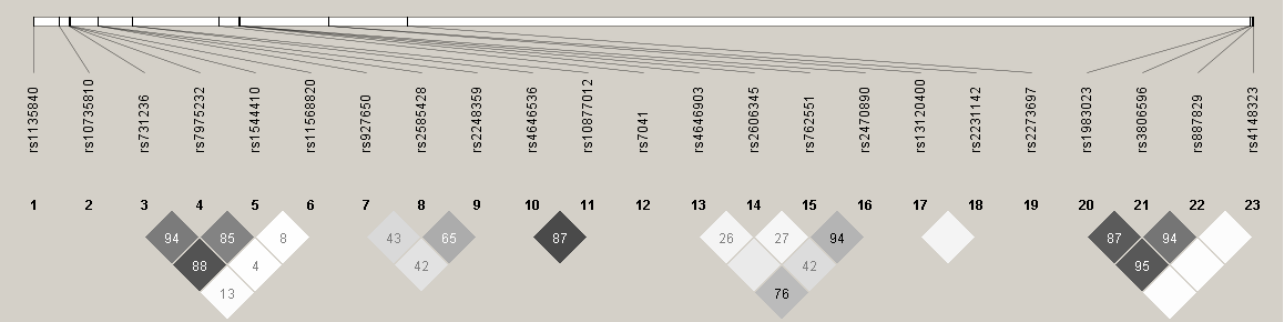

Figure 30 The panel shows pairwise LD of the studied population among the studied SNPs.

*2.3 Effect of UGT1A1, UGT1A3, CYP1A1, CYP1A2, CYP2D6, ABCC2 and ABCG2 SNPs on cardiac T2**

CYP1A1 *1189 CC (*p*= 0.038, Figure 31) and *ABCG2* 421 GA (*p*= 0.008, Figure 32) genotypes influenced T2* values. *CYP1A1* *1189 TT/TC (N=99) group showed a median T2* value of 42.30 ms mean/year (IQR 32.40-47.46 ms mean/year), whereas CC (N=6) 27.70 ms mean/year (IQR 15.91-39.88 ms mean/year) (Figure 31); *ABCG2* 421 GG (N=86) median T2* value was 42.50 ms mean/year (IQR 35.90-47.55 ms mean/year) and GA (N=19) showed 30.20 ms mean/year (IQR 15.70-43.30 ms mean/year) (Figure 32).

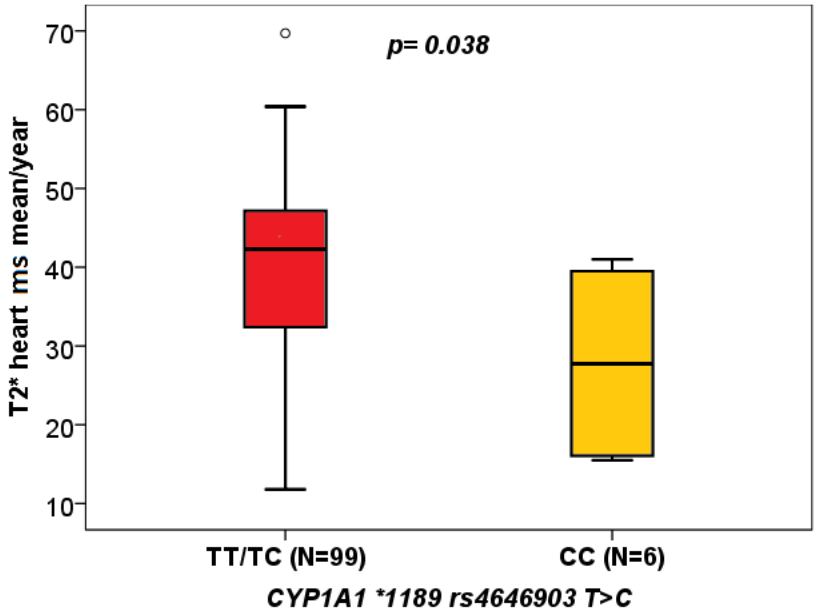

Figure 31 Influence of *CYP1A1* *1189 SNP on T2* values (ms mean/year).
***CYP1A1* *1189 TT/TC (N=99; median value 42.30 ms mean/year; IQR 32.40-47.46 ms mean/year) versus CC (N=6; median value 27.70 ms mean/year; IQR 15.91-39.88 ms mean/year).**

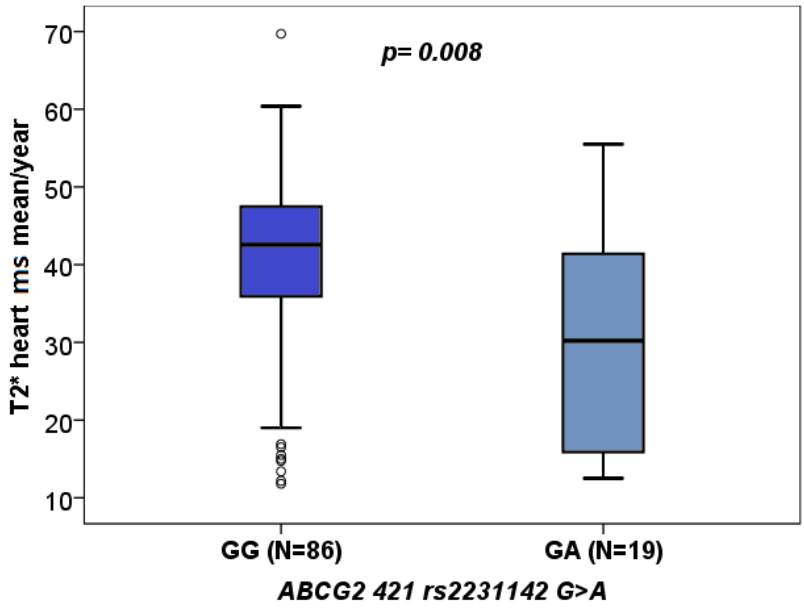

Figure 32 Influence of *ABCG2* 421 SNP on T2* values (ms mean/year).
***ABCG2* 421 GG (N=86; median value 42.50 ms mean/year; IQR 35.90-47.55 ms mean/year) versus GA (N=19; median value 30.20 ms mean/year; IQR 15.70-43.30 ms mean/year).**

2.4 Effect of VDR, CYP24A1, CYP27B1 and GC SNPs on cardiac T2.*

CYP24A1 8620 GG (p= 0.021, Figure 33) and *VDR* TaqI CC (p= 0.006, Figure 34) genotypes influenced T2* values. *CYP24A1* 8620 AA/AG (N=76) group showed a median T2* value of 43.60 ms mean/year (IQR 35.95-47.70 ms mean/year), whereas GG genotype (N=29) had 36.10 ms mean/year (IQR 22.75-42.90 ms mean/year) (Figure 33); *VDR* TaqI TT/TC (N=85) group median T2* value was 39.80 ms mean/year (IQR 24.99-46.10 ms mean/year) and CC (N=20) showed 45.80 ms mean/year (IQR 39.28-49.40 ms mean/year) (Figure 34).

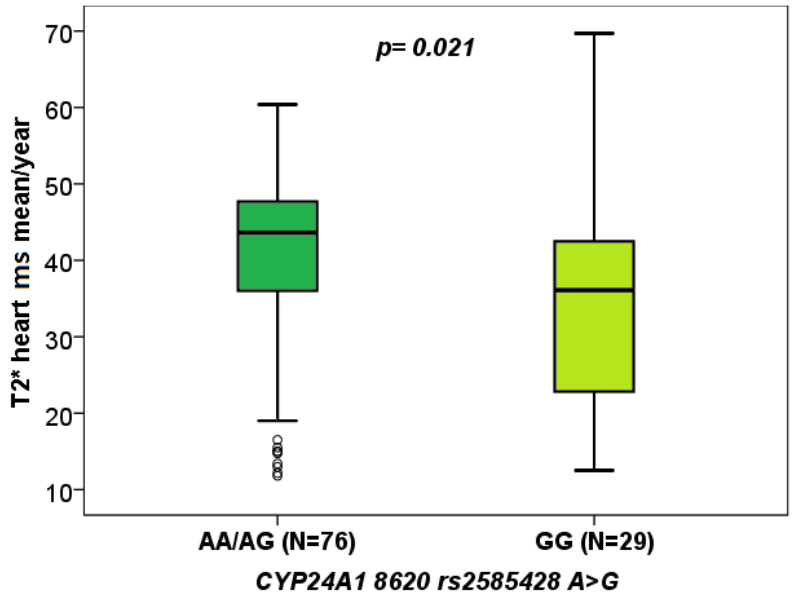

Figure 33 Influence of *CYP24A1* 8620 SNP on T2* values (ms mean/year).
***CYP24A1* 8620 AA/AG (N=76; median value 43.60 ms mean/year; IQR 35.95-47.70 ms mean/year) versus GG (N=29; median value 36.10 ms mean/year; IQR 22.75-42.90 ms mean/year).**

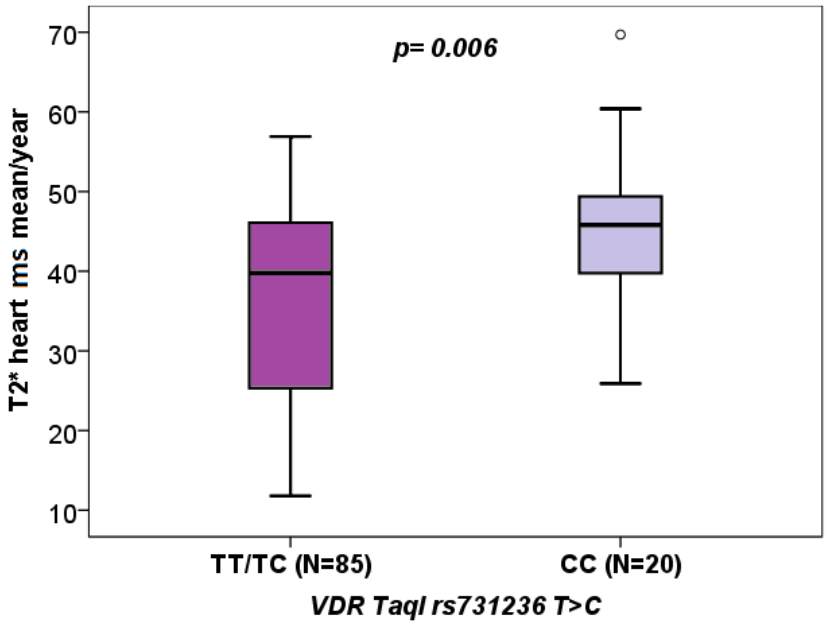

Figure 34 Influence of *VDR* TaqI SNP on T2* values (ms mean/year).
***VDR* TaqI TT/TC (N=85; median value 39.80 ms mean/year; IQR 24.99-46.10 ms mean/year) versus CC (N=20; median value 45.80 ms mean/year; IQR 39.28-49.40 ms mean/year).**

*2.5 Factors able to predict cardiac T2*cut-off*

Only serum ferritin (*p*= 0.007; Exp(B)= 0.999; IC95%: 0.99; 1) had a significant *p value* in logistic regression model (Table 17).

		UNIVARIATE	*q*	MULTIVARIATE
FACTOR	***GENOTYPE***	***p; ExpB* (IC95%)**		***p; ExpB* (IC95%)**
Age		**0.081; 0.911 (0.82; 1.01)**		0.098; 0.901 (0.80;1.02)
Gender		**0.191; 0.419 (0.11; 1.55)**		0.760; 0.733 (0.10; 5.36)
BMI		0.831; 1.023 (0.83; 1.26)		
Ethnicity		0.600; 0.651 (0.10; 3.79)		
DFX dose (mg/Kg/day)		**0.269; 0.947 (0.86; 1.04)**		0.175; 0.907 (0.79; 1.04)
Serum ferritin (ng/mL)		**0.008; 0.999 (0.99; 1)**		**0.007; 0.999 (0.99; 1)**
UGT1A1 -364	***CT/TT***	0.634; 0.705 (0.17; 2.97)	0.770	
	TT	0.406; 2.528 (0.28; 22.57)	0.767	
UGT1A1 -66	***AG/GG***	0.684; 0.772 (0.22; 2.69)	0.802	
	GG	0.805; 1.333 (0.14; 13.03)	0.912	
UGT1A3 -751	***CT/TT***	0.406; 0.396 (0.04; 3.53)	0.767	
	TT	0.558; 1.481 (0.40; 5.51)	0.825	
CYP1A1 -27+606	***CA/AA***	0.411; 2.222 (0.33; 14.89)	0.735	
	AA	0.955; 0.964 (0.27; 3.40)	0.955	
CYP1A1*1189	***TC/CC***	0.245; 0.483 (0.14; 1.65)	0.595	
	CC	0.243; 0.293 (0.04; 2.30)	0.636	
CYP1A2 -9-154	***AC/CC***	0.379; 1.800 (0.49; 6.66)	0.758	
	CC	0.418; 0.310 (0.02; 5.30)	0.711	
CYP1A2 1548	***CT/TT***	**0.144; 3.64 (0.64; 20.59)**	0.612	0.992; 1.023 (0.10; 103.08)
	TT	0.684; 1.296 (0.37; 4.52)	0.802	
CYP2D6 1457	***CG/GG***	0.600; 1.625 (0.26; 9.99)	0.756	
	GG	0.578; 1.425 (0.41; 4.96)	0.819	
ABCC2 1249	***GA/AA***	0.999		
	AA	0.828; 0.869 (0.25; 3.08)	0.853	
ABCG2 421	***GA***	0.684; 1.022 (0,92; 1.14)	0.802	
ABCG2 1194+928	***TC/CC***	**0.191; 0.419 (0.11; 1.55)**	0.649	0.295; 0.396 (0.07; 2.24)
	CC	0.999		
CYP27B1 +2838	***CT/TT***	0.242; 2.659 (0.52; 13.70)	0.686	
	TT	0.322; 1.852 (0.55; 6.27)	0.684	
CYP27B1 -1260	***GT/TT***	**0.113; 0.363 (0.10; 1.27)**	0.754	0.430; 0.467 (0.07; 2.24)
	TT	0.243; 0.293 (0.04; 2.30)	0.636	
CYP24A1 8620	***AG/GG***	0.816; 1.193 (0.27; 5.29)	0.895	
	GG	0.580; 0.697 (0.19; 2.51)	0.789	
CYP24A1 22776	***CT/TT***	0.479; 0.550 (0.11; 2.88)	0.740	
	TT	0.479; 1.818 (0.35;, 9.52)	0.776	
CYP24A1 3999	***TC/CC***	**0.130; 2.875 (0.73; 11.14)**	0.884	0.197; 4.374 (0.41; 74.61)
	CC	0.592; 0.714 (0.21; 2.44)	0.774	
FokI	***TC/CC***	0.242; 2.66 (0.52; 13.70)	0.686	
	CC	0.820; 1.150 (0.34; 3.85)	0.871	

Cdx2	***AG/GG***	0.999		
	GG	**0.082; 0.286 (0.07; 1.17)**	1.394	0.639; 0.619 (0.08; 4.62)
ApaI	***CA/AA***	0.221; 22.47 (0.58; 10.47)	0.683	
	AA	**0.178; 2.640 (0.64; 10.85)**	0.672	0.681; 0.581 (0.04; 7.76)
TaqI	***TC/CC***	**0.064; 3.300 (0.93; 11.68)**	2.176	0.654; 1.941 (0.11; 35.25)
	CC	0.999		
BsmI	***GA/AA***	**0.095; 2.909 (0.83; 10.17)**	0.808	0.133; 4.135 (0.065; 26.35)
	AA	0.313; 2.323 (0.45; 11.96)	0.709	
GC 1296	***TG/GG***	**0.085; 0.317 (0.09; 1.17)**	0.963	0.529; 0.440 (0.04; 5.36)
	GG	**0.143; 0.329 (0.07; 1.46)**	0.695	0.121; 0.224 (0.03; 1.49)

Table 17 Factors, in univariate and multivariate logistic regression analyses, able to predict cardiac T2* cut-off (>7 ms). Significant q = 0.0098.

3. Role of deferasirox and vitamin D pharmacogenetics on liver iron accumulation.

3.1 Study population

One-hundred and five patients, treated with DFX, have been enrolled. Our cohort demographical, clinical and pharmacokinetic features were resumed in Table 15.

3.2 Hardy-Weinberg and Linkage Disequilibrium analyses

All the SNPs were in Hardy-Weinberg equilibrium (Table 16). LD analysis was shown in Figure 27.

3.3 Effect of UGT1A1, UGT1A3, CYP1A1, CYP1A2, CYP2D6, ABCC2 and ABCG2 SNPs on liver stiffness.

UGT1A1 -364 CT/TT (p= 0.005, Figure 35) and *UGT1A3* -751 TT (p= 0.009, Figure 36) influenced liver stiffness values. *UGT1A1* -364 CC (N=43) genotype showed a median liver stiffness value of 5.10 KPa mean/year (IQR 4.20 - 6.40 KPa mean/year), whereas CT/TT (N=62) showed 6.15 KPa mean/year (IQR 4.90 - 8.93 KPa mean/year) (Figure 35); *UGT1A3* -751 CC/CT (N=73) group median liver stiffness value was 6.10 KPa mean/year (IQR 4.85 - 8.53 KPa mean/year) and TT (N=32) one was 4.95 KPa mean/year (IQR 4.13 - 8.94 KPa mean/year) (Figure 36).

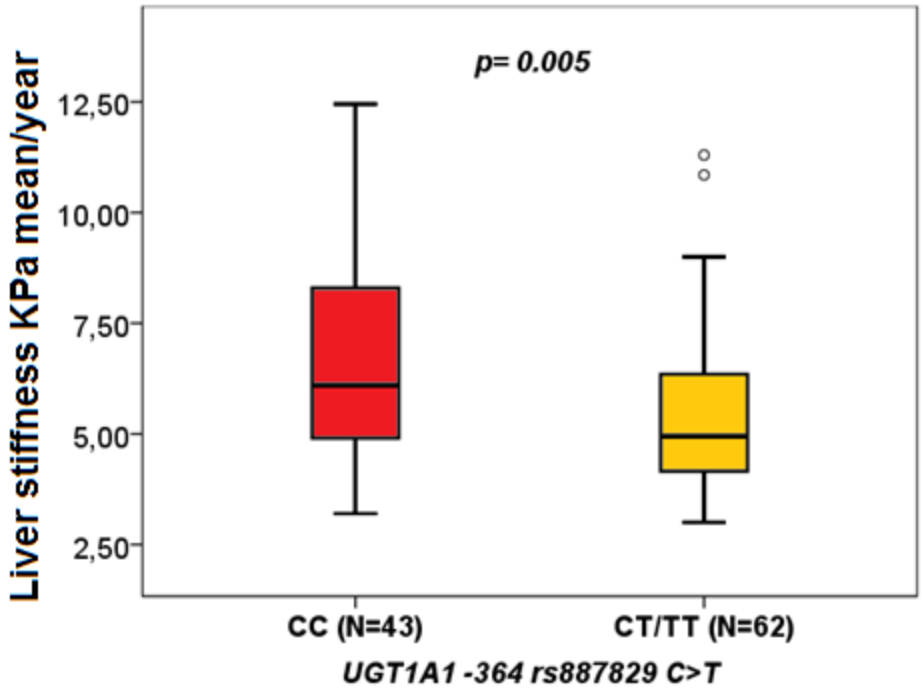

Figure 35 Influence of *UGT1A1* -364 SNP on liver stiffness values (KPa mean/year).
***UGT1A1* -364 CC (N=43; median value 5.10 KPa mean/year; IQR 4.20 - 6.40 KPa mean/year) versus CT/TT (N=62; versus median value 6.15 KPa mean/year; IQR 4.90 - 8.93 KPa mean/year).**

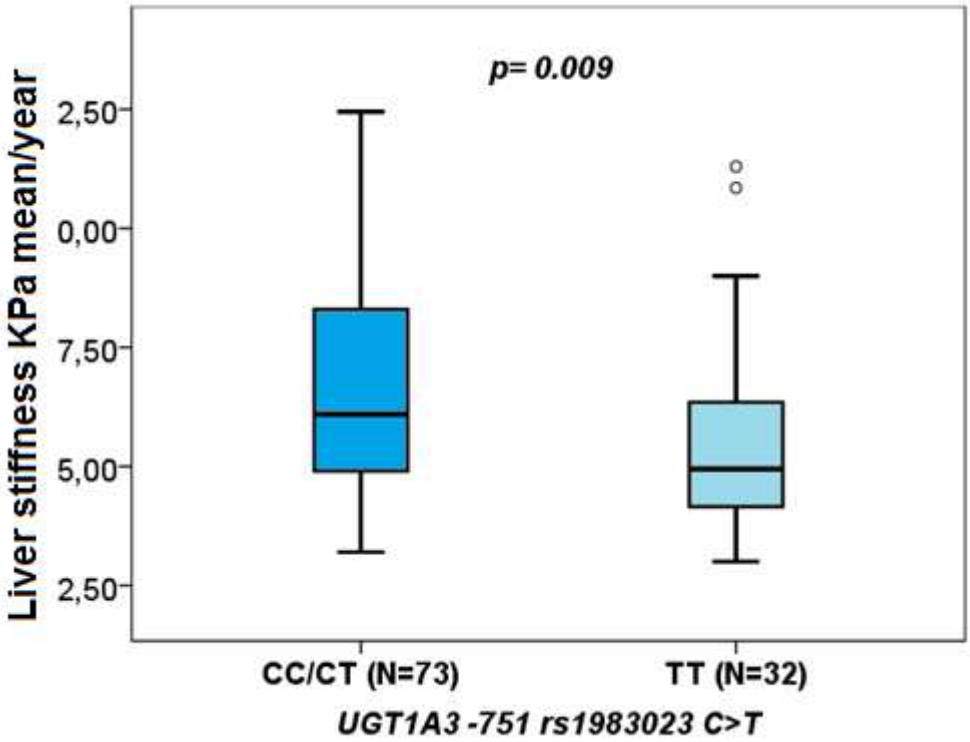

Figure 36 Influence of *UGT1A3* -751 SNP on liver stiffness values (KPa mean/year).
***UGT1A3* -751 CC/CT (N=73; median value 6.10 KPa mean/year; IQR 4.85 - 8.53 KPa mean/year) versus TT (N=32; median value 4.95 KPa mean/year; IQR 4.13 - 8.94 KPa mean/year).**

3.4 Effect of VDR, CYP24A1, CYP27B1 and GC SNPs on liver stiffness.

CYP27B1 -1260 GT/TT (p= 0.010, Figure 37), *VDR* TaqI CC (p= 0.016, Figure 38), *VDR* BsmI AA (p= 0.015, Figure 39) and *GC* 1296 TG/GG (p= 0.042, Figure 40) genotypes were related to liver stiffness values. *CYP27B1* -1260 GG (N=58) genotype showed 5.15 KPa mean/year (IQR 4.30 - 6.60 KPa mean/year) median liver stiffness value, whereas GT/TT (N=47) had 6.30 KPa mean/year (IQR 4.90 - 9.00 KPa mean/year) (Figure 37); *VDR* TaqI TT/TC (N=85) group median Cmin was 5.75 KPa mean/year (IQR 4.79 - 8.53 KPa mean/year) and CC (N=20) one was 4.70 KPa mean/year (IQR 3.56 - 6.70 KPa mean/year) (Figure 38); considering *VDR* BsmI, median Cmin was 14.430 KPa mean/year (IQR 0-85.95 KPa mean/year) for GG/GA (N=83) and 5.70 KPa mean/year (IQR 4.80 – 8.75 KPa mean/year) for AA (N=22) (IQR 3.69 - 6.45 KPa mean/year) (Figure 39); eventually *GC* 1296 TT (N=44) group median liver stiffness value was 5.23 KPa mean/year (IQR 4.21 - 6.80 KPa mean/year) and TG/GG (N=61) was 5.75 KPa mean/year (IQR 4.90 - 8.53 KPa mean/year) (Figure 40).

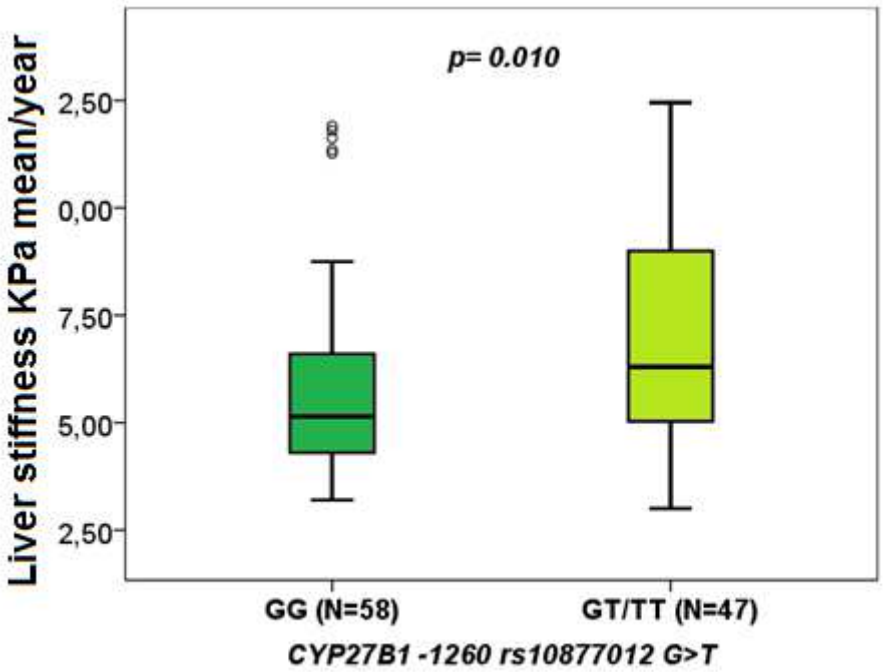

Figure 37 Influence of *CYP27B1* -1260 SNP on liver stiffness values (KPa mean/year). *CYP27B1* -1260 GG (N=58; median value 5.15 KPa mean/year; IQR 4.30 - 6.60 KPa mean/year) versus GT/TT (N=47; median value 6.30 KPa mean/year; IQR 4.90 - 9.00 KPa mean/year).

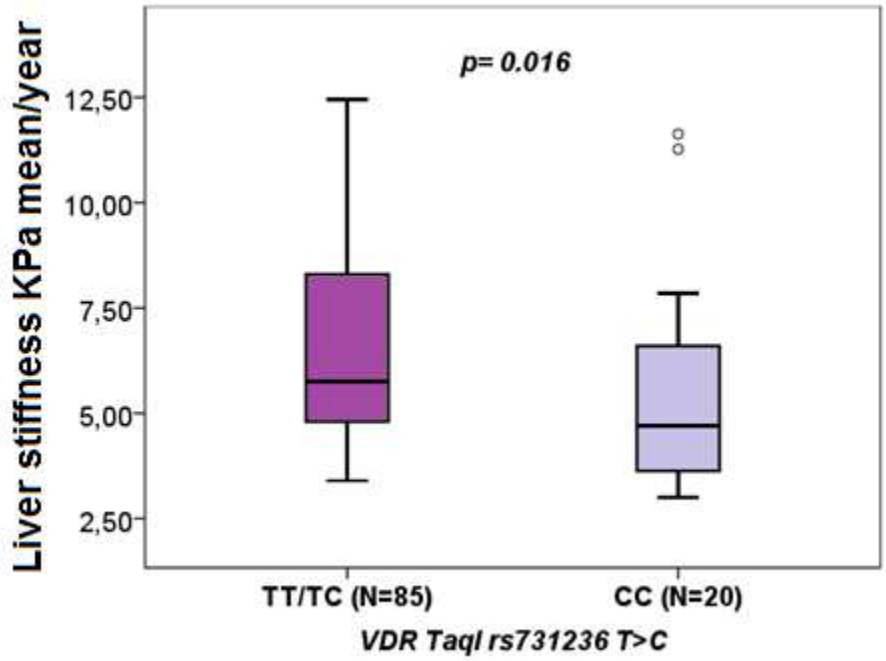

Figure 38 Influence of *VDR* TaqI SNP on liver stiffness values (KPa mean/year).
***VDR* TaqI TT/TC (N=85; median value 5.75 KPa mean/year; IQR 4.79 - 8.53 KPa mean/year) versus CC (N=20; median value 4.70 KPa mean/year; IQR 3.56 - 6.70 KPa mean/year).**

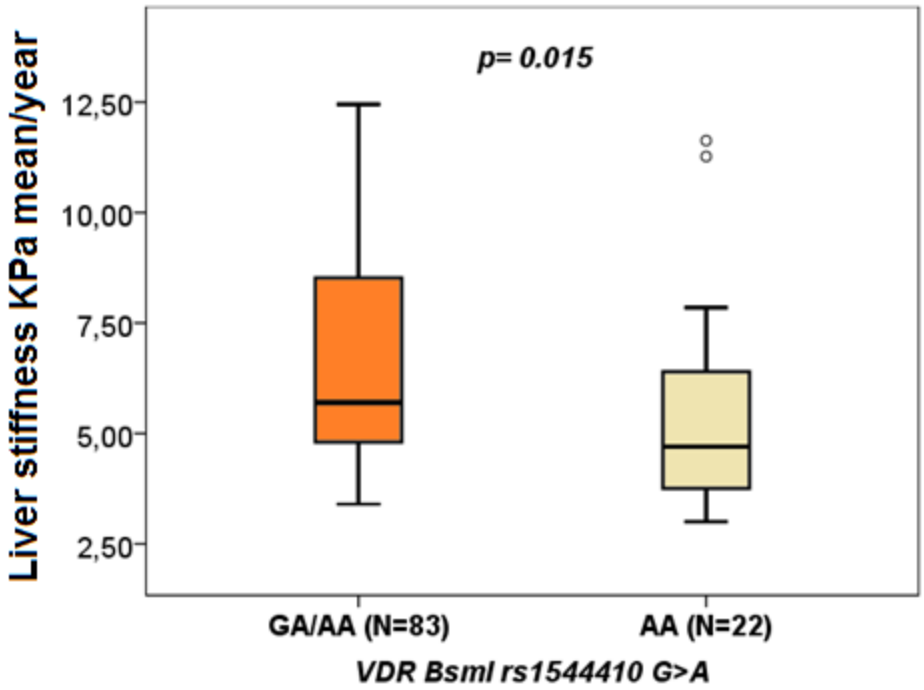

Figure 39 Influence of *VDR* BsmI SNP on liver stiffness values (KPa mean/year).
***VDR* BsmI GG/GA (N=83; median value 5.70 KPa mean/year; IQR 4.80 – 8.75 KPa mean/year) versus AA (N=22; median value 4.70 KPa mean/year; IQR 3.69 - 6.45 KPa mean/year).**

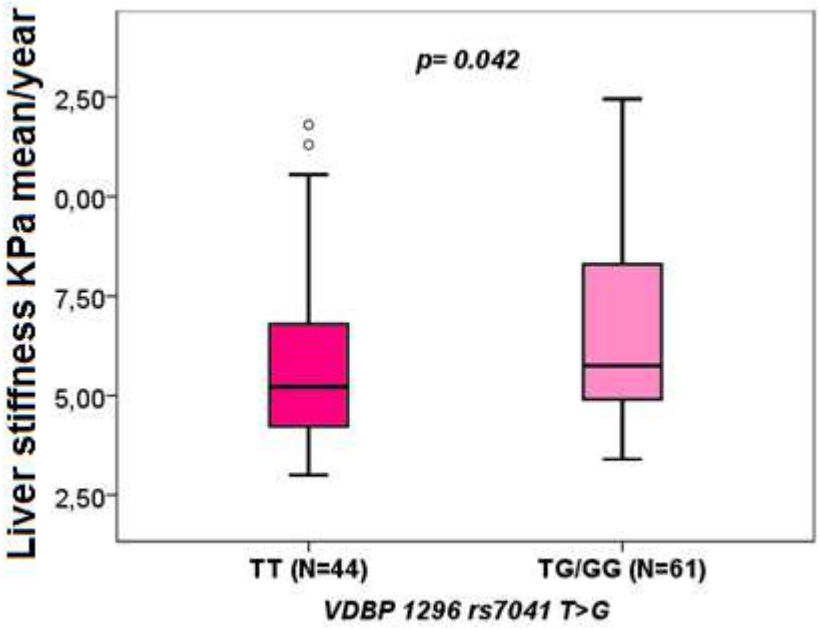

Figure 40 Influence of *GC* 1296 SNP on liver stiffness values (KPa mean/year). *GC* 1296 TT (N=44; median value 5.23 KPa mean/year; IQR 4.21 - 6.80 KPa mean/year) versus TG/GG (N=61; median value 5.75 KPa mean/year; IQR 4.90 - 8.53 KPa mean/year).

3.5 Factors able to predict liver stiffness cut-off

Serum ferritin (*p*= 0.001; Exp(B)= 0.999; IC95%: 0.99; 1) and *CYP27B1* -1260 GT/TT (*p*= 0.016; β= 0.297; IC95%: 0.11; 0.80) has been retained in logistic regression model (Table 18).

		UNIVARIATE	*q*	MULTIVARIATE
FACTOR	***GENOTYPE***	***p; ExpB* (IC95%)**		***p; ExpB* (IC95%)**
Age		**0.191; 0.957 (0.90; 1.02)**		0.058; 0.929 (0.86; 1.01)
Gender		**0.139; 0.514 (0.21; 1.24)**		0.480; 0.693 (0.25; 1.92)
BMI		0.298; 1.079 (0.94; 1.24)		
Ethnicity		0.699; 0.776 (0.22; 2.80)		
DFX dose (mg/Kg/day)		0.955; 1.002 (0.94; 1.07)		
Serum ferritin (ng/mL)		**0.001; 0.999 (0.99; 1)**		**0.001; 0.999 (0.99; 1)**
UGT1A1 -364	***CT/TT***	0.471; 0.717 (0.29; 1.77)	1.016	
	TT	0.497; 1.466 (0.49; 4.41)	1.019	
UGT1A1 -66	***AG/GG***	0.317; 0.636 (0.26; 1.54)	0.928	
	GG	**0.108; 5.524 (0.69; 44.52)**	0.886	0.195; 4.236 (0.48; 37.67)
UGT1A3 -751	***CT/TT***	0.514; 0.670 (0.20; 2.23)	1.004	
	TT	0.592; 1.1294 (0.50; 3.23)	0.971	
CYP1A1 -27+606	***CA/AA***	0.641; 0.722 (0.18; 2.83)	1.011	

	AA	0.659; 0.824 (0.35; 1.95)	1.001	
CYP1A1*1189	***TC/CC***	**0.106; 0.492 (0.21; 1.61)**	1.087	0.203; 0.528 (0.29; 1.41)
	CC	0.791; 0.789 (0.14; 4.55)	1.046	
CYP1A2 -9-154	***AC/CC***	0.949; 1.029 (0.43; 2.48)	0.973	
	CC	**0.181; 0.189 (0.02; 2.17)**	0.742	0.806; 0.627 (0.02; 25.80)
CYP1A2 1548	***CT/TT***	0.641; 0.722 (0.18; 2.83)	1.011	
	TT	0.947; 1.032 (0,41; 2.60)	0.996	
CYP2D6 1457	***CG/GG***	0.851; 1.128 (0.32; 3.99)	1.057	
	GG	0.317; 1.571 (0.65; 3.81)	0.928	
ABCC2 1249	***GA/AA***	0.853; 0.795 (0.07; 9.10)	1.029	
	AA	0.492; 1.357 (0,57; 3.24)	1.016	
ABCG2 421	***GA***	0.555; 0.947 (0.79; 1.3)	0.989	
ABCG2 1194+928	***TC/CC***	0.578; 0.785 (0.34; 1.84)	0.987	
	CC	0.405; 0.565 (0.15; 2.17)	0.977	
CYP27B1 +2838	***CT/TT***	**0.142; 2.429 (0.74; 7.95)**	0.832	0.856; 1.161 (0.23; 5.83)
	TT	**0.086; 2.129 (0.90; 5.05)**	1.763	0.576; 1.65 (0.29;9.52)
CYP27B1 -1260	***GT/TT***	**0.017; 0.345 (0.14; 0.83)**	0.697	**0.016; 0.297 (0.11; 0.80)**
	TT	0.916; 0.926 (0.22; 3.85)	1.073	
CYP24A1 8620	***AG/GG***	0.935; 0.954 (0.31; 2.96)	1.065	
	GG	0.535; 1.364 (0.51; 3.64)	0.997	
CYP24A1 22776	***CT/TT***	0.332; 0.602 (0.22; 1.68)	0.907	
	TT	0.433; 0.684 (0.27; 1.77)	0.986	
CYP24A1 3999	***TC/CC***	0.749; 1.192 (0.41; 3.50)	1.097	
	CC	**0.188; 0.563 (0.24; 1.33)**	0.701	0.967; 1.023 (0.35; 3.01)
FokI	***TC/CC***	0.771; 0.815 (0.21; 3.24)	1.054	
	CC	0.388; 0.685 (0.29; 1.62)	0.994	
Cdx2	***AG/GG***	1; 1 (0.29; 3.48)	1.000	
	GG	0.242; 1.664 (0.71; 3.91)	0.827	
ApaI	***CA/AA***	0.941; 1.038 (0.38; 2.83)	1.043	
	AA	**0.116; 2.250 (0,82; 6.19)**	0.793	0.986; 0.986 (0.20; 4.82)
TaqI	***TC/CC***	0.796; 0.889 (0.36; 2.17)	1.020	
	CC	**0.147; 2.638 (0.71; 9.77)**	0.753	0.953; 0.940 (0.12; 7.36)
BsmI	***GA/AA***	0.769; 0.889 (0.36; 2.17)	1.087	
	AA	**0.093; 3.054 (0.83; 11.22)**	1.271	0.542; 1.590 (0.36; 7.06)
GC 1296	***TG/GG***	0.262; 0.603 (0.25; 1.46)	0.826	
	GG	**0.151; 0.448 (0.15; 1.34)**	0.688	0.291; 0.510 (0.15; 1.78)

Table 18 Factors, in univariate and multivariate logistic regression analyses, able to predict liver stiffness cut-off (< 7 KPa). Significant q = 0.0098.

*3.6 Effect of pharmacogenetic on hepatic T2**

Mann Whitney tests revealed no genetic factors associated to liver T2* values (data not shown).

3.7 Factors able to predict hepatic T2 cut-off*

Regression analysis showed the predictive role of serum ferritin (p< 0.001; Exp(B)= 0.999; IC95%: 0.99; 1) and *UGT1A1 -364* CT/TT (p= 0.018; Exp(B)=5.080; IC95%: 1.33; 19.48) (Table 19).

		UNIVARIATE	***q***	**MULTIVARIATE**
FACTOR	***GENOTYPE***	***p; ExpB* (IC95%)**		***p; ExpB* (IC95%)**
Age		0.768; 1.012 (0.94; 1.09)		
Gender		0.829; 0,890 (0.31; 2.55)		
BMI		**0.074; 1.194 (0.98; 1.45)**		0.054; 1.257 (0.99; 1.59)
Ethnicity		0.287; 0.379 (0.06; 2.62)		
DFX dose (mg/Kg/day)		**0.109; 0.933 (0.86; 1.02)**		0.865; 1.013 (0.88; 1.17)
Serum ferritin (ng/mL)		**0.001; 0.999 (0.99; 1)**		**<0.001; 0.999 (0.99; 1)**
UGT1A1 -364	***CT/TT***	**0.060; 2.852 (0.96; 8.15)**	1.110	**0.018; 5.080 (1.33; 19.48)**
	TT	0.256; 3.704 (0.39; 35.42)	1.052	
UGT1A1 -66	***AG/GG***	**0.197; 2.206 (0.66; 7.34)**	1.041	0.148; 0.178 (0.02; 1.85)
	GG	**0.073; 7.29 (0.83; 63.79)**	0.675	0.289; 3.838 (0.32; 46.10)
UGT1A3 -751	***CT/TT***	0.221; 0.347 (0.06; 1.89)	1.022	
	TT	0.298; 0.558 (0,19; 1.67)	0.919	
CYP1A1 -27+606	***CA/AA***	0.504; 1.891 (0.29; 12.28)	0.981	
	AA	0.625; 0.762 (0.26; 2.27)	1.051	
CYP1A1*1189	***TC/CC***	0.434; 0.649 (0.22; 1.92)	1.147	
	CC	0.999		
CYP1A2 -9-154	***AC/CC***	0.985; 1.011 (0.35; 2.95)	0.985	
	CC	0.999		
CYP1A2 1548	***CT/TT***	0.287; 2.636 (0.44; 15.72)	1.062	
	TT	0.783; 0.861 (0.30; 2.49)	0.999	
CYP2D6 1457	***CG/GG***	0.820; 1.217 (0.22; 6.62)	0.948	
	GG	**0.037; 3.296 (1.08; 10.09)**	1.369	0.519; 1.700 (0.34; 8.52)
ABCC2 1249	***GA/AA***	0.899; 0.833 (0,05; 14.01)	0.950	
	AA	0.453; 0.655 (0.22; 1.98)	1.117	
ABCG2 421	***GA***	0.287; 0.469 (0.12; 1.89)	1.062	
ABCG2 1194+928	***TC/CC***	**0.071; 0.366 (0,12; 1.09)**	0.876	0.459; 0.565 (0.12; 2.66)
	CC	0.792; 1.286 (0,20; 8.35)	0.977	
CYP27B1 +2838	***CT/TT***	**0.161; 3.452 (0.61; 19.54)**	1.489	0.386; 0.272 (0.01; 5.16)
	TT	0.940; 1.041 (0.37; 2.96)	0.966	
CYP27B1 -1260	***GT/TT***	0.543; 0.722 (0.25; 2.06)	0.957	
	TT	0.855; 0.828 (0.11; 6.32)	0.959	
CYP24A1 8620	***AG/GG***	0.459; 0.623 (0.16; 2.42)	1.061	
	GG	0.886; 0.920 (0.30; 2.87)	0.964	
CYP24A1 22776	***CT/TT***	0.732; 1.250 (0.35; 4.74)	1.083	

	TT	0.324; 0.522 (0,14; 1.90)	0.922	
CYP24A1 3999	***TC/CC***	0.758; 0,816 (0.23; 2.96)	1.039	
	CC	**0.185; 0.477 (0.16; 1.43)**	1.141	0.395; 0.370 (0.04; 3.65)
FokI	***TC/CC***	**0.161; 3.452 (0.61; 19.54)**	1.191	0.534; 2.138 (0.20; 23.43)
	CC	0.716; 1.214 (0,43; 3.45)	1.104	
Cdx2	***AG/GG***	0.792; 0.778 (0,12; 5.05)	0.977	
	GG	0.296; 0.565 (0,19; 1.65)	0.996	
ApaI	***CA/AA***	0.695; 0.758 (0.19; 3.04)	1.118	
	AA	0.750; 1.193 (0,40; 3.53)	1.067	
TaqI	***TC/CC***	0.470; 1.552 (0,49; 4.76)	1.023	
	CC	0.759; 0.808 (0.21; 3.17)	1.003	
BsmI	***GA/AA***	0.490; 0.670 (0.22; 2.09)	1.007	
	AA	0.812; 1.159 (0.34; 3.91)	0.969	
GC 1296	***TG/GG***	0.514; 1.417 (0.50; 4.03)	0.951	
	GG	**0.179; 0.357 (0.08; 1.60)**	1.325	0.115; 0.205 (0.03; 1.47)

Table 19 Factors, in univariate and multivariate logistic regression analyses, able to predict hepatic T2* cut-off (> 6.3 ms). Significant q = 0.0098.

DISCUSSION

Thalassaemia is a significant health problem in the 71% of 229 countries; approximately 7% of the world population is carrier of this disease and about 56,000 have a major form, including at least 30,000 who need regular transfusions to survive and 5,500 who die perinatally due to α-thalassaemia major [159]. These disorders belong to a heterogeneous group of haemoglobin derangement in which the normal haemoglobin production is partly or completely suppressed as a result in one or more globin chains defective synthesis. Reduced or absent production of beta-globin chains, associated with nearly 300 genetic defects in and around the *beta-globin* gene, results in autosomal recessive beta-thalassaemia syndromes, the most clinically significant form [10]. It is by definition a transfusion dependent anaemia and iron overload is the leading cause of death and morbidity.

Since the correlation between iron burden and vitamin D deficiency has been demonstrated [123], our aim was to retrospectively evaluate the role of SNPs in genes encoding proteins involved in vitamin D metabolism (*CYP24A1* and *CYP27B1* genes), transport (*GC* gene) and activity (*VDR* gene) on DFX plasma pharmacokinetics, treatment response and on hepatic and cardiac iron overload.

1. Effect of vitamin D pathway gene polymorphisms on deferasirox pharmacokinetic and treatment outcome and on hepatic and cardiac iron overload

CYP24A1 (20q13.2) encodes 24-hydroxylase, dragged in vitamin D degradation; its high expression in prostate cancer cells has been observed [150, 151, 160]. Our findings showed the involvement of 22776 C>T, 3999 T>C and 8620 A>G gene SNPs in DFX pharmacokinetic and hepatic T2* parameters [152]. These three variants are located in intronic region; therefore, during the RNA processing, this kind of polymorphisms may result in alternative splice site, competing with the normal one, leading to a mature messenger RNA with improperly spliced intron sequences. In addition, intronic SNPs could be in high LD with others associated to various genes expression [161].

8620 polymorphism is significantly associated with prostate cancer risk [162]; our group recently suggested its predictive role on peg-interferon plus ribavirin treatment outcomes and S-telaprevir intracellular concentrations [163, 164]. Besides, GG genotype resulted as negative predictor of plasma ETA Cmax, suggesting an enhanced drug metabolism, leading to its minor extracellular concentration [165]. According to this hypothesis, we here observed an important influence on DFX pharmacokinetics: GG genotype had significantly lower Ctrough (p= 0.047; Figure 26A), AUC (p= 0.021; Figure 27), $t_{1/2}$ (p= 0.031; Figure 28) and Cmin (p= 0.010; Figure 29A) median values, than AA/AG group. Furthermore, GG profile resulted statistically significant in linear regression analysis (p= 0.031) as AUC negative predictor; however, the statistical significance was lost after Bonferroni correction, when we considered all the SNPs (Table 11) [152]. Carrying out the evaluation of cardiac iron burden, we showed significantly higher T2* values in patients with at least one wild-type allele (p= 0.021; Figure 33). CYP enzymes involved in vitamin D metabolism have been mapped in heart, making it plausible vitamin may acts as a cardiac intracrine or paracrine factor. Thus, normal circulating 25(OH)D substrate level is required to maintain an optimal

intracrine actions of 1,25(OH)2D, leading to a reduced risk of chronic diseases [166]. However, in literature there are no evidence about the 8620 gene variant and cardiac iron overload.

The 22776 C>T variant has been associated with decreased risk of prostate cancer recurrence/regression [167]. Although in literature there are no evidence about this SNP and drug pharmacokinetics, we observed significantly lower Cmin in TT carriers, compared to CC/CT (p= 0.011; Figure 29C); its role is confirmed by the multivariate regression analysis, in which it remained as Cmin negative predictor factor (p= 0.036; Table 12) [152].

The 3999 T>C is less than 4 kb upstream of *CYP24A1* gene in a promoter associated region, thus it probably operates by changing gene expression. It was recently associated with increased leukocyte count in Chinese gestational diabetes mellitus and with prostate cancer risk [162, 168, 169]. Hallau *et al.* identified C allele over-representation in adults with severe atopic dermatitis compared with healthy controls [170]. Higher C frequency has been identified in allergic asthma patients, in whom beneficial functions of vitamin D signalling are known [171-173]. This allele is also broadly associated with *CYP24A1* enhanced expression in frontal cortex, but not white matter, providing a genetic link among multiple sclerosis and vitamin D metabolism and predicting the active form physiologically protective role [168]. In our population, CC genotype resulted significantly able to influence Ctrough (p= 0.010; Figure 26B) and Cmin (p= 0.040; Figure 29B) median values: carrier of at least one T allele had higher concentrations than homozygous mutant ones. In regression analysis, CC profile remained, with DFX dose (p= 0.013), as Tmax negative predictor (p= 0.008) (Table 13) [152].

CYP27B1 gene (12q14.1) encodes a member of the CYP monooxygenases family (the 1α-hydroxylase enzyme), localized to the inner mitochondrial membrane of renal cells; here it activates 25(OH)D3 to 1,25(OH)2D3 [174]. Available data on the *CYP27B1* -1260 promoter polymorphism are inconsistent: Lange and colleagues suggested its influence on 1–25(OH)2 vitamin D serum concentrations, in contrast of what observed by Kitanaka *et al.* [175-177]. We suggested a correlation among T allele and raised liver stiffness levels: Mann-Whitney test reported higher

median values in GT/TT group (p= 0.010; Figure 37), compared to GG and, in the regression analysis, it resulted as liver stiffness normal values negative predictor (p= 0.016; Table 18).

VDR mediates most of calcitriol biological effects; it is a ligand-activated transcription factor [178-180]. Its gene maps on chromosome 12q13.11 and consists of 9 exons with at least 6 isoforms of exon 1 and encodes a 427 amino acids protein [181]; alternative splicing results in multiple transcript variants, thus different length proteins [182]. It is expressed in at least 37 tissues such as pancreatic β cells, muscle, cardiovascular, brain and lung [183, 184]. By binding vitamin D, VDR modulates several physiological systems: neural, immune, endocrine, calcium and phosphorous homeostasis, apoptosis and cell differentiation [140, 185]. Several potentially functional *VDR* genes SNPs were identified and related to different diseases, as advanced non-small-cell lung cancer, prostate cancer, end-stage renal disease, primary biliary cirrhosis and autoimmune hepatitis [150].

Rs11568820 variant is commonly known as Cdx2, due to its location in the binding site of transcription factor Cdx2. Its A to G base substitution eliminates the Cdx binding site and reduces transcriptional activity of VDR to 70% of the A allele [186]. Moreover, GG/GA genotypes were associated with increased midazolam clearance as compared to AA [187]. In our cohort A allele resulted, together with *GC* 1296 variant (TT/TG genotypes), as AUC efficacy cut-off negative predictor (Table 14) [69, 152]; this was probably due to a non-reduced VDR transcriptional activity, maintenance of normal vitamin D pathway, higher vitamin D levels and subsequently minor iron overload, which consists in treatment efficacy likelihood [123].

BsmI intronic variant has no functional consequences [150]. It could influence *VDR* gene expression, with a consequent disruption of a splice site for *VDR* mRNA transcription, resulting in trenched or alternatively spliced protein product [188]. In a previous study, we found that AA genotype is a predictive factor of ribavirin-induced anaemia at 2 weeks, presuming a gene enhanced transcriptional activity [163]. Moreover, we observed a raising rifampicin intracellular maximum concentration at week 2 of treatment, probably due to a major presence of an influx transporter with

a VDR-dependent expression [189]. Evaluating DFX treatment and liver stiffness, we observed reduced median values in AA genotype (p= 0.015; Figure 39).

The non synonymous exonic variant TaqI is located on CpG island and the C allele is always methylated [190]. A correlation among T allele and rifampicin plasma maximum concentration at week 2 of treatment has been reported, supposing a role of this variant on the expression of an efflux transporter, such as ABCB1 [189, 191]. Here, CC resulted associated with lower liver stiffness median values, compared to TC/CC genotype group (p= 0.016; Figure 38). In addition, CC was associated with higher cardiac T2*, compared to TC/CC genotype group (p= 0.006; Figure 34).

GC gene (4q12-q13) is a multigene family member that includes albumin, α-fetoprotein and α-albumin/afamin [192]. Various *GC* genetic variants are known; the two most common polymorphisms, 1296 T>G (rs7041, Glu432Asp) and 1307 C>A (rs4588, Thr436Lys) are localized in exon 11 and they are in complete LD [193]. Circulating VDBP levels are not influenced by rs7041 variant, however, considering 1296/1307 diplotype, there is a slight transport increase in TG/CA, compared to TT/CA. Probably, lysine to threonine substitution at position 436 eliminates an O-glycosylation site from the molecule and the loss of glycosylation affect VDBP half-life. Moreover, glutamine to asparagine change in 432 position, influences the extent of O-glycosylation at the 436. It is not known how changes in VDBP molecule affect its serum concentration, but the described substitutions could result in altered rates of transcription, changes in mRNA stability or in a self-clearance of the protein [194]. A transmission disequilibrium testing of more than 200 families from the German Asthma Family Study found a significant 1296 T>G association with total serum IgE (p< 0.03) [195]. Moreover, in a recent study on Caucasian women, TT genotype resulted associated with an increased risk of breast cancer, compared to healthy controls [196]. We observed a negative influence of TT/TG genotype group (p= 0.010; Table 14) on DFX treatment outcome prediction (cut-off of 360 µg/mL/h) [152]. Furthermore, TT genotype resulted weakly associated with lower liver stiffness values as compared to TG/GG genotype group (p= 0.042; Figure 40).

2. Effect of SNPs in genes encoding for proteins involved in DFX metabolism on hepatic and cardiac iron burden

CYP1A1 gene (15q24.1) encodes a member of the CYP superfamily enzymes. The proteins are monooxygenases able to catalyze many reactions involved in drugs metabolism and cholesterol, steroids and other lipids synthesis. *CYP1A1* *1189 T>C intronic variant has been related to an increased activity in carrier of C allele [95-97]. In addition, it has been associated to risk of lung, head, neck and oral cancers [197, 198]. Carried out analyses on DFX pharmacokinetics and efficacy, we observed higher creatinine levels and Tmax in TC/CC [59, 69]. Considering the effect on cardiac T2* parameter, TT/TC group showed raised median values, compared to CC genotype (p= 0.038; Figure 31).

The ABC transporter encoded by *ABCG2* gene (4q22.1), also known as *BCRP1* (breast cancer resistance protein), is expressed in the gastrointestinal tract and in liver and it is involved in absorption, distribution and excretion of many drugs. This gene SNPs have been related to changes in gene expression, cellular localization and substrate recognition of the protein; more than 24 variations have been reported [102, 199]. *ABCG2* 1194+928 C allele has been associated with a cumulative incidence of major molecular response in patients affected by chronic myelogenous leukaemia and treated with imatinib. It positively affects response to methotrexate in patients with psoriasis [109, 110]. In a study on DFX treatment in paediatrics, higher Vd median values in CC genotype has been observed, supporting a decreased efflux rate [81].

Another *ABCG2* gene variant, the missense SNP 421 G>A, has been related to different drug pharmacokinetics: AA genotype resulted in osuvastatin, atorvastatin, fluvastatin, simvastatin, sulfasalazine, sunitinib and imatinib higher plasma concentrations [103-108]. Moreover, this GA/AA genotype group was retained in multivariate linear regression analysis as predictive factor of longer DFX Tmax in paediatrics [81]. In this cohort, no patients with the homozygous mutant

genotype were present; however, we observed lower T2* values in GA carriers (p= 0.008; Figure 32).

The *UGT1A* gene cluster (2q37.1) encodes for a set of enzymes involved in the glucuronidation pathway, thus the conversion of lipophilic to water soluble molecules; moreover, UGT1A protein contributes to the bilirubin clearance regulation [68]. *UGT1A1* -364 C>T was associated with a reduction in enzyme activity of up to 70% [73-75, 78, 200, 201]. Our previous studies on DFX pharmacokinetics suggested a correlation between TT genotype and raised drug Ctrough levels, lower $t_{1/2}$ and reduced ferritin serum levels [58, 59, 69]. Here we observed lower liver stiffness values in CC carriers, compared to CT and TT ones (p= 0.005; Figure 35). Considering *UGT1A3*-751 T>C SNP, we reported reduced DFX exposure (AUC) and raised drug Vd in T allele carriers, hypothesizing an enhanced DFX via UGT elimination [59, 69]. This is confirmed by the lower liver stiffness showed in TT genotype carriers (p= 0.009; Figure 36); moreover T allele has been retained in regression model as hepatic T2* normal values negative predictor (p= 0.018; Table 19)

3. Effect of serum ferritin on hepatic and cardiac iron overload

Serum ferritin, measured through a drawn blood, is the easiest and the least expensive test used to evaluate iron overload, furthermore its levels correlate with total body ion burden and are still used to define DFX adequate and inadequate responders [57, 202]. DFX reduces serum ferritin levels in dose dependent manner and it stabilizes serum ferritin and liver iron concentrations when used in a dose of 20mg/kg/day [203]. In this study, serum ferritin levels resulted able to predict hepatic (p< 0.001; Table 19) and cardiac (p= 0.007; Table 17) T2* and liver stiffness (p= 0.001; Table 18) normal values. This probably suggests a minor iron entry in cardiac myocytes, when circulating ion levels are higher [204, 205].

CONCLUSIONS

To our knowledge, this is the first study aimed at evaluating the role of DFX and vitamin D pharmacogenetics on cardiac and hepatic iron accumulation and on drug pharmacokinetic and efficacy.

Our results indicated the influence of *CYP24A1* 22776, 3999 and 8620 variants on DFX pharmacokinetics. Furthermore, *VDR* Cdx2 and *GC* 1296 variants resulted as AUC efficacy cut-off predictors. Considering liver parameters, *UGT1A1* -364 and *CYP27B1* -1260 showed a predictive role on T2* and stiffness cut-offs, respectively. In addition *UGT1A1* -364 and *VDR* TaqI and BsmI, *GC* 1269 and *CYP27B1* -1260 polymorphisms influenced liver stiffness values. Eventually, we observe the association between *CYP1A1* +1189, *ABCG2* 421, *UGT1A1* -364, *UGT1A3* -751, *CYP24A1* 8620 and *VDR* TaqI variants and cardiac T2* parameter. We also highlighted the influence of serum ferritin levels on cardiac and hepatic iron burden prediction.

Larger prospective studies, incorporating other markers (such as *GC 1307* variant), vitamin D serum levels, and comparative studies with other diseases are warranted. Moreover, we had not evaluated calcitriol plasma levels (considering it is a retrospective study), but we think it is not a limitation because some factors could be confounding as sunlight exposition and seasonal variability, reduced alimentary sources of vitamin D and intestinal malabsorption. In our opinion, the use of genetic factors affecting vitamin D pathway should be the novel approach without the described above limitations. Eventually, we did not compare the obtained results of hepatic iron overload to that of liver biopsy. Despite this, the accuracy of transient elastografy and T2* magnetic resonance imaging for liver fibrosis evaluation in thalassaemia patients have been assessed in previous studies [19, 27, 29, 30, 206-208].

The discoveries of this research may be useful for personalized medicine field and the proposed method could be applied in other populations. For instance, DFX is used also in patients with

hereditary hemochromatosis, myelodysplastic syndromes and it may be a safe alternative to phlebotomy in selected patients [209-212].

REFERENCES

[1] Li Q, Li LY, Huang SW, Li L, Chen XW, Zhou WJ, et al. Rapid genotyping of known mutations and polymorphisms in beta-globin gene based on the DHPLC profile patterns of homoduplexes and heteroduplexes. Clin Biochem 2008;41:681-687.

[2] Galanello R, Origa R. Beta-thalassemia. Orphanet J Rare Dis 2010;5:11.

[3] Mader SS. Inquiry into Life, 8th edition, McGraw-Hill Higher Education ed; 1997.

[4] Thein SL, Menzel S. Discovering the genetics underlying foetal haemoglobin production in adults. Br J Haematol 2009;145:455-467.

[5] Tanner MA, Galanello R, Dessi C, Smith GC, Westwood MA, Agus A, et al. Combined chelation therapy in thalassemia major for the treatment of severe myocardial siderosis with left ventricular dysfunction. J Cardiovasc Magn Reson 2008;10:12.

[6] Aessopos A, Kati M, Meletis J. Thalassemia intermedia today: should patients regularly receive transfusions? Transfusion 2007;47:792-800.

[7] Taher A, Isma'eel H, Cappellini MD. Thalassemia intermedia: revisited. Blood Cells Mol Dis 2006;37:12-20.

[8] Rund D, Rachmilewitz E. Beta-thalassemia. N Engl J Med 2005;353:1135-1146.

[9] Quek L, Thein SL. Molecular therapies in beta-thalassaemia. Br J Haematol 2007;136:353-365.

[10] Thein SL. The molecular basis of beta-thalassemia. Cold Spring Harb Perspect Med 2013;3:a011700.

[11] Li CK. New trend in the epidemiology of thalassaemia. Best Pract Res Clin Obstet Gynaecol 2016;39:16-26.

[12] Abbaspour N, Hurrell R, Kelishadi R. Review on iron and its importance for human health. J Res Med Sci 2014;19:164-174.

[13] Sebastiani G, Walker AP. HFE gene in primary and secondary hepatic iron overload. World J Gastroenterol 2007;13:4673-4689.

[14] Queiroz-Andrade M, Blasbalg R, Ortega CD, Rodstein MA, Baroni RH, Rocha MS, et al. MR imaging findings of iron overload. Radiographics 2009;29:1575-1589.

[15] Saito H. Metabolism of Iron Stores. Nagoya J Med Sci 2014;76:235-254.

[16] Waldvogel-Abramowski S, Waeber G, Gassner C, Buser A, Frey BM, Favrat B, et al. Physiology of iron metabolism. Transfus Med Hemother 2014;41:213-221.

[17] Silva B, Faustino P. An overview of molecular basis of iron metabolism regulation and the associated pathologies. Biochim Biophys Acta 2015;1852:1347-1359.

[18] Marsella M, Borgna-Pignatti C. Transfusional iron overload and iron chelation therapy in thalassemia major and sickle cell disease. Hematol Oncol Clin North Am 2014;28:703-727, vi.

[19] Wood JC, Enriquez C, Ghugre N, Tyzka JM, Carson S, Nelson MD, et al. MRI R2 and R2* mapping accurately estimates hepatic iron concentration in transfusion-dependent thalassemia and sickle cell disease patients. Blood 2005;106:1460-1465.

[20] Siri-Angkul N, Chattipakorn SC, Chattipakorn N. Diagnosis and treatment of cardiac iron overload in transfusion-dependent thalassemia patients. Expert Rev Hematol 2018:1-9.

[21] Brissot P, Troadec MB, Bardou-Jacquet E, Le Lan C, Jouanolle AM, Deugnier Y, et al. Current approach to hemochromatosis. Blood Rev 2008;22:195-210.

[22] Anderson LJ, Holden S, Davis B, Prescott E, Charrier CC, Bunce NH, et al. Cardiovascular T2-star (T2*) magnetic resonance for the early diagnosis of myocardial iron overload. Eur Heart J 2001;22:2171-2179.

[23] Musallam KM, Motta I, Salvatori M, Fraquelli M, Marcon A, Taher AT, et al. Longitudinal changes in serum ferritin levels correlate with measures of hepatic stiffness in transfusion-independent patients with beta-thalassemia intermedia. Blood Cells Mol Dis 2012;49:136-139.

[24] Richardson KJ, McNamee AP, Simmonds MJ. Haemochromatosis: Pathophysiology and the red blood cell1. Clin Hemorheol Microcirc 2018;69:295-304.

[25] Batts KP. Iron overload syndromes and the liver. Mod Pathol 2007;20 Suppl 1:S31-39.

[26] Cournane S, Browne JE, Fagan AJ. The effects of fatty deposits on the accuracy of the Fibroscan(R) liver transient elastography ultrasound system. Phys Med Biol 2012;57:3901-3914.

[27] Sandrin L, Fourquet B, Hasquenoph JM, Yon S, Fournier C, Mal F, et al. Transient elastography: a new noninvasive method for assessment of hepatic fibrosis. Ultrasound Med Biol 2003;29:1705-1713.
[28] Bedossa P, Poynard T. An algorithm for the grading of activity in chronic hepatitis C. The METAVIR Cooperative Study Group. Hepatology 1996;24:289-293.
[29] Castera L, Forns X, Alberti A. Non-invasive evaluation of liver fibrosis using transient elastography. J Hepatol 2008;48:835-847.
[30] Tsochatzis EA, Gurusamy KS, Ntaoula S, Cholongitas E, Davidson BR, Burroughs AK. Elastography for the diagnosis of severity of fibrosis in chronic liver disease: a meta-analysis of diagnostic accuracy. J Hepatol 2010;54:650-659.
[31] Sharma SD, Fischer R, Schoennagel BP, Nielsen P, Kooijman H, Yamamura J, et al. MRI-based quantitative susceptibility mapping (QSM) and R2* mapping of liver iron overload: Comparison with SQUID-based biomagnetic liver susceptometry. Magn Reson Med 2016;78:264-270.
[32] Wood JC. Guidelines for quantifying iron overload. Hematology Am Soc Hematol Educ Program 2015;2014:210-215.
[33] Fovargue D, Nordsletten D, Sinkus R. Stiffness reconstruction methods for MR elastography. NMR Biomed 2018:e3935.
[34] Pennell DJ, Porter JB, Piga A, Lai YR, El-Beshlawy A, Elalfy M, et al. Sustained improvements in myocardial T2* over 2 years in severely iron-overloaded patients with beta thalassemia major treated with deferasirox or deferoxamine. Am J Hematol 2014;90:91-96.
[35] Chaudhary P, Pullarkat V. Deferasirox: appraisal of safety and efficacy in long-term therapy. J Blood Med;4:101-110.
[36] Lai YR, Liu RR, Li CF, Huang SL, Li Q, Habr D, et al. Efficacy of Deferasirox for the treatment of iron overload in Chinese thalassaemia major patients: results from a prospective, open-label, multicentre clinical trial. Transfus Med 2013;23:389-396.
[37] Naderi M, Sadeghi-Bojd S, Valeshabad AK, Jahantigh A, Alizadeh S, Dorgalaleh A, et al. A prospective study of tubular dysfunction in pediatric patients with Beta thalassemia major receiving deferasirox. Pediatr Hematol Oncol 2013;30:748-754.
[38] Cappellini MD. Exjade(R) (deferasirox, ICL670) in the treatment of chronic iron overload associated with blood transfusion. Ther Clin Risk Manag 2007;3:291-299.
[39] Neufeld EJ. Oral chelators deferasirox and deferiprone for transfusional iron overload in thalassemia major: new data, new questions. Blood 2006;107:3436-3441.
[40] Cunningham MJ, Macklin EA, Neufeld EJ, Cohen AR. Complications of beta-thalassemia major in North America. Blood 2004;104:34-39.
[41] Pennell DJ, Berdoukas V, Karagiorga M, Ladis V, Piga A, Aessopos A, et al. Randomized controlled trial of deferiprone or deferoxamine in beta-thalassemia major patients with asymptomatic myocardial siderosis. Blood 2006;107:3738-3744.
[42] Taher A, Sheikh-Taha M, Sharara A, Inati A, Koussa S, Ellis G, et al. Safety and effectiveness of 100 mg/kg/day deferiprone in patients with thalassemia major: a two-year study. Acta Haematol 2005;114:146-149.
[43] Farmaki K, Tzoumari I, Pappa C, Chouliaras G, Berdoukas V. Normalisation of total body iron load with very intensive combined chelation reverses cardiac and endocrine complications of thalassaemia major. Br J Haematol 2010;148:466-475.
[44] Novartis Pharmaceuticals. Exjade (deferasirox) tablets for oral suspension [prescribing information]. East Hanover (NJ): Novartis Pharmaceuticals 2006.
[45] Cappellini MD, Cohen A, Piga A, Bejaoui M, Perrotta S, Agaoglu L, et al. A phase 3 study of deferasirox (ICL670), a once-daily oral iron chelator, in patients with beta-thalassemia. Blood 2006;107:3455-3462.
[46] EPAR E. Exjade (deferasirox) Prescribing Information. Novartis Pharmaceuticals Corporation. 2007.
[47] Novartis. Exjade (deferasirox) tablets for oral suspension [prescribing information]. East Hanover (NJ): Novartis Pharmaceuticals 2006.

[48] Vichinsky E, Onyekwere O, Porter J, Swerdlow P, Eckman J, Lane P, et al. A randomised comparison of deferasirox versus deferoxamine for the treatment of transfusional iron overload in sickle cell disease. Br J Haematol 2007;136:501-508.
[49] Bruin GJ, Faller T, Wiegand H, Schweitzer A, Nick H, Schneider J, et al. Pharmacokinetics, distribution, metabolism, and excretion of deferasirox and its iron complex in rats. Drug Metab Dispos 2008;36:2523-2538.
[50] Hershko C, Konijn AM, Nick HP, Breuer W, Cabantchik ZI, Link G. ICL670A: a new synthetic oral chelator: evaluation in hypertransfused rats with selective radioiron probes of hepatocellular and reticuloendothelial iron stores and in iron-loaded rat heart cells in culture. Blood 2001;97:1115-1122.
[51] Nick H, Acklin P, Lattmann R, Buehlmayer P, Hauffe S, Schupp J, et al. Development of tridentate iron chelators: from desferrithiocin to ICL670. Curr Med Chem 2003;10:1065-1076.
[52] Waldmeier F, Bruin GJ, Glaenzel U, Hazell K, Sechaud R, Warrington S, et al. Pharmacokinetics, metabolism, and disposition of deferasirox in beta-thalassemic patients with transfusion-dependent iron overload who are at pharmacokinetic steady state. Drug Metab Dispos 2010;38:808-816.
[53] Mao Q, Unadkat JD. Role of the breast cancer resistance protein (ABCG2) in drug transport. AAPS J 2005;7:E118-133.
[54] Iyer L, Das S, Janisch L, Wen M, Ramirez J, Karrison T, et al. UGT1A1*28 polymorphism as a determinant of irinotecan disposition and toxicity. Pharmacogenomics J 2002;2:43-47.
[55] De Francia S, Massano D, Piccione FM, Pirro E, Racca S, Di Carlo F, et al. A new HPLC UV validated method for therapeutic monitoring of deferasirox in thalassaemic patients. J Chromatogr B Analyt Technol Biomed Life Sci 2012;893-894:127-133.
[56] Lee JW, Kang HJ, Choi JY, Kim NH, Jang MK, Yeo CW, et al. Pharmacogenetic study of deferasirox, an iron chelating agent. PLoS One 2013;8:e64114.
[57] Chirnomas D, Smith AL, Braunstein J, Finkelstein Y, Pereira L, Bergmann AK, et al. Deferasirox pharmacokinetics in patients with adequate versus inadequate response. Blood 2009;114:4009-4013.
[58] Cusato J, Allegra S, Massano D, De Francia S, Piga A, D'Avolio A. Influence of single-nucleotide polymorphisms on deferasirox C trough levels and effectiveness. Pharmacogenomics J 2014;15:263-271.
[59] Cusato J, Allegra S, De Francia S, Massano D, Piga A, D'Avolio A. Role of pharmacogenetics on deferasirox AUC and efficacy. Pharmacogenomics 2016;17:561-572.
[60] Vichinsky E. Clinical application of deferasirox: practical patient management. Am J Hematol 2008;83:398-402.
[61] Mehrotra N, Gupta M, Kovar A, Meibohm B. The role of pharmacokinetics and pharmacodynamics in phosphodiesterase-5 inhibitor therapy. Int J Impot Res 2007;19:253-264.
[62] Rxkinetics. Therapeutic drug monitoring. 2009 [cited; Available from: http://www.rxkinetics.com/pktutorial/1_6.html
[63] Nisbet-Brown E, Olivieri NF, Giardina PJ, Grady RW, Neufeld EJ, Sechaud R, et al. Effectiveness and safety of ICL670 in iron-loaded patients with thalassaemia: a randomised, double-blind, placebo-controlled, dose-escalation trial. Lancet 2003;361:1597-1602.
[64] Galanello R, Origa R. Once-daily oral deferasirox for the treatment of transfusional iron overload. Expert Rev Clin Pharmacol 2008;1:231-240.
[65] Galanello R, Piga A, Alberti D, Rouan MC, Bigler H, Sechaud R. Safety, tolerability, and pharmacokinetics of ICL670, a new orally active iron-chelating agent in patients with transfusion-dependent iron overload due to beta-thalassemia. J Clin Pharmacol 2003;43:565-572.
[66] Clemerson JP, Payne K, Bissell P, Anderson C. Pharmacogenetics, the next challenge for pharmacy? Pharm World Sci 2006;28:126-130.
[67] Evans WE, Relling MV. Moving towards individualized medicine with pharmacogenomics. Nature 2004;429:464-468.
[68] Schwertner HA, Vitek L. Gilbert syndrome, UGT1A1*28 allele, and cardiovascular disease risk: possible protective effects and therapeutic applications of bilirubin. Atherosclerosis 2008;198:1-11.
[69] Allegra S, Cusato J, De Francia S, Massano D, Piga A, D'Avolio A. Deferasirox AUC efficacy cutoff and role of pharmacogenetics. Eur J Clin Pharmacol 2016;72:1155-1157.

[70] Riedmaier S, Klein K, Hofmann U, Keskitalo JE, Neuvonen PJ, Schwab M, et al. UDP-glucuronosyltransferase (UGT) polymorphisms affect atorvastatin lactonization in vitro and in vivo. Clin Pharmacol Ther 2010;87:65-73.
[71] Cho SK, Oh ES, Park K, Park MS, Chung JY. The UGT1A3*2 polymorphism affects atorvastatin lactonization and lipid-lowering effect in healthy volunteers. Pharmacogenet Genomics 2012;22:598-605.
[72] Lankisch TO, Moebius U, Wehmeier M, Behrens G, Manns MP, Schmidt RE, et al. Gilbert's disease and atazanavir: from phenotype to UDP-glucuronosyltransferase haplotype. Hepatology 2006;44:1324-1332.
[73] Argikar UA, Iwuchukwu OF, Nagar S. Update on tools for evaluation of uridine diphosphoglucuronosyltransferase polymorphisms. Expert Opin Drug Metab Toxicol 2008;4:879-894.
[74] Bosma PJ, Chowdhury JR, Bakker C, Gantla S, de Boer A, Oostra BA, et al. The genetic basis of the reduced expression of bilirubin UDP-glucuronosyltransferase 1 in Gilbert's syndrome. N Engl J Med 1995;333:1171-1175.
[75] Mimura Y, Maruo Y, Ohta Y, Sato H, Takeuchi Y. Effect of common exon variant (p.P364L) on drug glucuronidation by the human UDP-glucuronosyltransferase 1 family. Basic Clin Pharmacol Toxicol 2011;109:486-493.
[76] Chen G, Ramos E, Adeyemo A, Shriner D, Zhou J, Doumatey AP, et al. UGT1A1 is a major locus influencing bilirubin levels in African Americans. Eur J Hum Genet 2012;20:463-468.
[77] Lin R, Wang Y, Fu W, Zhang D, Zheng H, Yu T, et al. Common variants of four bilirubin metabolism genes and their association with serum bilirubin and coronary artery disease in Chinese Han population. Pharmacogenet Genomics 2009;19:310-318.
[78] Johnson AD, Kavousi M, Smith AV, Chen MH, Dehghan A, Aspelund T, et al. Genome-wide association meta-analysis for total serum bilirubin levels. Hum Mol Genet 2009;18:2700-2710.
[79] Zhou Y, Wang SN, Li H, Zha W, Peng Q, Li S, et al. Quantitative trait analysis of polymorphisms in two bilirubin metabolism enzymes to physiologic bilirubin levels in Chinese newborns. J Pediatr 2014;165:1154-1160 e1151.
[80] Cusato J, Allegra S, Massano D, De Francia S, Piga A, D'Avolio A. Influence of single-nucleotide polymorphisms on deferasirox C trough levels and effectiveness. Pharmacogenomics J 2015;15:263-271.
[81] Allegra S, De Francia S, Cusato J, Arduino A, Massano D, Longo F, et al. Deferasirox pharmacogenetic influence on pharmacokinetic, efficacy and toxicity in a cohort of pediatric patients. Pharmacogenomics 2017;18:539-554.
[82] Martin P, Giardiello M, McDonald TO, Rannard SP, Owen A. Mediation of in Vitro Cytochrome P450 Activity by Common Pharmaceutical Excipients. Mol Pharm 2013.
[83] Singh AP, Pant MC, Ruwali M, Shah PP, Prasad R, Mathur N, et al. Polymorphism in cytochrome P450 1A2 and their interaction with risk factors in determining risk of squamous cell lung carcinoma in men. Cancer Biomark;8:351-359.
[84] B'Chir F, Pavanello S, Knani J, Boughattas S, Arnaud MJ, Saguem S. CYP1A2 genetic polymorphisms and adenocarcinoma lung cancer risk in the Tunisian population. Life Sci 2009;84:779-784.
[85] Nakajima M, Yokoi T, Mizutani M, Kinoshita M, Funayama M, Kamataki T. Genetic polymorphism in the 5'-flanking region of human CYP1A2 gene: effect on the CYP1A2 inducibility in humans. J Biochem 1999;125:803-808.
[86] Sachse C, Bhambra U, Smith G, Lightfoot TJ, Barrett JH, Scollay J, et al. Polymorphisms in the cytochrome P450 CYP1A2 gene (CYP1A2) in colorectal cancer patients and controls: allele frequencies, linkage disequilibrium and influence on caffeine metabolism. Br J Clin Pharmacol 2003;55:68-76.
[87] Luna-Tortos C, Fedrowitz M, Loscher W. Evaluation of transport of common antiepileptic drugs by human multidrug resistance-associated proteins (MRP1, 2 and 5) that are overexpressed in pharmacoresistant epilepsy. Neuropharmacology;58:1019-1032.
[88] Catterall WA. Molecular properties of brain sodium channels: an important target for anticonvulsant drugs. Adv Neurol 1999;79:441-456.
[89] Lipkind GM, Fozzard HA. Molecular model of anticonvulsant drug binding to the voltage-gated sodium channel inner pore. Mol Pharmacol;78:631-638.

[90] Koopmann TT, Bezzina CR, Wilde AA. Voltage-gated sodium channels: action players with many faces. Ann Med 2006;38:472-482.
[91] Meisler MH, O'Brien JE, Sharkey LM. Sodium channel gene family: epilepsy mutations, gene interactions and modifier effects. J Physiol;588:1841-1848.
[92] Tiwari AK, Deshpande SN, Lerer B, Nimgaonkar VL, Thelma BK. Genetic susceptibility to Tardive Dyskinesia in chronic schizophrenia subjects: V. Association of CYP1A2 1545 C>T polymorphism. Pharmacogenomics J 2007;7:305-311.
[93] Rotunno M, Yu K, Lubin JH, Consonni D, Pesatori AC, Goldstein AM, et al. Phase I metabolic genes and risk of lung cancer: multiple polymorphisms and mRNA expression. PLoS One 2009;4:e5652.
[94] Wang S, Chanock S, Tang D, Li Z, Jedrychowski W, Perera FP. Assessment of interactions between PAH exposure and genetic polymorphisms on PAH-DNA adducts in African American, Dominican, and Caucasian mothers and newborns. Cancer Epidemiol Biomarkers Prev 2008;17:405-413.
[95] Hayashi SI, Watanabe J, Nakachi K, Kawajiri K. PCR detection of an A/G polymorphism within exon 7 of the CYP1A1 gene. Nucleic Acids Res 1991;19:4797.
[96] Kawajiri K, Nakachi K, Imai K, Yoshii A, Shinoda N, Watanabe J. Identification of genetically high risk individuals to lung cancer by DNA polymorphisms of the cytochrome P450IA1 gene. FEBS Lett 1990;263:131-133.
[97] Mitrunen K, Hirvonen A. Molecular epidemiology of sporadic breast cancer. The role of polymorphic genes involved in oestrogen biosynthesis and metabolism. Mutat Res 2003;544:9-41.
[98] Surekha D, Sailaja K, Rao DN, Padma T, Raghunadharao D, Vishnupriya S. Association of a CYP17 gene polymorphism with development of breast cancer in India. Asian Pac J Cancer Prev 2011;11:1653-1657.
[99] Vasiliou V, Vasiliou K, Nebert DW. Human ATP-binding cassette (ABC) transporter family. Hum Genomics 2009;3:281-290.
[100] Engstrom K, Ameer S, Bernaudat L, Drasch G, Baeuml J, Skerfving S, et al. Polymorphisms in genes encoding potential mercury transporters and urine mercury concentrations in populations exposed to mercury vapor from gold mining. Environ Health Perspect 2012;121:85-91.
[101] Grover S, Kukreti R. A systematic review and meta-analysis of the role of ABCC2 variants on drug response in patients with epilepsy. Epilepsia 2013;54:936-945.
[102] Ieiri I. Functional significance of genetic polymorphisms in P-glycoprotein (MDR1, ABCB1) and breast cancer resistance protein (BCRP, ABCG2). Drug Metab Pharmacokinet 2012;27:85-105.
[103] Birmingham BK, Bujac SR, Elsby R, Azumaya CT, Wei C, Chen Y, et al. Impact of ABCG2 and SLCO1B1 polymorphisms on pharmacokinetics of rosuvastatin, atorvastatin and simvastatin acid in Caucasian and Asian subjects: a class effect? Eur J Clin Pharmacol 2015;71:341-355.
[104] Chu YH, Li H, Tan HS, Koh V, Lai J, Phyo WM, et al. Association of ABCB1 and FLT3 Polymorphisms with Toxicities and Survival in Asian Patients Receiving Sunitinib for Renal Cell Carcinoma. PLoS One 2015;10:e0134102.
[105] Gotanda K, Tokumoto T, Hirota T, Fukae M, Ieiri I. Sulfasalazine disposition in a subject with 376C>T (nonsense mutation) and 421C>A variants in the ABCG2 gene. Br J Clin Pharmacol 2015;80:1236-1237.
[106] Keskitalo JE, Pasanen MK, Neuvonen PJ, Niemi M. Different effects of the ABCG2 c.421C>A SNP on the pharmacokinetics of fluvastatin, pravastatin and simvastatin. Pharmacogenomics 2009;10:1617-1624.
[107] Keskitalo JE, Zolk O, Fromm MF, Kurkinen KJ, Neuvonen PJ, Niemi M. ABCG2 polymorphism markedly affects the pharmacokinetics of atorvastatin and rosuvastatin. Clin Pharmacol Ther 2009;86:197-203.
[108] Skoglund K, Boiso Moreno S, Jonsson JI, Vikingsson S, Carlsson B, Green H. Single-nucleotide polymorphisms of ABCG2 increase the efficacy of tyrosine kinase inhibitors in the K562 chronic myeloid leukemia cell line. Pharmacogenet Genomics 2013;24:52-61.
[109] Warren RB, Smith RL, Campalani E, Eyre S, Smith CH, Barker JN, et al. Genetic variation in efflux transporters influences outcome to methotrexate therapy in patients with psoriasis. J Invest Dermatol 2008;128:1925-1929.

[110] Delord M, Rousselot P, Cayuela JM, Sigaux F, Guilhot J, Preudhomme C, et al. High imatinib dose overcomes insufficient response associated with ABCG2 haplotype in chronic myelogenous leukemia patients. Oncotarget 2013;4:1582-1591.
[111] Mattioli F, Puntoni M, Marini V, Fucile C, Milano G, Robbiano L, et al. Determination of deferasirox plasma concentrations: do gender, physical and genetic differences affect chelation efficacy? Eur J Haematol 2014;94:310-317.
[112] Allegra S, Cusato J, De Francia S, Pirro E, Massano D, Piga A, et al. Deferasirox pharmacokinetic evaluation in beta-thalassaemia paediatric patients. J Pharm Pharmacol 2016;69:525-528.
[113] Allegra S, De Francia S, Cusato J, Pirro E, Massano D, Piga A, et al. Deferasirox pharmacokinetic and toxicity correlation in beta-thalassaemia major treatment. J Pharm Pharmacol 2016;68:1417-1421.
[114] Allegra S, De Francia S, Longo F, Massano D, Cusato J, Arduino A, et al. Deferasirox pharmacokinetics evaluation in a woman with hereditary haemochromatosis and heterozygous beta-thalassaemia. Biomed Pharmacother 2016;84:1510-1512.
[115] Allegra S, Massano D, De Francia S, Longo F, Piccione F, Pirro E, et al. Clinical relevance of deferasirox trough levels in beta-thalassemia patients. Clin Exp Pharmacol Physiol 2017;45:213-216.
[116] Daar S, Pathare A, Nick H, Kriemler-Krahn U, Hmissi A, Habr D, et al. Reduction in labile plasma iron during treatment with deferasirox, a once-daily oral iron chelator, in heavily iron-overloaded patients with beta-thalassaemia. Eur J Haematol 2009;82:454-457.
[117] Chauzit E, Bouchet S, Micheau M, Mahon FX, Moore N, Titier K, et al. A method to measure deferasirox in plasma using HPLC coupled with MS/MS detection and its potential application. Ther Drug Monit 2010;32:476-481.
[118] Sechaud R, Dutreix C, Balez S, Pommier F, Dumortier T, Morisson S, et al. Relative bioavailability of deferasirox tablets administered without dispersion and dispersed in various drinks. Int J Clin Pharmacol Ther 2008;46:102-108.
[119] Piga A, Galanello R, Forni GL, Cappellini MD, Origa R, Zappu A, et al. Randomized phase II trial of deferasirox (Exjade, ICL670), a once-daily, orally-administered iron chelator, in comparison to deferoxamine in thalassemia patients with transfusional iron overload. Haematologica 2006;91:873-880.
[120] Rouan MC, Marfil F, Mangoni P, Sechaud R, Humbert H, Maurer G. Determination of a new oral iron chelator, ICL670, and its iron complex in plasma by high-performance liquid chromatography and ultraviolet detection. J Chromatogr B Biomed Sci Appl 2001;755:203-213.
[121] Dimitriadou M, Christoforidis A, Fidani L, Economou M, Vlachaki E, Athanassiou-Metaxa M, et al. A 2-year prospective densitometric study on the influence of Fok-I gene polymorphism in young patients with thalassaemia major. Osteoporos Int 2015.
[122] Moulas A, Challa A, Chaliasos N, Lapatsanis PD. Vitamin D metabolites (25-hydroxyvitamin D, 24,25-dihydroxyvitamin D and 1,25-dihydroxyvitamin D) and osteocalcin in beta-thalassaemia. Acta Paediatr 1997;86:594-599.
[123] Napoli N, Carmina E, Bucchieri S, Sferrazza C, Rini GB, Di Fede G. Low serum levels of 25-hydroxy vitamin D in adults affected by thalassemia major or intermedia. Bone 2006;38:888-892.
[124] Wood JC, Claster S, Carson S, Menteer JD, Hofstra T, Khanna R, et al. Vitamin D deficiency, cardiac iron and cardiac function in thalassaemia major. Br J Haematol 2008;141:891-894.
[125] Soliman A, De Sanctis V, Yassin M. Vitamin d status in thalassemia major: an update. Mediterr J Hematol Infect Dis 2013;5:e2013057.
[126] Chung M, Balk EM, Brendel M, Ip S, Lau J, Lee J, et al. Vitamin D and calcium: a systematic review of health outcomes. Evid Rep Technol Assess (Full Rep) 2009:1-420.
[127] He F, Hockemeyer JA, Sedlock D. Does combined antioxidant vitamin supplementation blunt repeated bout effect? Int J Sports Med 2015;36:407-413.
[128] Wolf G. The discovery of vitamin D: the contribution of Adolf Windaus. J Nutr 2004;134:1299-1302.
[129] Calvo MS, Whiting SJ, Barton CN. Vitamin D intake: a global perspective of current status. J Nutr 2005;135:310-316.
[130] Christakos S, Ajibade DV, Dhawan P, Fechner AJ, Mady LJ. Vitamin D: metabolism. Rheum Dis Clin North Am 2012;38:1-11, vii.

[131] Nykjaer A, Dragun D, Walther D, Vorum H, Jacobsen C, Herz J, et al. An endocytic pathway essential for renal uptake and activation of the steroid 25-(OH) vitamin D3. Cell 1999;96:507-515.
[132] Weisman Y, Harell A, Edelstein S, David M, Spirer Z, Golander A. 1 alpha, 25-Dihydroxyvitamin D3 and 24,25-dihydroxyvitamin D3 in vitro synthesis by human decidua and placenta. Nature 1979;281:317-319.
[133] Gray TK, Lester GE, Lorenc RS. Evidence for extra-renal 1 alpha-hydroxylation of 25-hydroxyvitamin D3 in pregnancy. Science 1979;204:1311-1313.
[134] Stoffels K, Overbergh L, Bouillon R, Mathieu C. Immune regulation of 1alpha-hydroxylase in murine peritoneal macrophages: unravelling the IFNgamma pathway. J Steroid Biochem Mol Biol 2007;103:567-571.
[135] Esteban L, Vidal M, Dusso A. 1alpha-Hydroxylase transactivation by gamma-interferon in murine macrophages requires enhanced C/EBPbeta expression and activation. J Steroid Biochem Mol Biol 2004;89-90:131-137.
[136] Jones G, Prosser DE, Kaufmann M. 25-Hydroxyvitamin D-24-hydroxylase (CYP24A1): its important role in the degradation of vitamin D. Arch Biochem Biophys 2011;523:9-18.
[137] Knutson JC, DeLuca HF. 25-Hydroxyvitamin D3-24-hydroxylase. Subcellular location and properties. Biochemistry 1974;13:1543-1548.
[138] Jones G, Strugnell SA, DeLuca HF. Current understanding of the molecular actions of vitamin D. Physiol Rev 1998;78:1193-1231.
[139] Hewison M. Vitamin D and the immune system: new perspectives on an old theme. Endocrinol Metab Clin North Am 2010;39:365-379, table of contents.
[140] Plum LA, DeLuca HF. Vitamin D, disease and therapeutic opportunities. Nat Rev Drug Discov 2010;9:941-955.
[141] Bikle DD. Vitamin D: an ancient hormone. Exp Dermatol 2011;20:7-13.
[142] Baker AR, McDonnell DP, Hughes M, Crisp TM, Mangelsdorf DJ, Haussler MR, et al. Cloning and expression of full-length cDNA encoding human vitamin D receptor. Proc Natl Acad Sci U S A 1988;85:3294-3298.
[143] Lin R, Nagai Y, Sladek R, Bastien Y, Ho J, Petrecca K, et al. Expression profiling in squamous carcinoma cells reveals pleiotropic effects of vitamin D3 analog EB1089 signaling on cell proliferation, differentiation, and immune system regulation. Mol Endocrinol 2002;16:1243-1256.
[144] Wood RJ, Tchack L, Angelo G, Pratt RE, Sonna LA. DNA microarray analysis of vitamin D-induced gene expression in a human colon carcinoma cell line. Physiol Genomics 2004;17:122-129.
[145] Wang TT, Tavera-Mendoza LE, Laperriere D, Libby E, MacLeod NB, Nagai Y, et al. Large-scale in silico and microarray-based identification of direct 1,25-dihydroxyvitamin D3 target genes. Mol Endocrinol 2005;19:2685-2695.
[146] Feldman D, Krishnan AV, Swami S, Giovannucci E, Feldman BJ. The role of vitamin D in reducing cancer risk and progression. Nat Rev Cancer 2014;14:342-357.
[147] Fujiki R, Kim MS, Sasaki Y, Yoshimura K, Kitagawa H, Kato S. Ligand-induced transrepression by VDR through association of WSTF with acetylated histones. EMBO J 2005;24:3881-3894.
[148] Huhtakangas JA, Olivera CJ, Bishop JE, Zanello LP, Norman AW. The vitamin D receptor is present in caveolae-enriched plasma membranes and binds 1 alpha,25(OH)2-vitamin D3 in vivo and in vitro. Mol Endocrinol 2004;18:2660-2671.
[149] Rebsamen MC, Sun J, Norman AW, Liao JK. 1alpha,25-dihydroxyvitamin D3 induces vascular smooth muscle cell migration via activation of phosphatidylinositol 3-kinase. Circ Res 2002;91:17-24.
[150] Poon AH, Gong L, Brasch-Andersen C, Litonjua AA, Raby BA, Hamid Q, et al. Very important pharmacogene summary for VDR. Pharmacogenet Genomics 2012;22:758-763.
[151] Deeb KK, Trump DL, Johnson CS. Vitamin D signalling pathways in cancer: potential for anticancer therapeutics. Nat Rev Cancer 2007;7:684-700.
[152] Allegra S, Cusato J, De Francia S, Arduino A, Longo F, Pirro E, et al. Role of CYP24A1, VDR and GC gene polymorphisms on deferasirox pharmacokinetics and clinical outcomes. Pharmacogenomics J 2017.

[153] Allegra S, Cusato J, De Francia S, Longo F, Pirro E, Massano D, et al. Effect of pharmacogenetic markers of vitamin D pathway on deferasirox pharmacokinetics in children. Pharmacogenet Genomics 2017;28:17-22.
[154] Westwood M, Anderson LJ, Firmin DN, Gatehouse PD, Charrier CC, Wonke B, et al. A single breath-hold multiecho T2* cardiovascular magnetic resonance technique for diagnosis of myocardial iron overload. J Magn Reson Imaging 2003;18:33-39.
[155] Maceira AM, Prasad SK, Khan M, Pennell DJ. Normalized left ventricular systolic and diastolic function by steady state free precession cardiovascular magnetic resonance. J Cardiovasc Magn Reson 2006;8:417-426.
[156] Di Tucci AA, Matta G, Deplano S, Gabbas A, Depau C, Derudas D, et al. Myocardial iron overload assessment by T2* magnetic resonance imaging in adult transfusion dependent patients with acquired anemias. Haematologica 2008;93:1385-1388.
[157] Rodriguez S, Gaunt TR, Day IN. Hardy-Weinberg equilibrium testing of biological ascertainment for Mendelian randomization studies. Am J Epidemiol 2009;169:505-514.
[158] Reich DE, Cargill M, Bolk S, Ireland J, Sabeti PC, Richter DJ, et al. Linkage disequilibrium in the human genome. Nature 2001;411:199-204.
[159] Modell B, Darlison M. Global epidemiology of haemoglobin disorders and derived service indicators. Bull World Health Organ 2008;86:480-487.
[160] Lou YR, Qiao S, Talonpoika R, Syvala H, Tuohimaa P. The role of Vitamin D3 metabolism in prostate cancer. J Steroid Biochem Mol Biol 2004;92:317-325.
[161] Syvanen AC. Accessing genetic variation: genotyping single nucleotide polymorphisms. Nat Rev Genet 2001;2:930-942.
[162] Oh JJ, Byun SS, Lee SE, Hong SK, Jeong CW, Choi WS, et al. Genetic variants in the CYP24A1 gene are associated with prostate cancer risk and aggressiveness in a Korean study population. Prostate Cancer Prostatic Dis 2014;17:149-156.
[163] Cusato J, Allegra S, Boglione L, De Nicolo A, Baietto L, Cariti G, et al. Vitamin D pathway gene variants and HCV-2/3 therapy outcomes. Antivir Ther 2014;20:335-341.
[164] Cusato J, Allegra S, De Nicolo A, Boglione L, Fatiguso G, Mohamed Abdi A, et al. Intracellular and Plasma Trough Concentration and Pharmacogenetics of Telaprevir. J Pharm Pharm Sci 2015;18:171-176.
[165] Fatiguso G, Allegra S, Calcagno A, Baietto L, Motta I, Favata F, et al. Ethambutol plasma and intracellular pharmacokinetics: A pharmacogenetic study. Int J Pharm 2015;497:287-292.
[166] Bouillon R, Carmeliet G, Verlinden L, van Etten E, Verstuyf A, Luderer HF, et al. Vitamin D and human health: lessons from vitamin D receptor null mice. Endocr Rev 2008;29:726-776.
[167] Holt SK, Kwon EM, Koopmeiners JS, Lin DW, Feng Z, Ostrander EA, et al. Vitamin D pathway gene variants and prostate cancer prognosis. Prostate 2010;70:1448-1460.
[168] Ramasamy A, Trabzuni D, Forabosco P, Smith C, Walker R, Dillman A, et al. Genetic evidence for a pathogenic role for the vitamin D3 metabolizing enzyme in multiple sclerosis. Mult Scler Relat Disord 2015;3:211-219.
[169] Wang Y, Wang O, Li W, Ma L, Ping F, Chen L, et al. Variants in Vitamin D Binding Protein Gene Are Associated With Gestational Diabetes Mellitus. Medicine (Baltimore) 2015;94:e1693.
[170] Hallau J, Hamann L, Schumann RR, Worm M, Heine G. A Promoter Polymorphism of the Vitamin D Metabolism Gene Cyp24a1 is Associated with Severe Atopic Dermatitis in Adults. Acta Derm Venereol 2015.
[171] Bosse Y, Lemire M, Poon AH, Daley D, He JQ, Sandford A, et al. Asthma and genes encoding components of the vitamin D pathway. Respir Res 2009;10:98.
[172] Wjst M. Variants in the vitamin D receptor gene and asthma. BMC Genet 2005;6:2.
[173] Brehm JM, Schuemann B, Fuhlbrigge AL, Hollis BW, Strunk RC, Zeiger RS, et al. Serum vitamin D levels and severe asthma exacerbations in the Childhood Asthma Management Program study. J Allergy Clin Immunol 2010;126:52-58 e55.
[174] DeLuca HF. Evolution of our understanding of vitamin D. Nutr Rev 2008;66:S73-87.
[175] Lange CM, Bojunga J, Ramos-Lopez E, von Wagner M, Hassler A, Vermehren J, et al. Vitamin D deficiency and a CYP27B1-1260 promoter polymorphism are associated with chronic hepatitis C and poor response to interferon-alfa based therapy. J Hepatol 2010;54:887-893.

[176] Lange CM, Bibert S, Kutalik Z, Burgisser P, Cerny A, Dufour JF, et al. A genetic validation study reveals a role of vitamin D metabolism in the response to interferon-alfa-based therapy of chronic hepatitis C. PLoS One 2012;7:e40159.
[177] Kitanaka S, Isojima T, Takaki M, Numakura C, Hayasaka K, Igarashi T. Association of vitamin D-related gene polymorphisms with manifestation of vitamin D deficiency in children. Endocr J 2012;59:1007-1014.
[178] Rukin NJ, Strange RC. What are the frequency, distribution, and functional effects of vitamin D receptor polymorphisms as related to cancer risk? Nutr Rev 2007;65:S96-101.
[179] Uitterlinden AG, Fang Y, Van Meurs JB, Pols HA, Van Leeuwen JP. Genetics and biology of vitamin D receptor polymorphisms. Gene 2004;338:143-156.
[180] Wang TJ, Zhang F, Richards JB, Kestenbaum B, van Meurs JB, Berry D, et al. Common genetic determinants of vitamin D insufficiency: a genome-wide association study. Lancet;376:180-188.
[181] Miyamoto K, Kesterson RA, Yamamoto H, Taketani Y, Nishiwaki E, Tatsumi S, et al. Structural organization of the human vitamin D receptor chromosomal gene and its promoter. Mol Endocrinol 1997;11:1165-1179.
[182] Crofts LA, Hancock MS, Morrison NA, Eisman JA. Multiple promoters direct the tissue-specific expression of novel N-terminal variant human vitamin D receptor gene transcripts. Proc Natl Acad Sci U S A 1998;95:10529-10534.
[183] Bouillon R, Okamura WH, Norman AW. Structure-function relationships in the vitamin D endocrine system. Endocr Rev 1995;16:200-257.
[184] Menezes RJ, Cheney RT, Husain A, Tretiakova M, Loewen G, Johnson CS, et al. Vitamin D receptor expression in normal, premalignant, and malignant human lung tissue. Cancer Epidemiol Biomarkers Prev 2008;17:1104-1110.
[185] Bikle DD. Vitamin D regulation of immune function. Vitam Horm 2011;86:1-21.
[186] Jehan F, Gaucher C, Nguyen TM, Walrant-Debray O, Lahlou N, Sinding C, et al. Vitamin D receptor genotype in hypophosphatemic rickets as a predictor of growth and response to treatment. J Clin Endocrinol Metab 2008;93:4672-4682.
[187] Thirumaran RK, Lamba JK, Kim RB, Urquhart BL, Gregor JC, Chande N, et al. Intestinal CYP3A4 and midazolam disposition in vivo associate with VDR polymorphisms and show seasonal variation. Biochem Pharmacol 2012;84:104-112.
[188] Nesic D, Cheng J, Maquat LE. Sequences within the last intron function in RNA 3'-end formation in cultured cells. Mol Cell Biol 1993;13:3359-3369.
[189] Allegra S, Fatiguso G, Calcagno A, Baietto L, Motta I, Favata F, et al. Role of vitamin D pathway gene polymorphisms on rifampicin plasma and intracellular pharmacokinetics. Pharmacogenomics 2017;18:865-880.
[190] Andraos C, Koorsen G, Knight JC, Bornman L. Vitamin D receptor gene methylation is associated with ethnicity, tuberculosis, and TaqI polymorphism. Hum Immunol 2011;72:262-268.
[191] Saeki M, Kurose K, Tohkin M, Hasegawa R. Identification of the functional vitamin D response elements in the human MDR1 gene. Biochem Pharmacol 2008;76:531-542.
[192] Song YH, Naumova AK, Liebhaber SA, Cooke NE. Physical and meiotic mapping of the region of human chromosome 4q11-q13 encompassing the vitamin D binding protein DBP/Gc-globulin and albumin multigene cluster. Genome Res 1999;9:581-587.
[193] Malik S, Fu L, Juras DJ, Karmali M, Wong BY, Gozdzik A, et al. Common variants of the vitamin D binding protein gene and adverse health outcomes. Crit Rev Clin Lab Sci 2013;50:1-22.
[194] Carpenter TO, Zhang JH, Parra E, Ellis BK, Simpson C, Lee WM, et al. Vitamin D binding protein is a key determinant of 25-hydroxyvitamin D levels in infants and toddlers. J Bone Miner Res 2013;28:213-221.
[195] Wjst M, Altmuller J, Faus-Kessler T, Braig C, Bahnweg M, Andre E. Asthma families show transmission disequilibrium of gene variants in the vitamin D metabolism and signalling pathway. Respir Res 2006;7:60.
[196] Anderson LN, Cotterchio M, Cole DE, Knight JA. Vitamin D-related genetic variants, interactions with vitamin D exposure, and breast cancer risk among Caucasian women in Ontario. Cancer Epidemiol Biomarkers Prev 2011;20:1708-1717.

[197] Hashibe M, Brennan P, Strange RC, Bhisey R, Cascorbi I, Lazarus P, et al. Meta- and pooled analyses of GSTM1, GSTT1, GSTP1, and CYP1A1 genotypes and risk of head and neck cancer. Cancer Epidemiol Biomarkers Prev 2003;12:1509-1517.
[198] Liu H, Jia J, Mao X, Lin Z. Association of CYP1A1 and GSTM1 Polymorphisms With Oral Cancer Susceptibility: A Meta-Analysis. Medicine (Baltimore) 2015;94:e895.
[199] Mo W, Zhang JT. Human ABCG2: structure, function, and its role in multidrug resistance. Int J Biochem Mol Biol 2012;3:1-27.
[200] Kang TW, Kim HJ, Ju H, Kim JH, Jeon YJ, Lee HC, et al. Genome-wide association of serum bilirubin levels in Korean population. Hum Mol Genet;19:3672-3678.
[201] Sanna S, Busonero F, Maschio A, McArdle PF, Usala G, Dei M, et al. Common variants in the SLCO1B3 locus are associated with bilirubin levels and unconjugated hyperbilirubinemia. Hum Mol Genet 2009;18:2711-2718.
[202] Brittenham GM, Cohen AR, McLaren CE, Martin MB, Griffith PM, Nienhuis AW, et al. Hepatic iron stores and plasma ferritin concentration in patients with sickle cell anemia and thalassemia major. Am J Hematol 1993;42:81-85.
[203] Cappellini MD, Taher A. Deferasirox (Exjade) for the treatment of iron overload. Acta Haematol 2009;122:165-173.
[204] Glickstein H, El RB, Shvartsman M, Cabantchik ZI. Intracellular labile iron pools as direct targets of iron chelators: a fluorescence study of chelator action in living cells. Blood 2005;106:3242-3250.
[205] Glickstein H, El RB, Link G, Breuer W, Konijn AM, Hershko C, et al. Action of chelators in iron-loaded cardiac cells: Accessibility to intracellular labile iron and functional consequences. Blood 2006;108:3195-3203.
[206] Brittenham GM, Farrell DE, Harris JW, Feldman ES, Danish EH, Muir WA, et al. Magnetic-susceptibility measurement of human iron stores. N Engl J Med 1982;307:1671-1675.
[207] Fischer R, Tiemann CD, Engelhardt R, Nielsen P, Durken M, Gabbe EE, et al. Assessment of iron stores in children with transfusion siderosis by biomagnetic liver susceptometry. Am J Hematol 1999;60:289-299.
[208] Berzigotti A, Castera L. Update on ultrasound imaging of liver fibrosis. J Hepatol 2013;59:180-182.
[209] Cancado R, Melo MR, de Moraes Bastos R, Santos PC, Guerra-Shinohara EM, Ballas SK, et al. Deferasirox in patients with iron overload secondary to hereditary hemochromatosis: results of a 1-year Phase 2 study. Eur J Haematol 2015.
[210] Rose C, Brechignac S, Vassilief D, Pascal L, Stamatoullas A, Guerci A, et al. Does iron chelation therapy improve survival in regularly transfused lower risk MDS patients? A multicenter study by the GFM (Groupe Francophone des Myelodysplasies). Leuk Res 2010;34:864-870.
[211] Neukirchen J, Fox F, Kundgen A, Nachtkamp K, Strupp C, Haas R, et al. Improved survival in MDS patients receiving iron chelation therapy - a matched pair analysis of 188 patients from the Dusseldorf MDS registry. Leuk Res 2012;36:1067-1070.
[212] Leitch HA, Chan C, Leger CS, Foltz LM, Ramadan KM, Vickars LM. Improved survival with iron chelation therapy for red blood cell transfusion dependent lower IPSS risk MDS may be more significant in patients with a non-RARS diagnosis. Leuk Res 2012;36:1380-1386.